

UNCLASSIFIED

AD NUMBER

AD903215

LIMITATION CHANGES

TO:

Approved for public release; distribution is unlimited.

FROM:

Distribution authorized to U.S. Gov't. agencies only; Test and Evaluation; 21 JUL 1972. Other requests shall be referred to Air Force Cambridge Research Laboratories, Attn: OPR, L. G. Hancorn Field, Bedford, MA.

AUTHORITY

AFGL ltr, 15 Jan 1981

THIS PAGE IS UNCLASSIFIED

AD903215

DESIGN AND DEVELOPMENT OF A CRYOGENICALLY COOLED HIGH RESOLUTION INTERFEROMETER

by

Henry H. Blau, Jr.

Richard B. Hinckley

Frank E. Ruccia

ARTHUR D. LITTLE, INC.

Acorn Park

Cambridge, Massachusetts 02140

Contract No. F19628-71-C-0090

Project No. 8692

FINAL REPORT

12 November 1970 – 3 November 1971

November 1971

Contract Monitor: Dean F. Kimball

Optical Physics Laboratory

Distribution limited to U.S. Government agencies only;
Test and Evaluation, 21 July 1972. Other requests for this
document must be referred to AFCRL (OPR), L. G. Hanscom
Field, Bedford, Massachusetts 01730.

Sponsored by

Advanced Research Projects Agency

ARPA Order No. 1366

Monitored by

AIR FORCE CAMBRIDGE RESEARCH LABORATORIES

AIR FORCE SYSTEMS COMMAND

UNITED STATES AIR FORCE

BEDFORD, MASSACHUSETTS 01730



THIS REPORT HAS BEEN DELIMITED
AND CLEARED FOR PUBLIC RELEASE
UNDER DOD DIRECTIVE 5200.20 AND
NO RESTRICTIONS ARE IMPOSED UPON
ITS USE AND DISCLOSURE.

DISTRIBUTION STATEMENT A

APPROVED FOR PUBLIC RELEASE;
DISTRIBUTION UNLIMITED.

Program Code No. OE50

Effective Date of Contract 12 November 1970

Contract Expiration Date 3 November 1971

Principal Investigator and Phone No. Dr. Henry H. Blau, Jr. (617) 861-1490

AFCRL Project Scientist and Phone No. Dean F. Kimball (617) 861-4909

Contract No. F19628-71-C-0090

ARPA Order No. 1366

Contractor Arthur D. Little, Inc.

DESIGN AND DEVELOPMENT OF A CRYOGENICALLY COOLED HIGH RESOLUTION INTERFEROMETER

by

Henry H. Blau, Jr.
Richard B. Hinckley
Frank E. Ruccia

ARTHUR D. LITTLE, INC.
Acorn Park
Cambridge, Massachusetts 02140

Contract No. F19628-71-C-0090
Project No. 8692

FINAL REPORT

12 November 1970 — 3 November 1971
November 1971

Contract Monitor: Dean F. Kimball
Optical Physics Laboratory

Distribution limited to U.S. Government agencies only;
Test and Evaluation, 21 July 1972. Other requests for this
document must be referred to AFCRL (OPR), L. G. Hanscom
Field, Bedford, Massachusetts 01730.

Sponsored by
Advanced Research Projects Agency
ARPA Order No. 1366

Monitored by
AIR FORCE CAMBRIDGE RESEARCH LABORATORIES
AIR FORCE SYSTEMS COMMAND
UNITED STATES AIR FORCE
BEDFORD, MASSACHUSETTS 01730

ABSTRACT

The intent of the development called for under this contract is to produce a prototype liquid-helium cooled instrument, consisting of a cooled interferometer spectrometer, telescope, optical system and sensor, having a resolution of about two wave numbers and suitable for flight on vertical sounding rockets such as the Black Brant V for the purpose of making measurements of the spectral radiance of the airglow and aurora. This development was initiated under Contract No. F1928-70-C-0068.

Development, fabrication and testing of a prototype optical cube suitable for use at liquid helium temperatures and capable of surviving the environment of a rocket launch is described. A prototype interferometer was exposed to mechanical vibration at room temperature; the results of these tests are reported. The results of an experimental program to determine the feasibility of using a laser diode as a fringe reference source at liquid helium temperatures are cited. The preliminary design of a test dewar designed to permit both vibration and optical tests of the interferometer at cryogenic temperatures is presented.

PRECEDING PAGE BLANK - NOT FILMED

TABLE OF CONTENTS

	<u>Page</u>
List of Figures	vii
List of Tables	ix
1. INTRODUCTION	1
2. SUMMARY AND CONCLUSIONS	3
2.1 Summary	3
2.2 Consulisons	3
3. DEVELOPMENT AND TESTS OF PROTOTYPE INTERFEROMETER	5
3.1 Mechanical Tests of Optical H-Cube	5
3.2 Optical Tests of H-Cube Before and After Vibration	14
3.3 Mechanical Tests of H-Cube	15
3.4 Low Temperature Tests of Prototype V-Cube Interferometer	20
3.5 Mechanical Tests of Prototype Interferometer	23
3.6 Interferometer Servo Response	27
3.7 Slide Velocity Tests	32
3.8 Monochromatic Fringe Reference	36
3.9 Monochromatic Fringe Reference Detector	42
3.10 White Light Reference	43
3.11 Detector Optics	44
3.12 Low Temperature Tests of KRS-5 for Beam Splitter	48
3.13 Beam Splitter Support System	53
3.14 Interferometer Slide Lock	55
4. APPENDICES	59
4.1 Mechanical Environment Specification for Interferometer Tests	59
4.2 Interferometer Mounting Plate	61
4.4 System Operating Temperature Requirement	76
4.5 Idealab, Inc. Final Report, "Servo Controlled Michelson Interferometer Spectrometer"	

PRECEDING PAGE BLANK - NOT FILMED

LIST OF FIGURES

<u>No.</u>	<u>Title</u>	<u>Page</u>
3.1.1.1	Schematic of Optical Test of H-Cube	7
3.1.2.1	H-Cube with A-Z Steel Mirrors (Photo 11334-4)	9
3.1.2.2	Steel Mirrors - Fringe Patterns for Unmounted State - Produced by Fringe Fields Low Efficiency	10
3.1.2.3	Quartz Air-Gap Beam Splitter	11
3.1.2.4	H-Cube Cryogenic-Optical Test Arrangement	12
3.1.2.5	H-Cube with A-Z Steel Mirrors - Scanned Fringe Patterns	13
3.3.1	Mechanical Environment Tests of H-Cube X Input, 5 g, Location 2	17
3.3.2	Mechanical Environment Tests of H-Cube Z Input, 25 g, Location 4	18
3.4.1	Chamber and Optical Table Set Up for V-Cube Tests	21
3.4.2	Optical Arrangement for V-Cube Cryogenic Tests	22
3.5.1	Mechanical Environment Test of V-Cube Interferometer Y-Axis Input, 5 g, Response on Slide Near Cube	24
3.5.2	Mechanical Environment Tests of V-Cube Interferometer X-Axis Input, 5 g, Response on Slide Near Cube	25
3.5.3	Mechanical Environment Tests of V-Cube Interferometer Z-Axis Input, 10 g, Response on Moving Mirror	26
3.6.1	Interferometer Servo System - Simplified Schematic	29
3.6.2	Amplitude Response - Interferometer Servo	30
3.7.1	Slide Velocity Test Set Block Diagram	31
3.7.2	Slide Velocity Tests at Liquid Helium Temperature	33
3.7.3	Slide Velocity Tests, Liquid Helium Temperature	35

LIST OF FIGURES (Continued)

<u>No.</u>	<u>Title</u>	<u>Page</u>
3.8.1	IBM Diode Spectral Output at 200MA and at 4.2K	38
3.8.2	Laser Diode Lab., Inc., LD-22 at 200MA and 4.2K	39
3.8.3	RCA 7606 Diode Spectral Output at 150MA and 4.2K	40
3.8.4	RCA 7606 Diode Spectral Output at 95MA and 4.2K	40
3.8.5	Junction Temperature Effect, Laser Diodes	41
3.11.1	Suggested Detector Optics	45
3.12.1	KRS-5 Sample Holder for Liquid Helium Tests	50
3.13.1	Beam Splitter Support System	54
4.3.1.1	Idealab Dewar	64
4.3.1.2	Liquid Nitrogen Test Chamber	65
4.3.2.1	Optical, Thermal, Vacuum Test Chamber for Helium Temperature Tests	68
4.3.2.2	Helium Thermal, Optical, Vacuum Test Facility	69
4.3.2.3	Helium Test Facility, Optical Set Up	70
4.3.2.4	Liquid Helium Test Chamber, Nitrogen and Helium Shroud Configuration	71
4.3.3.1	Helium Test Dewar	75

LIST OF TABLES

<u>No.</u>	<u>Title</u>	<u>Page</u>
1	H-Cube-Teflon Washer Experiment	6
3.1	Summary of Pertinent Vibration Results Obtained with H-Cube	19
3.8.1	Summary of Laser Diode Test Results	37
3.12.1	Beam Splitter Material Cold Shock Test Results	52
3.14.1	Interferometer Motor Slide Lock Test Results	56
4.4.1	Noise Equivalent Spectro Radiance	78
4.4.2	Mirror Radiance	79

1. INTRODUCTION

Under Contract F19628-71-C-0090, Idealab, Franklin, Mass. and Arthur D. Little, Inc., Cambridge, Mass. continued the development of a cryogenically-cooled, high resolution interferometer spectrometer. This development was initiated under Contract F19628-70-C-0068. The intent of the development is to produce a prototype liquid-helium-cooled instrument, consisting of a cooled interferometer spectrometer, telescope, optical system and sensors, having a resolution of two wave-numbers or better and a scan rate of at least four scans per second, suitable for flight on vertical sounding rockets such as the Black Brant V for the purpose of making measurements of the spectral radiance of the aurora and air glow.

The several tasks delineated in this effort were:

- a. Develop improved means of applying dry lubricants to the slide and rails of the interferometer.
- b. Test a commercially available velocity transducer.
- c. Increase the stiffness of the slide servo to obtain required velocity linearity for the slide.
- d. Manufacture a flight prototype slide.
- e. Develop and fabricate an optical cube suitable for liquid helium temperature.
- f. Design and test means for mounting the beam splitter and mirrors to the cube.

which tasks were assigned to Idealab; and

- g. Design and fabricate a test dewar and mounting structure for the prototype interferometer.
- h. Subject the slide to vibration tests at room and liquid nitrogen temperatures, and determine velocity linearity after the cold test.
- i. Test the optical cube to assure that alignment is maintained with no adjustment after vibration and at liquid helium temperature.
- j. Subject the prototype interferometer to a mechanical environment simulating launch of a Black Brant V rocket, while cooled to liquid helium temperature.
- k. While cold, and after vibration, operate the prototype interferometer to demonstrate required resolution at the required scan rate, demonstrating that alignment is maintained by monitoring monochromatic fringes from a CO₂ laser and required velocity linearity by monitoring fringe references.

which tasks were assigned to Arthur D. Little, Inc.

This report discusses progress to date, test results, design of the test dewar and presents the Idealab final report in Appendix 4.5.

2. SUMMARY AND CONCLUSIONS

2.1 Summary

Various components of the prototype interferometer have been designed, developed and tested. Beam splitter mounting and mirror mounting designs were established. A commercial velocity transducer was procured and tested at low temperature.

A prototype interferometer was exposed to mechanical vibration at room temperature and response measurements made to determine design areas that might require modification.

A series of optical tests have been conducted, as follows:

- a. H-Cube, before and after exposure to the mechanical environment at room temperature, and at low temperature.
- b. The prototype interferometer incorporating a V-Cube, operating at liquid nitrogen and liquid helium temperatures.

Cold shock tests were performed on KRS-5 beam splitter material to determine its suitability for use in an interferometer operating at liquid helium temperatures.

Velocity constancy tests were conducted on the prototype interferometer operating at liquid nitrogen and liquid helium temperatures. During these tests, the interferometer servo frequency response was measured.

An experimental program was undertaken to determine if solid state laser diodes could be used as a fringe reference source.

Measurements were made of silicon photodiodes for use as a fringe reference detector.

A test dewar was designed to permit both vibration and optical tests of the interferometer at liquid helium temperatures.

The Idealab final report on Contract F19628-71-C-0090 is included as Appendix 4.5 of this report.

2.2 Conclusions

The testing performed on the prototype interferometer has shown the feasibility of developing the instrument to meet the specified requirements when operating at liquid helium temperatures.

An H-Cube of all A-2 steel construction maintained very reasonable optical alignment when tested at low temperature. This same cube

developed a 40 arc second tilt as a result of mechanical vibration; the problem was traced to dirt and improper assembly techniques, and is amenable to solution.

Vibration tests of the H-Cube were successful and have shown that lower weight and higher stiffness to result in higher natural frequencies is the proper way to design further models.

A prototype V-Cube interferometer was operationally tested at low temperature. Slide performance was excellent, although the mirrors did exhibit bowing. Vibration tests of the same interferometer indicated the necessity of providing greater stiffness for the servo system.

It was shown that off-the-shelf gallium arsenide laser diodes, such as the RCA 7606 diode, can be used for a fringe reference source, and that silicon diffused photodiodes, such as PIN 040 diffused diode from United Detector Technology can be used as a detector, thereby providing a monochromatic fringe reference.

A low-power incandescent tungsten lamp is satisfactory for a white light source, with a silicon photodiode or lead selenide detector to provide a white light reference.

Low temperature tests of KRS-5 blanks, which were considered prime candidates for the beam splitter, have shown that the solid solution deteriorates below 77 K and the material becomes opaque.

A beam splitter support system was developed for use at low temperatures.

It is concluded that the interferometer motor can be used to lock the interferometer slide during launch by passing excess current through the motor coil. The detailed design of the interferometer electrical system should include this feature.

3. DEVELOPMENT AND TESTS OF PROTOTYPE INTERFEROMETER

3.1 Mechanical Tests of Optical H-Cube

3.1.1 H-Cube with Teflon Washers

An H-Cube consisting of two fixed pyrex mirrors, and a fixed beam splitter mounted to an A2 steel structure was received and prepared for tests in our thermal vacuum chamber. It was reported on the basis of fringe measurements, the H-Cube in this form had remained stable from room temperature to liquid nitrogen temperature in preliminary tests at Idealab. The H-Cube was basically of an A2 steel frame, with a beam splitter consisting of two quartz plates separated by an air gap mounted in a central web. A circular spring is located between one of the steel plates, and a third A2 steel plate presses down on the outer surface of one of the beam splitter elements. The details of this design are shown in Section 3.13 of this report.

The plain front surface pyrex mirrors were mounted against three pads that were ground to be co-planar and very flat. One hole was tapped in each pad and the mirror was attached to the pads by means of steel screws passing through holes in the mirrors. The holes in the mirrors were counterbored and teflon washers were mounted between the screw heads and the pyrex mirror. This arrangement was an Idealab design.

The H-Cube was mounted in the thermal vacuum chamber and thermocouples attached. It was cooled from room temperature to approximately 39.5 K and then returned to room temperature. During the cooling cycle, the alignment of the cube was observed by monitoring interference fringes produced by a parallel laser beam passed through the cube. The optical arrangement used is shown in Figure 3.1.1.1. In order to facilitate this process, the cube had initially been misaligned with a 63 arc second wedge. On cooling the 63 arc second tilt increased to 115 arc seconds as the temperature decreased from 291 to 134 K. At this point the wedge angle changed suddenly, returning to a value of about 56 arc seconds. This is consistent with the teflon shrinking, and the screws losing their grip on the mirrors. From this temperature to a minimum temperature of 39.5° the wedge angle decreased slowly to 32.5°. Upon warming to room temperature, the instrument returned to its initial condition with a wedge angle of 63°.

The experimental results are summarized in Table I.

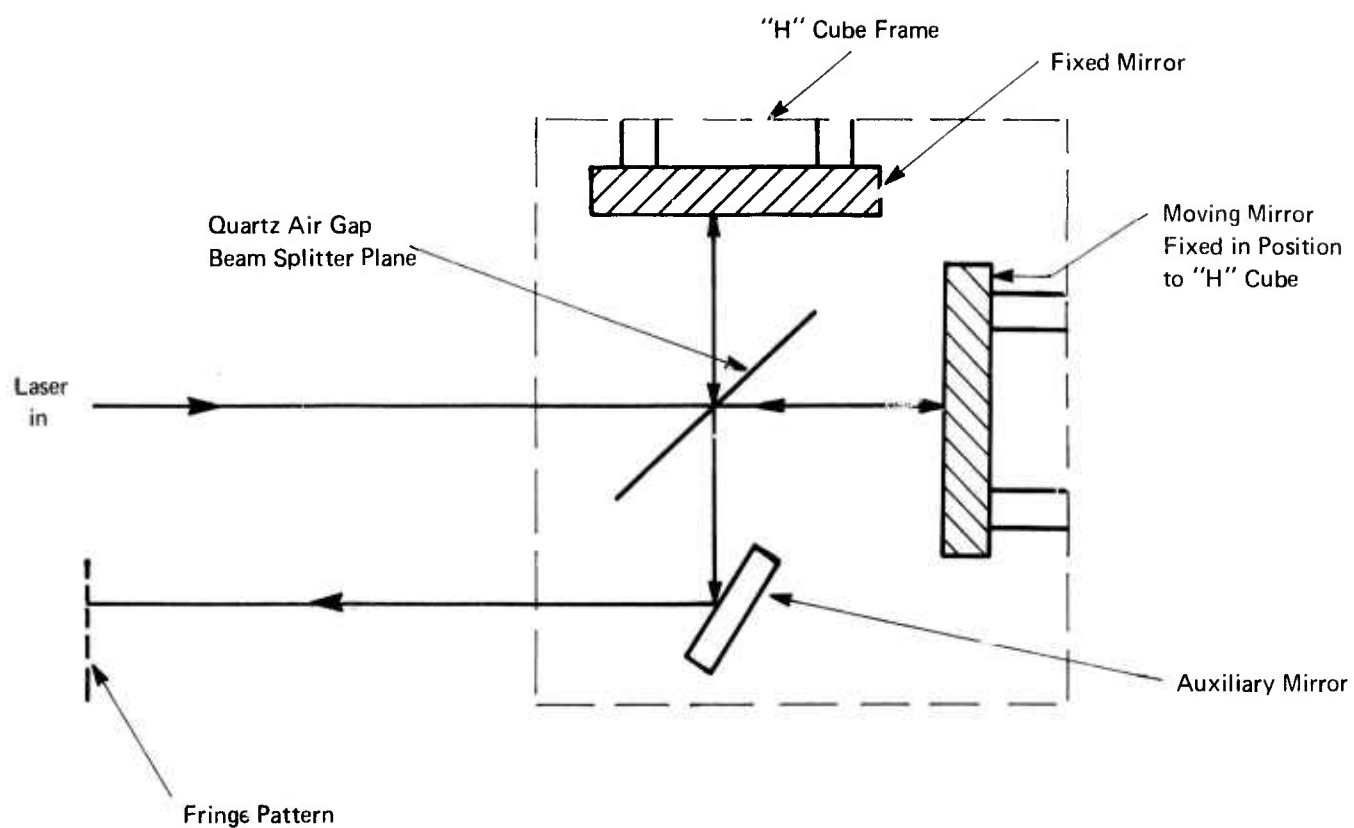
TABLE I

I²-CUBE - TEFLON WASHER EXPERIMENT

<u>Temp. K</u>	<u>Δ arc sec⁽¹⁾</u>
291	63
279	63
242	74
255	75
197	75
162	104
134	115
120	56
112	52
---	51
102	51.5
100.5	49
97	49
95	49
89	49
78	49
53	34.4
45	33.3
39.5	32.5
288	63

(1)

Δ measures from fringe pattern.



Note: "H" Cube located inside of thermal-vacuum test chamber during tests and laser and fringe screen located outside of chamber.

FIGURE 3.1.1.1 SCHEMATIC OF OPTICAL TEST OF H-CUBE

3.1.2 H-Cube with A-2 Steel Mirrors

An H-Cube with an air gapped quartz beam splitter mounted according to the A. D. Little design and A-2 steel metal mirrors was received, Fig. 3.1.2.1. The metal mirrors were mounted with three steel screws to three supporting pads. Belleville washers were located between the screw heads and the mirror front surface; in this case with the thermal expansion coefficients closely matched, the initial deflection of the Belleville washers probably was not critical. However, the mounting plates to which the mirrors were attached in turn mounted with three pads against a flat ground A-2 steel surface. Belleville washers and steel screws were used here as well. The screws holding the mounting plates were, however, torqued down hard so the Belleville washers were essentially flat.

The steel mirrors supplied with the H-Cube were of a very low quality. These mirrors had originally been prepared by ADL to test whether or not an optics shop could produce a good flat, highly reflecting surface on A-2 steel. Idealab had supplied us with 1 inch by 2 inch by 1/2 inch thick hardened and heat treated A-2 steel blanks, which we had sent out for polishing. The specification was "flat to a tenth of a wave over the center 1/2 inch of the mirrors, and flat to 1/4 of a wave over the center 5/8 inch". The mirrors, when received, were tested for spectral reflectivity and found suitable for use in the spectrometer. They were returned to Idealab, where a decision was made to attempt to use them in the test program even though they had been hardened. Three holes were bored in the mirrors to permit mounting them to the three pads using carbide tipped drills. Heat generated during the drilling operation, badly distorted the mirrors. When received at ADL (as determined after the cold tests) we found that one mirror was flat to about 1 fringe over something less than 1/2 inch zone in the center, while the better mirror was flat to 1 fringe over perhaps 3/4 inch near the center. Figure 3.1.2.2 shows hand-drawn sketches of fringe patterns observed in proof plate tests of the steel mirrors. The drilling process may also have caused phase transformations in the metal, effectively reversing in part the results of annealing the steel to helium temperature which is believed so important in obtaining dimensionally stable material for use in the cryospectrometer.

Because of the poor mirror quality it was not possible to make conclusive tests on the H-Cube with the autocollimator. To obviate this problem, a fringe pattern was used to monitor tilt in the H-Cube. There was a second difficulty with this unit. The beam splitter efficiency was very low, the air gap reflecting little more radiation than the surfaces of the plates. Consequently, three fringe fields were observed produced by reflection of the laser beam from the air gap surface in the beam splitter, as well

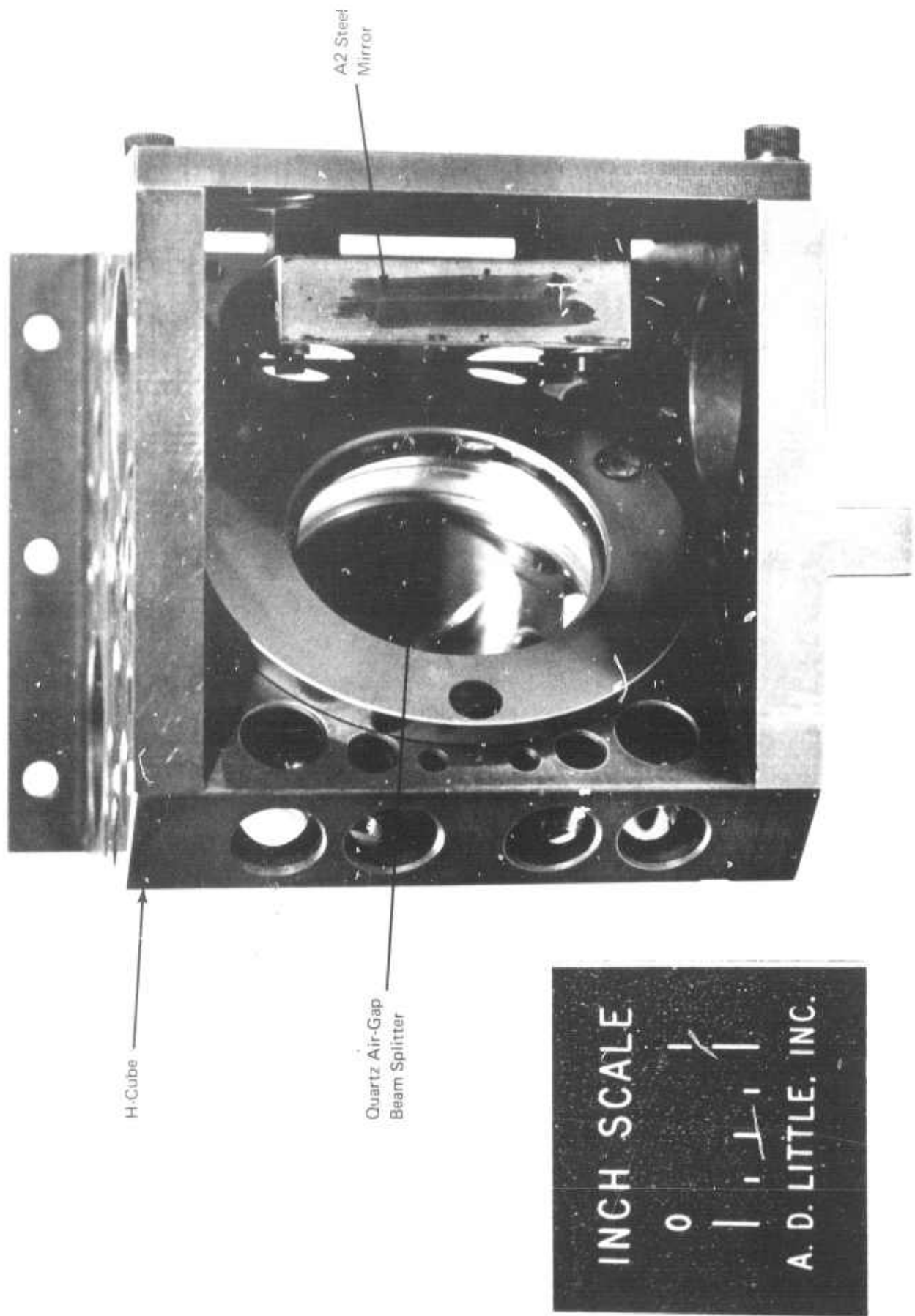


FIGURE 3.1.2.1 H-CUBE WITH A-2 STEEL MIRRORS (PHOTO 11334--4)



Mirror No. 1

At Best Central $\frac{1}{2}$ " Flat to 1 Fringe



Mirror No. 2

Estimate Central $\frac{1}{4}$ " Flat to 1 Fringe

Regular Spacing

FIGURE 3.1.2.2 STEEL MIRRORS – FRINGE PATTERNS FOR UNMOUNTED STATE

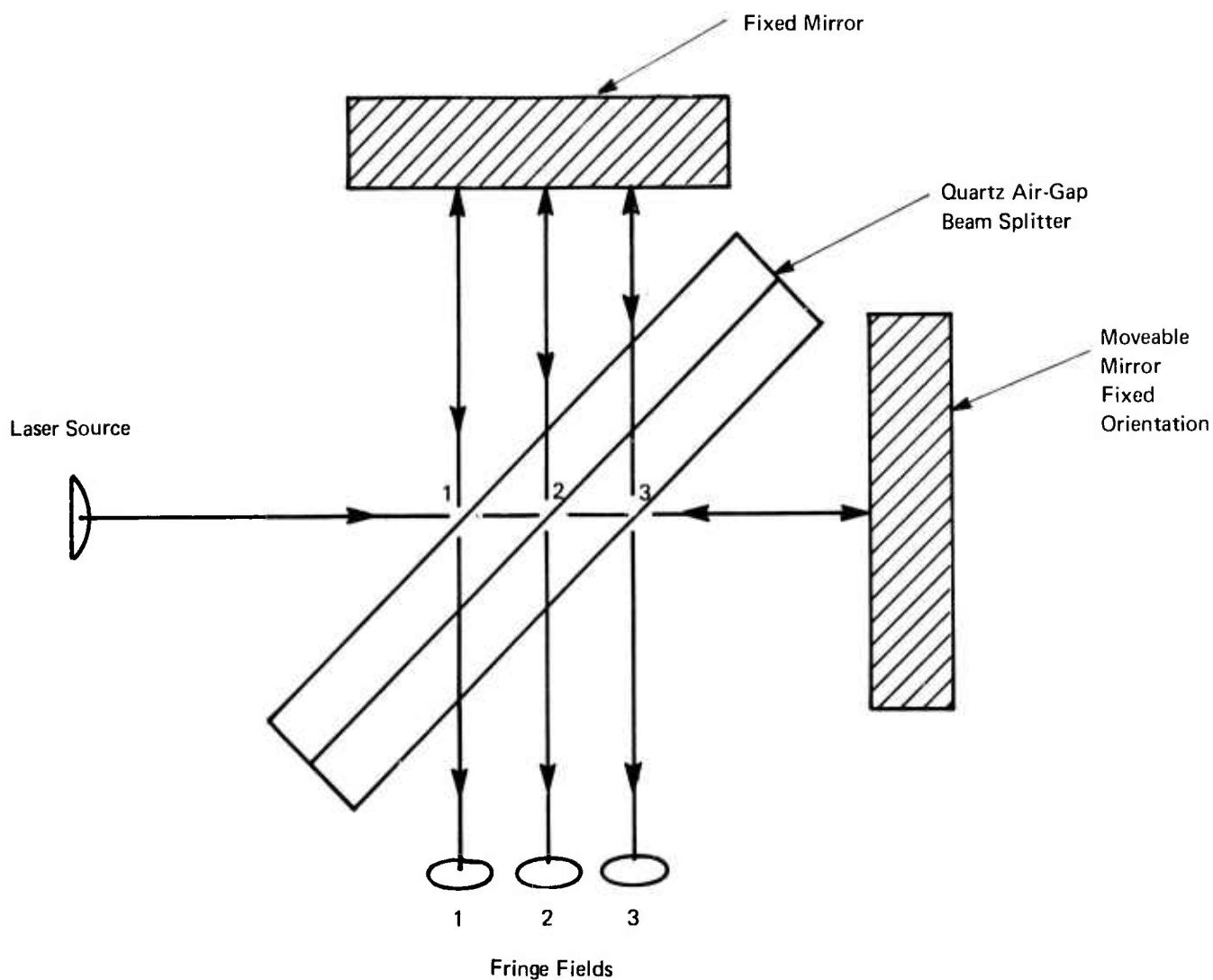
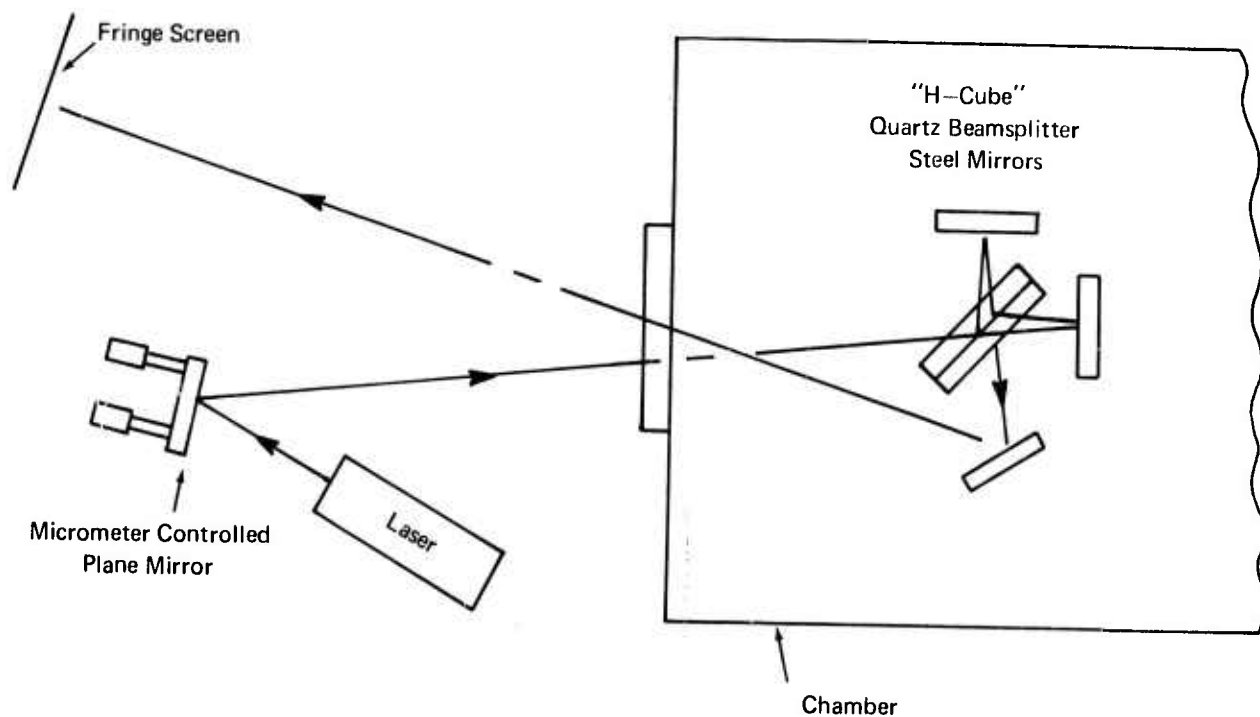


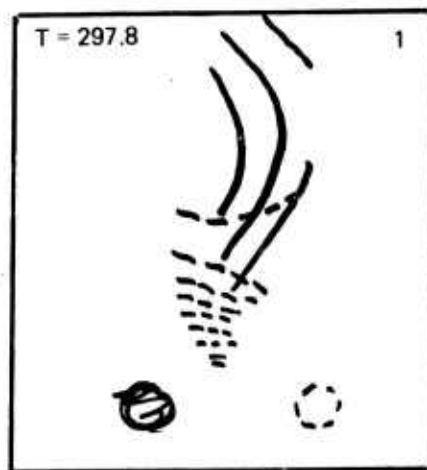
FIGURE 3.1.2.3 FRINGE FIELDS PRODUCED BY LOW EFFICIENCY QUARTZ AIR-GAP BEAM SPLITTER



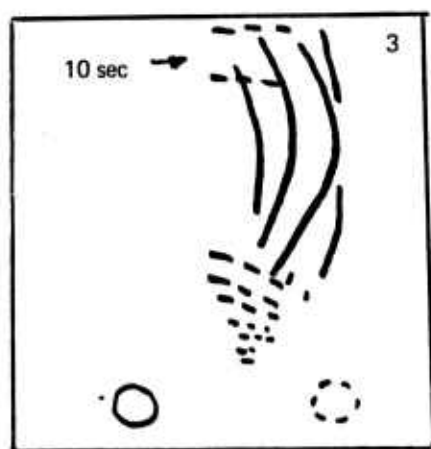
Poor Mirror Figure Rules Out Use of Autocollimator.
Tests Based on Fringe Pattern

FIGURE 3.1.2.4 H-CUBE CRYOGENIC-OPTICAL TEST ARRANGEMENT

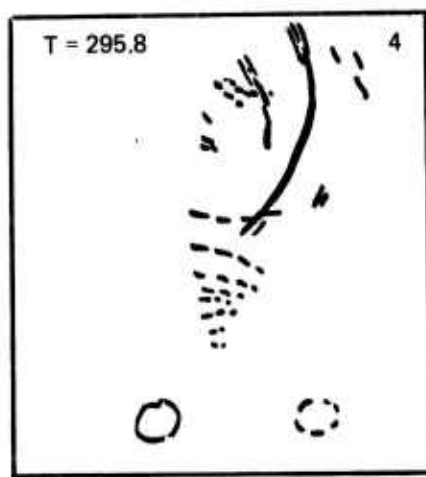
Initial Pattern



Start



Helium



Finish

Note: The solid lines are produced by reflection from the surface
1 Figure 3.1.2.3 and the dashed from surface 3 Figure 3.1.2.3.

FIGURE 3.1.2.5 H-CUBE WITH A-2 STEEL MIRRORS – SCANNED FRINGE PATTERNS

as from the two free quartz surfaces, Figure 3.1.2.3. The three fringe fields would overlap if the entire aperture of the instrument were filled. This together with the contoured appearance of the fringe fields produced by the low quality mirrors completely precluded any interpretation working with a filled aperture. To get around this problem, we used a pencil laser beam that was scanned in a reproducible manner, using a micrometer controlled mirror, Fig. 3.1.2.4, and traced the fringe pattern on a card with a pencil, Figure 3.1.2.5. Working this way it was possible to identify each of the three overlapping fringe patterns and to trace out the pattern produced by reflection from any of the three beam splitter surfaces.

In spite of these difficulties, we were able to carry out reasonably conclusive liquid helium tests of this unit. The results show that the cube maintained alignment within about 10 arc seconds on cooldown from room temperature to liquid helium temperature. Furthermore, the cube returned to very nearly its initial condition on rewarming to 300 K. Figure 3.1.2.5 shows fringe patterns initially before cooling, at helium temperature and at the conclusion of the experiment with the system again at room temperature.

3.2 Optical Tests of H- Cube Before and After Vibration

The same arrangement for measuring the fringe field of the H-Cube Figure 3.1.2.4 was used to determine the state of the instrument before the vibration tests. The experiment was repeated after the vibration tests and it was determined that a 40 arc second tilt had developed in the instrument. This was confirmed using the autocollimator. With such a large tilt, even with the poor image quality resulting from the distorted mirror surfaces, it was possible to use the autocollimator.

We undertook to determine the probable cause of this 40 arc second tilt. This was done by carefully disassembling the instrument. The screws on plate #2 were loosened and then retightened. The cube returned to very near its original condition. This was repeated with plate #1 with the same results. Plate #2 was then removed, the screws under the mirror loosened and then retightened, and plate #1 replaced. The cube returned very near its original condition. Finally the same procedure was repeated with plate #2 and mirror #2. It appeared from these tests that the Cube had developed a permanent change accounting for the 40 arc second wedge. We then removed both plates and both mirrors and cleaned the mirrors and the mounting plates with alcohol. The Cube was then reassembled and a 100 arc second tilt was observed. This tilt remained with ± 10 arc seconds on repeated disassembly and reassembly of the instrument. The change from 40 to 100 sec wedge was probably due to dirt under one or more of the pads of the instrument. It is very likely that the presence of this dirt also accounts for the wedge that developed during shake.

The beam splitter was then disassembled and reassembled and the cube was found to return to the same condition observed after cleaning of the mirrors and mounting plates. Throughout the vibration tests the beam splitter, as evidenced by the white light fringe pattern in the air gap, remained very stable. At the beginning of the shake 6 - 8 fringes of a given color could be observed. Interestingly these fringes could be observed during the actual vibration, except at very low frequencies where the physical displacements of the cube were so large as to preclude visual observation. During vibration the number of fringes of a given color decreased from about 6 to about 4, indicating that the vibration held the two halves of the beam splitter. After disassembly and reassembly, 9 fringes of a given color were observed. Two days later this number had decreased to 7, indicating that the beam splitter and mount were reasonably stable.

Upon disassembling the H-Cube after the vibration tests we discovered that we had not been supplied with a timely non-adjustable system. There were 3 pads on each of the mirror support plates for mounting to the cube. According to previous discussions with Idealab, it had been agreed that these three pads would be machined co-planar. On plate #1, we discovered that one of the pads was approximately two thousandths of an inch lower than the other two. Thus when the other two pads were held down with screws, the screw pressure on the third pad could be used as an adjustment, the plate effectively acting as a spring. This arrangement was very unfortunate and together with the poor mirror quality, effectively ruled out the possibility of performing a conclusive test on the thermal and probably vibrational stability of the H-Cube.

3.3 Mechanical Tests of H-Cube

In this series of mechanical environment exposure tests, an H-Cube with metal mirrors was used.

The testing sequence consisted of the following:

- A. Lateral, X and Y directions - 1 g sweeps to 3000 HZ were made to determine natural frequencies and mode shapes followed by a 5 g exposure, 20-2000 HZ. This was followed by a repeat of the 1 g sweep at the most sensitive location in the cube to establish the repeatability of the structural response. If the response was identical to the prior 1 g sweep, it was assumed that no major structural changes had occurred.
- B. Thrust, Z, direction - the same procedure was used as for the lateral directions. In addition there were 1 g sweeps after successive exposures of 15 g and 25 g.

The primary result was that the mirror and mirror holders exhibit a natural frequency of 1600 to 1750 HZ. As such, the entire structure is excited at this frequency. Amplification is 12, so during the 5 g

exposure, the mirrors experience between 60 and 70 g in either lateral direction. Extrapolating the results of a 1 g sweep, where the beam splitter surface was instrumented, it can be concluded that this optical element also experiences 60 to 70 g and the entire structure is being driven by the resonating mirrors. The response of one of the mirrors is shown in Figure 3.3.1.

In the thrust, or Z direction, the character of the resonances is the same as in the lateral directions because of the obvious symmetry. There was, in addition, a specimen-to-fixture-to-shaker core natural resonance at 2200 HZ, Figure 3.3.2 shows the response of the edge of mirror No. 1, during the 25 g input. Discernible is the mirror resonance at 1600 HZ. Again, the beam splitter surface was not instrumented because of the possible hazard of damage to the quartz surface should the accelerometer become loose at high acceleration levels. Mirror No. 1 has an acceleration of 140 g at 2000 HZ, not unlike the levels that might be expected of a cube mounted on an interferometer base. The rerun 1 g sweeps indicate that minor, if any, changes in the structure occurred.

From a purely structural point of view, fatigue and maximum mechanical stress, the components appear to function in an acceptable manner. The results of the functional optical examination are reported elsewhere.

An examination of the mirror holder plates indicates that lower weight and higher stiffness (and consequently higher natural frequencies) could be achieved with relatively simple modifications.

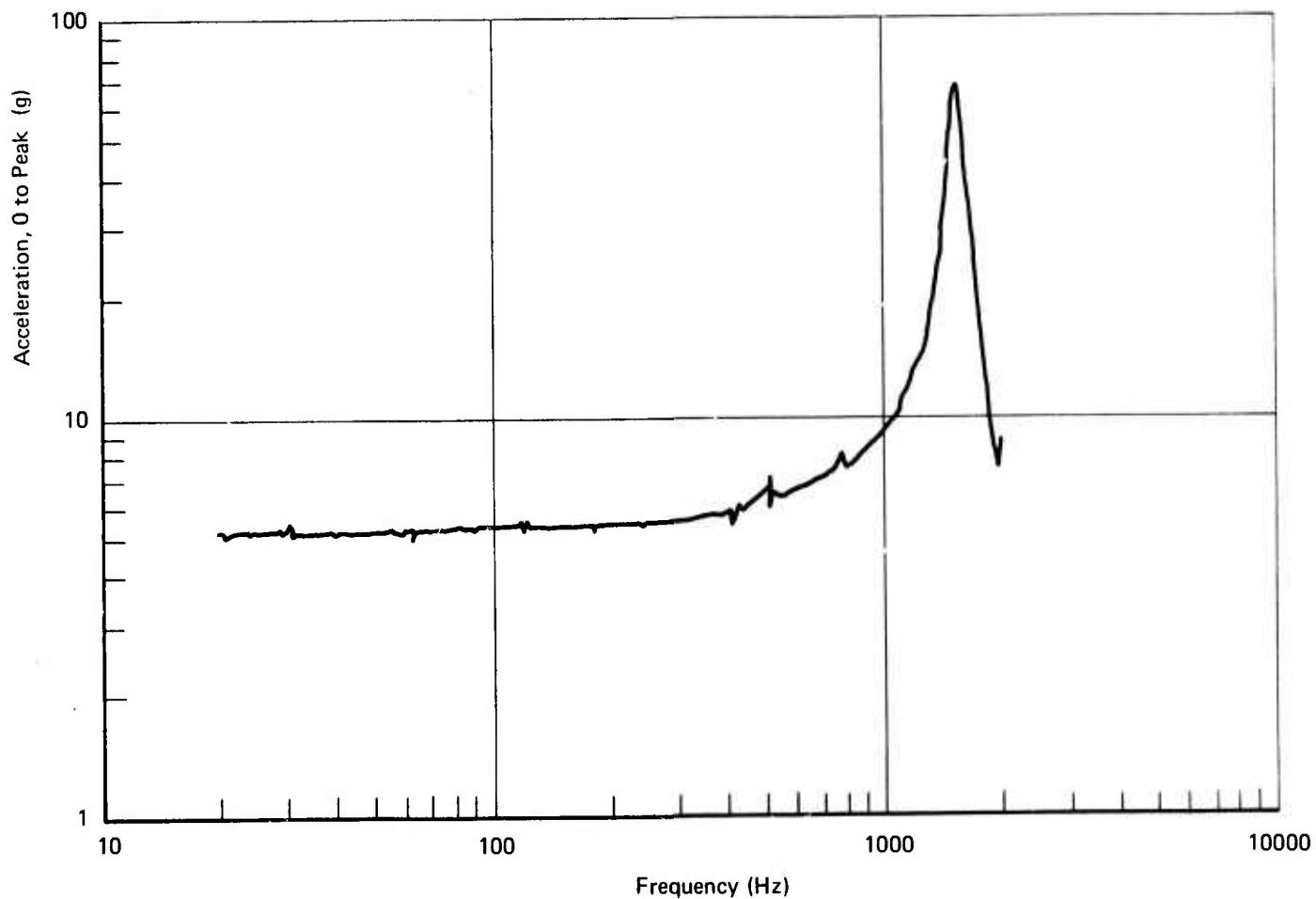


FIGURE 3.3.1 MECHANICAL ENVIRONMENT TESTS OF H-CUBE, X INPUT, 5 g, LOCATION 2

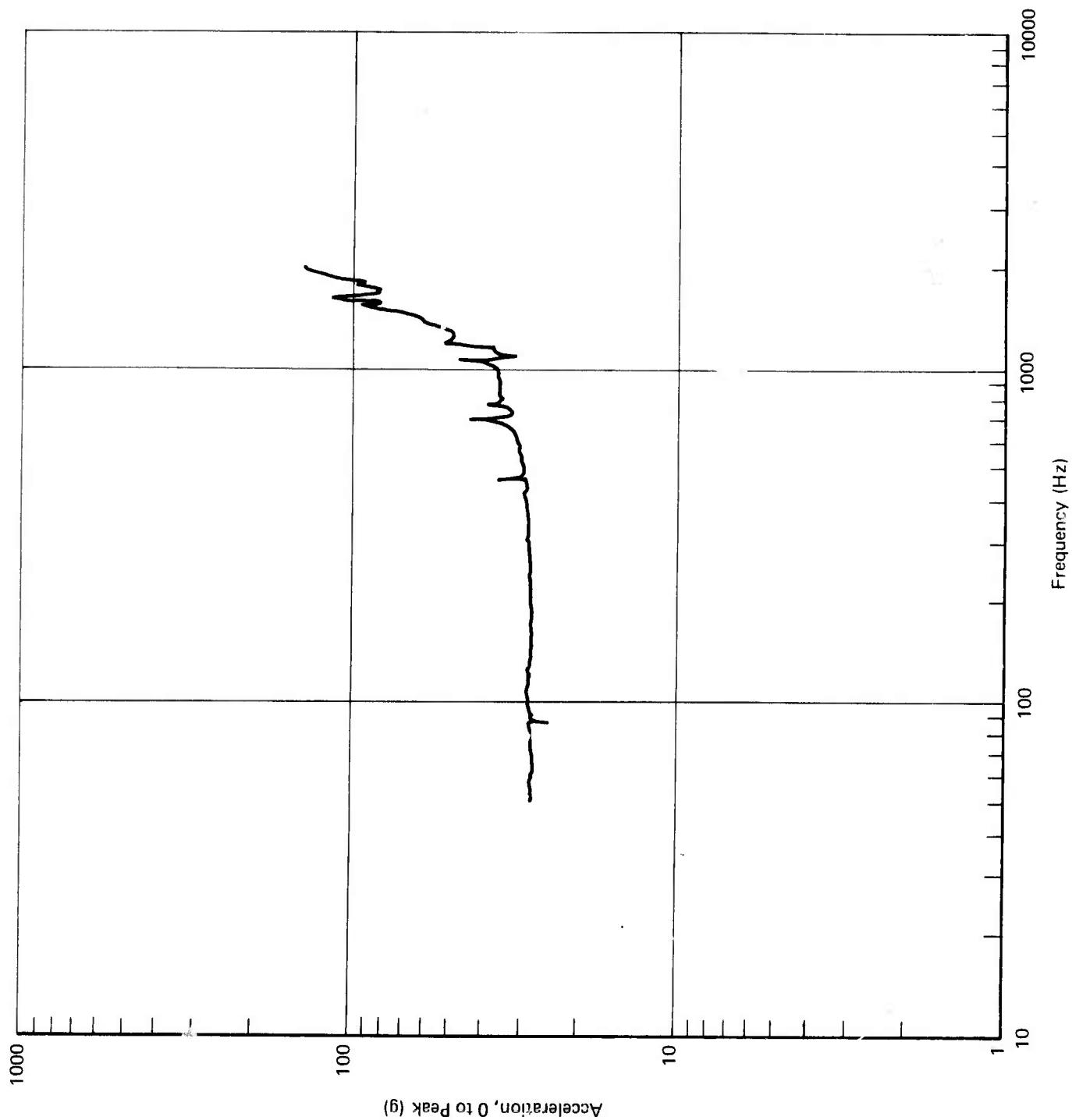
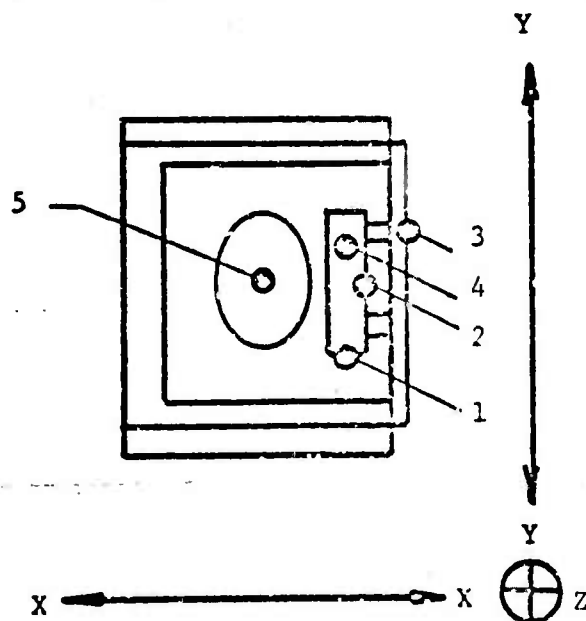


FIGURE 3.3.2 MECHANICAL ENVIRONMENT TESTS OF H-CUBE, Z INPUT, 25 g, LOCATION 4

TABLE 3.1

SUMMARY OF PERTINENT VIBRATION
RESULTS OBTAINED WITH H- CUBE

<u>Run No.</u>	<u>Input Axis</u>	<u>"g" Input</u>	<u>Acc Position</u>	<u>Meas "g"</u>	<u>Amp</u>	<u>Remarks</u>
1	Y	1	1	12	12	1750HZ
5	Y	5	1	60	12	1750HZ
6	X	1	2	26	26	1600HZ
7	X	1	3	24	24	1600HZ
8	X	1	5	10 14	10 14	X-Z } 1600HZ X
9	X	5	2	60	12	1600HZ
10	X	1	2	26	26	1600HZ
11	Z	1	4	~7	7	2000HZ
13	Z	5	4	31	6	2000HZ
14	Z	15	4	120	7.5	2000HZ
15	Z	1	4	~7	7	2000HZ
16	Z	25	4	140	5.6	2000HZ
17	Z	1	4	~7	7	2000HZ



View along flight axis looking into Interferometer entrance aperture

3.4 Low Temperature Tests of Prototype V-Cube Interferometer

A complete V-Cube interferometer spectrometer was received from Idealab for test to liquid helium temperature. It was indicated that the instrument had successfully survived cooldown to liquid nitrogen temperature in their test chamber.

The V-Cube instrument was equipped with an air gap quartz beam splitter and mount similar to that used in the V-Cube and front surface pyrex mirrors. The pyrex mirrors were attached to their pads with steel screws with Belleville washers. The Belleville washers unfortunately had not been properly set but were almost completely flattened out at room temperature. Consequently on cooldown, due to the differences in the expansion coefficients of steel and the pyrex, a controlled load was not maintained. Rather the mirrors were subjected to a continually increasing load as the temperature decreased. That eventually became very large, distorting the mirror. The fixed mirror was mounted to a plate which was in turn mounted to the side of the V-Cube with screws in a push pull arrangement rather than the preferred arrangement of mounting securely against co-planar pads. Low temperature tests, Figure 3.4.1, were performed using an autocollimator and observing the two sets of images of the cross hairs, one produced by reflection from the moving mirror, and the other produced by reflection from the fixed mirror, Figure 3.4.2. The air gapped pyrex beam splitter supplied with the instrument was very inefficient, transmitting far more radiation than it reflected. Consequently, it was necessary to use an apodizing stop mounted on the moving mirror to approximately equalize the brightness of the two images.

The cube went badly out of alignment on cooling. Initially there was no tilt within the accuracy of our measurement about a vertical axis through the cube and about 8 seconds of tilt about a horizontal axis. On cooling to nitrogen atmosphere, the tilt about the vertical axis remained zero, but about the horizontal had increased to 63 arc seconds. At 10 K the vertical tilt remained zero arc seconds, while the horizontal tilt had increased to 71 arc seconds. On warming to room temperature, the vertical tilt remained zero arc seconds, and the horizontal tilt became 28 arc seconds. Thus, there was some hysteresis in the instrument. In addition to these tilts, there was evidence that the mirrors bowed at low temperatures. This is consistent with the Belleville washers not acting as springs and the quartz mirrors being held tightly by the mounting screws. The bowing was greater about an axis parallel to the plane of the mirror, and perpendicular to the long dimension of the mirror than about the axis perpendicular to the narrow dimension of the mirror as one would expect on the basis of relative stiffness.

Measurements were made of slide wobble at room temperature, at 80 K and 10 K and upon warming to 300 K. At all times slide performance was excellent. During stroking, slide wobble was less than 2 arc seconds, which is near the resolving power of our autocollimator.

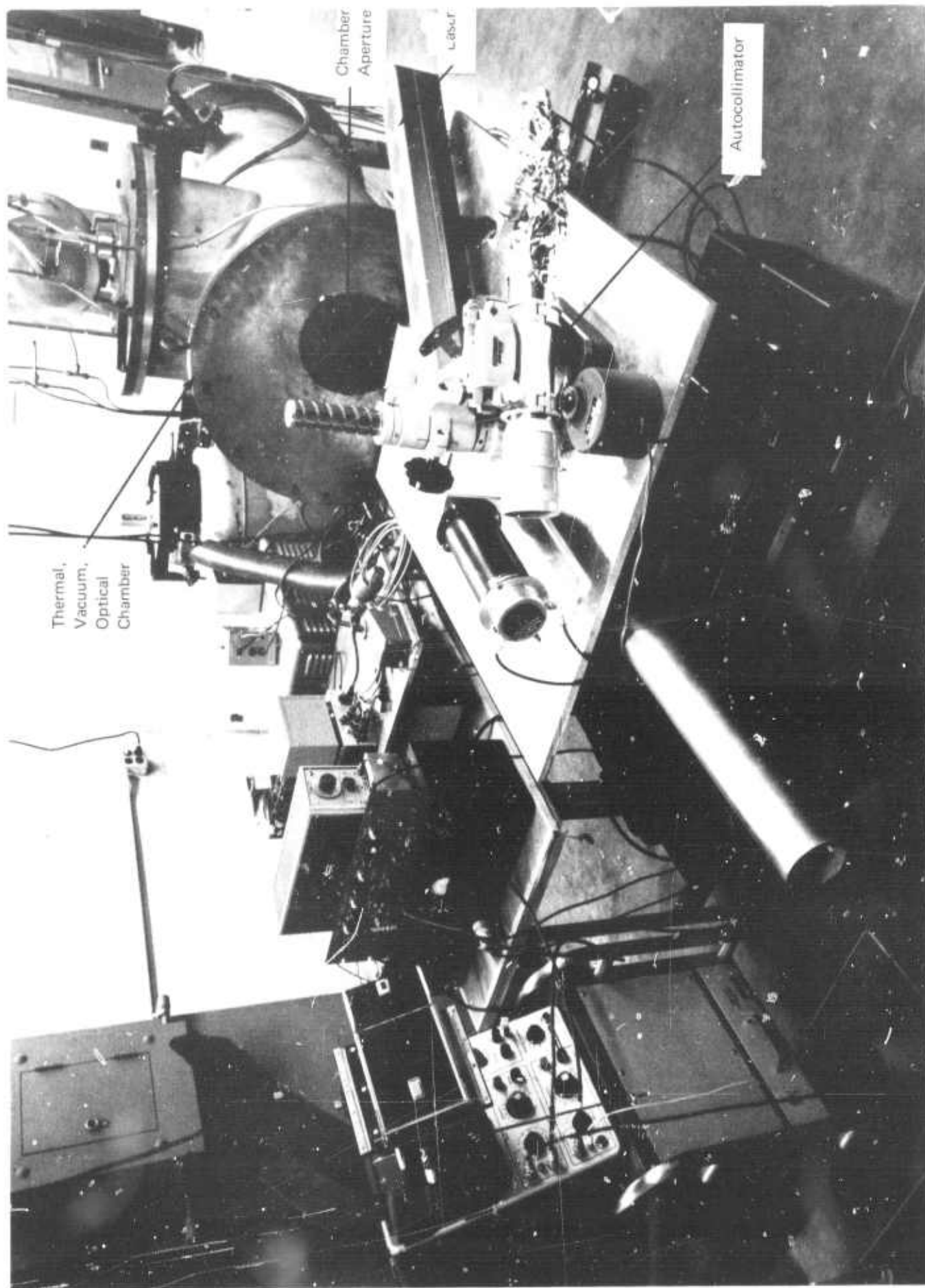


FIGURE 3.4.1 CHAMBER AND OPTICAL TABLE SET UP FOR V-CUBE TESTS

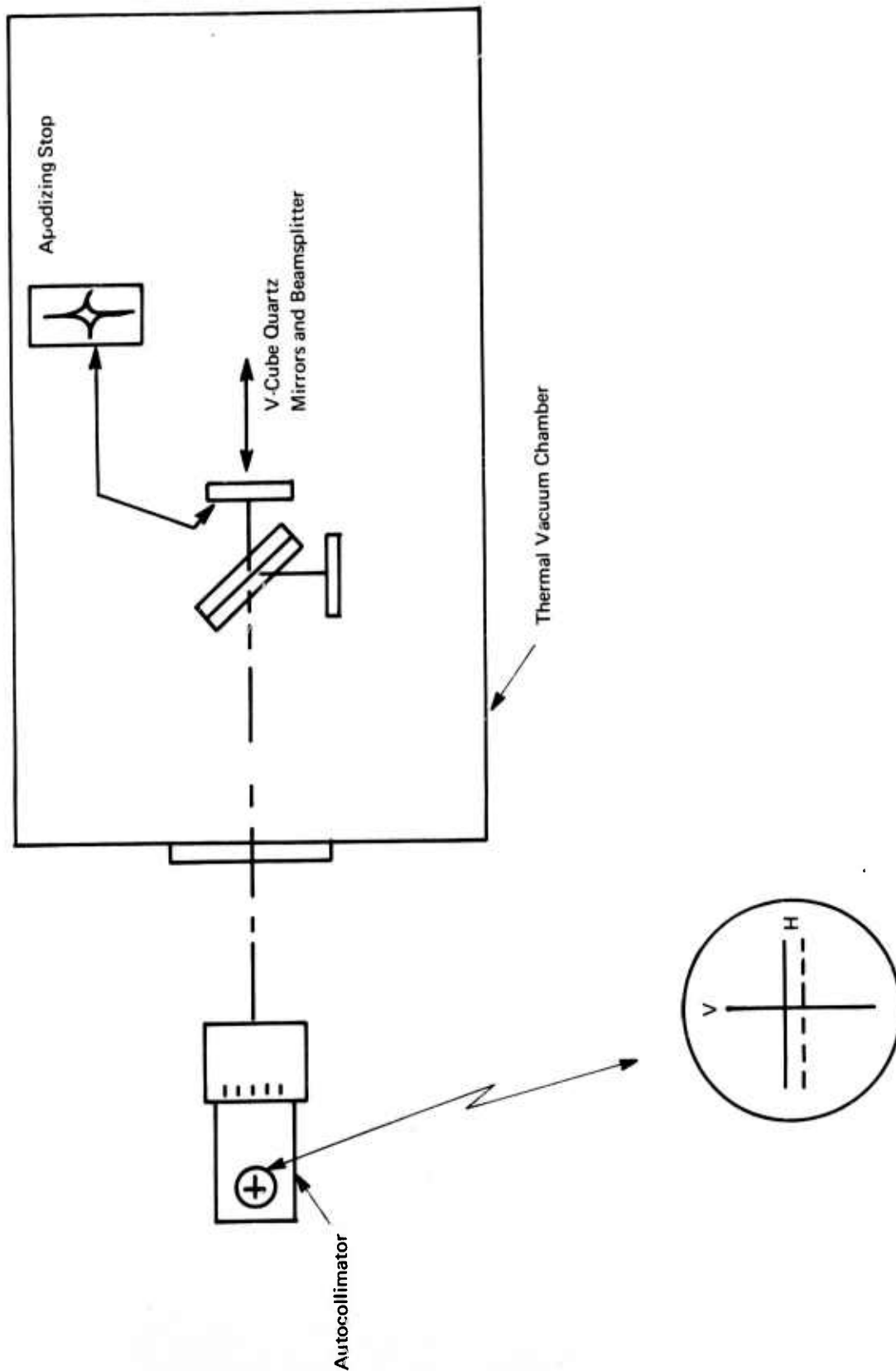


FIGURE 3.4.2 OPTICAL ARRANGEMENT FOR V-CUBE CRYOGENIC TESTS

3.5 Mechanical Tests of Prototype Interferometer

3.5.1 Room Temperature Test

With an interferometer instrument modified with motor-to-base stiffening members, we performed the following test sequence:

1. Both lateral directions - 1 g search to 2500 HZ
2. Flight direction (parallel to long dimension)
 - a. 1 g search to 2500 HZ
 - b. 5 g exposure to 2000 HZ
 - c. Functional test
 - d. 10 g exposure to 2000 HZ
 - e. Functional test
3. Both lateral directions, 5 g exposure to 2000 HZ, followed by a functional test
4. Flight direction, 25 g exposure to 2000 HZ, followed by a functional test.

In the lateral direction, Y, perpendicular to the plane of the balls of the slide, the first major resonance occurred at 700 HZ and was the first bending mode of the interferometer base and 1-1/2 inch thick fixture plate. Amplification was 5 at the input level of 1 or 5 g. The next significant resonance was at 1120 HZ. The mode shape was not determined exactly but the motor was rocking with an upper end amplification of 14; the aluminum cube, 24; and the moving mirror experienced an amplification of 30 to 40. Other resonances near 2000 HZ were observed also with high amplification, but the mode shapes were not defined. Figure 3.5.1 is shown as a typical response curve.

Parallel to the plane of the balls of the slide, X direction, the first resonance at 450 to 540 HZ consisted of general rocking with low amplification. The motor controlled the next resonance at 750 HZ with an amplification of 7.5 to 8. Figure 3.5.2 describes the 5 g exposure.

In the Z axis, or thrust direction, which is in line with the slide, the only resonance of interest is at 1150 HZ which was defined as a column resonance of the moving mirror, shaft, slide and motor shaft. (The motor coil was bolted to the motor magnet to simulate a clamp for use during launch.) The amplification was 10 with an input of 10 g resulting in 100 g acceleration level at the center of the moving mirror. Figure 3.5.3 illustrates this resonance.

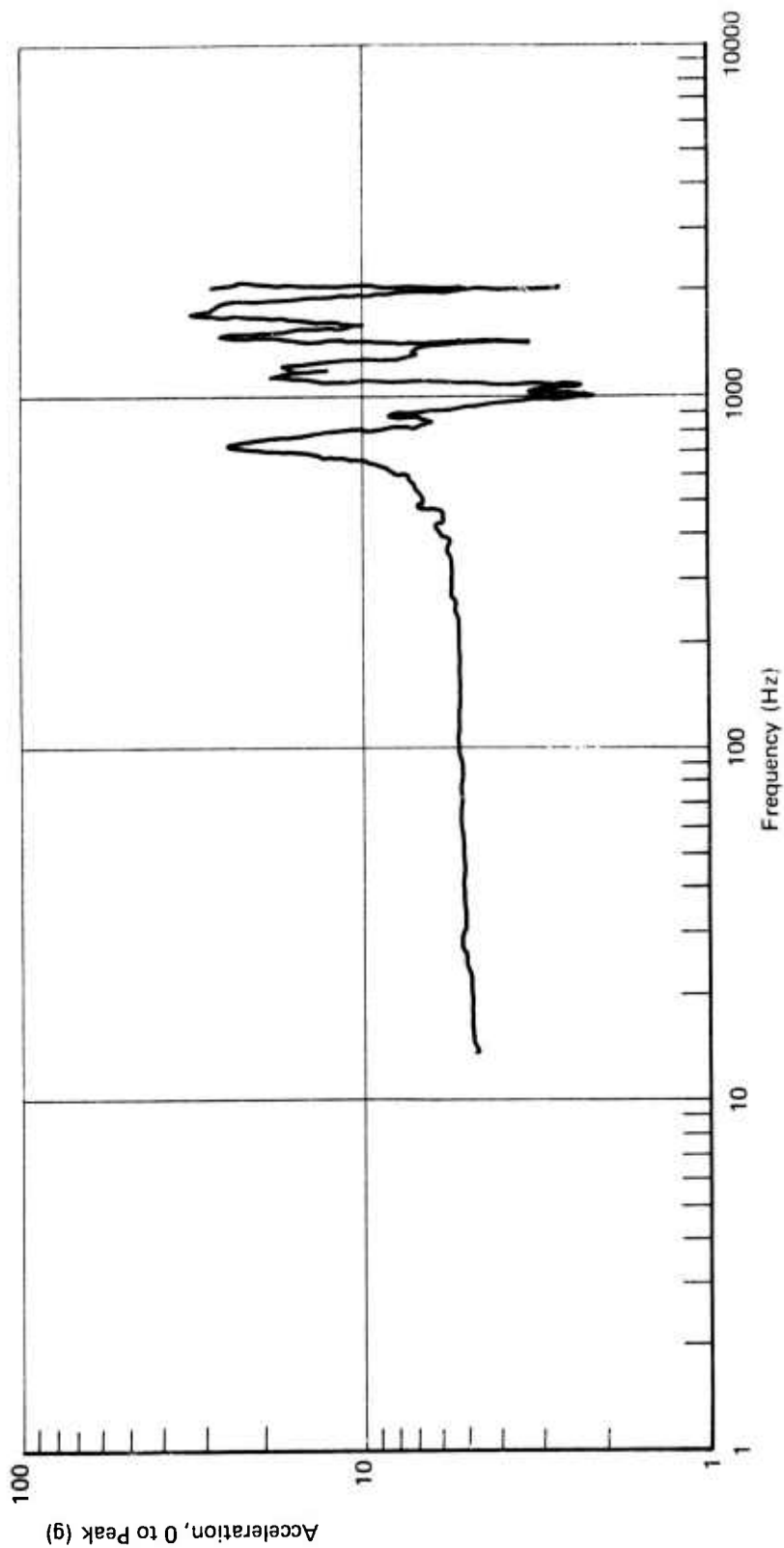


FIGURE 3.5.1 MECHANICAL ENVIRONMENT TEST OF V-CUBE INTERFEROMETER Y-AXIS INPUT, 5 g,
RESPONSE ON SLIDE NEAR CUBE

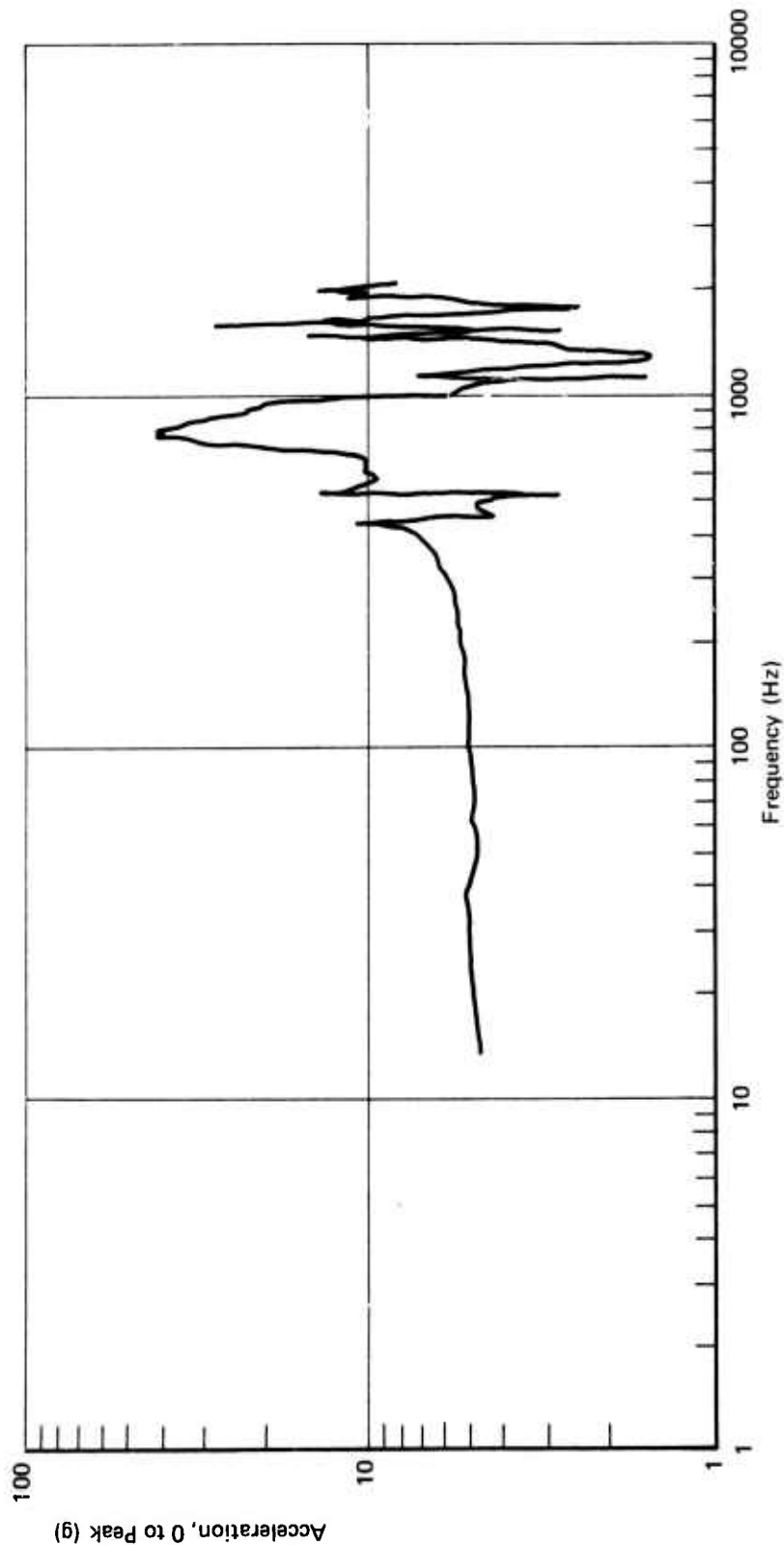


FIGURE 3.5.2 MECHANICAL ENVIRONMENT TESTS OF V-CUBE INTERFEROMETER, X-AXIS INPUT,
5 g, RESPONSE ON SLIDE NEAR CUBE

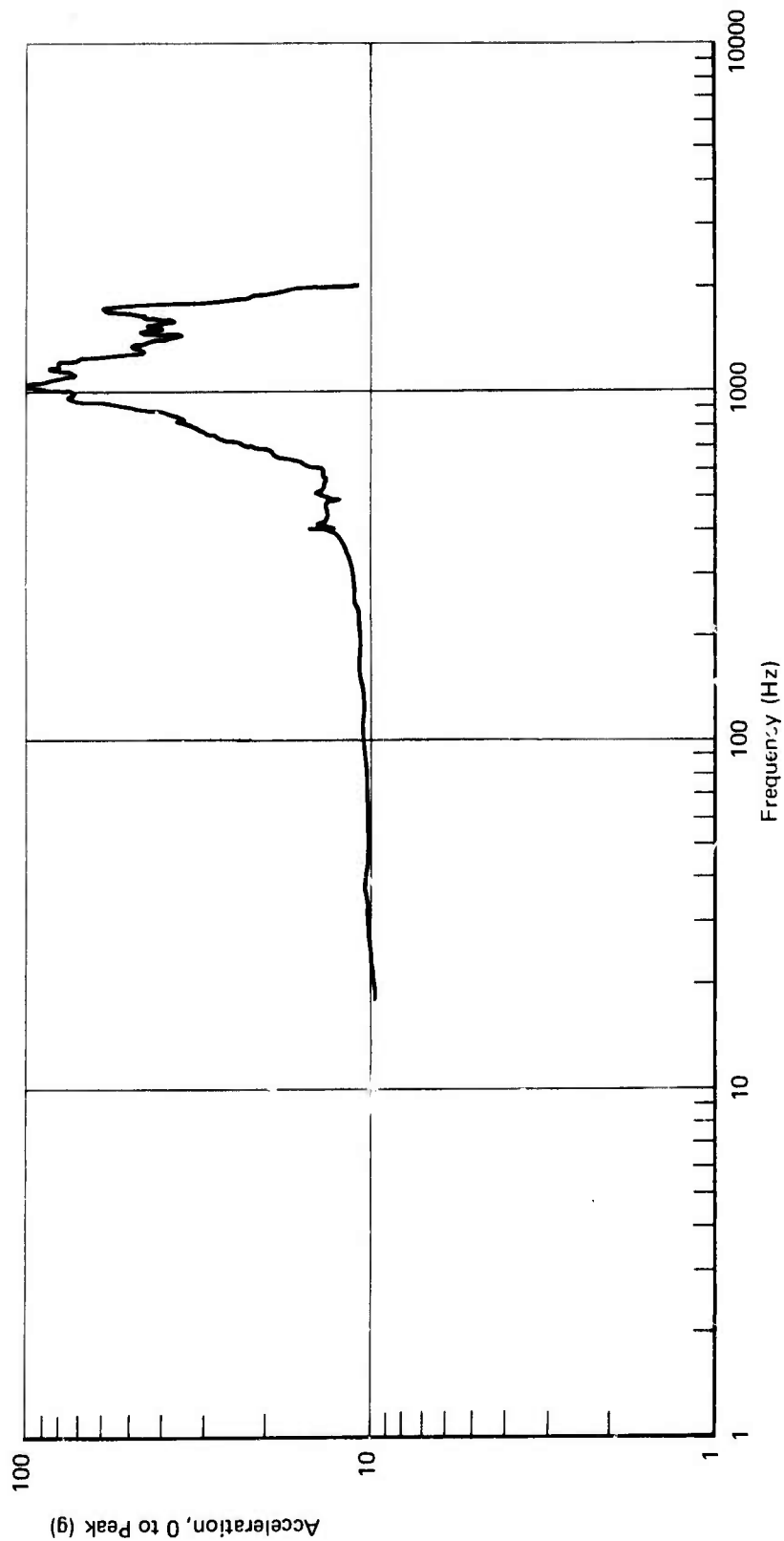


FIGURE 3.5.3 MECHANICAL ENVIRONMENT TESTS OF V-CUBE INTERFEROMETER, Z-AXIS INPUT,
10 g, RESPONSE ON MOVING MIRROR

At 25 g input in the thrust direction no response measurements were made due to the difficulty of attaching accelerometers at high levels. The amplification at the 1, 5, and 10 g inputs was extrapolated to be between 6.5 and 10 at the 25 g input. Hence, the acceleration level at the moving mirror is estimated to be between 160 and 250 g. The results of the functional tests after these exposures is reported elsewhere.

From these tests some conclusions with respect to the response of the structure to the mechanical environment were made. If the instrument is to preserve its usual configuration, stiffening members from the motor to the base are required. The moving mirror should have as rigid a connection as possible to the moving slide. Components attached to the basic structure (i.e., velocity sensor) must be fixed with the greatest possible rigidity. Acceleration levels of components of the interferometer (i.e., mirrors) will be quite high and consequently attention must be given to attachment means that will preserve alignment after such a severe exposure.

The problems of alignment far outweigh any stress or fatigue considerations. In essence the design must be based on the requirement for high stiffness.

3.5.2 Liquid Nitrogen Temperature

For this test a urethane foam box was designed to be placed between the interferometer (containing the instrument and liquid nitrogen) and the magnesium fixture plate. Because of shaker limitations, the instrument was exposed to only 10 g, 18 to 2000 HZ, in the axial direction and 5 g, 13-2000 HZ, in the plane of the balls of the slide. No accelerometer response measurements were made because of the low temperatures. The results of the functional tests after this exposure are reported in optical testing.

3.6 Interferometer Servo Response

The interferometer servo system response requirement may be treated from two points of view. First, one may consider the ability of the servo system to cause the output displacement of the interferometer mirror to correspond closely to the input electrical signal. Second, one may consider the ability of the servo system to prevent mechanical noise disturbances from causing unwanted motion of the mirror. The first consideration is the closed loop frequency response of the servo system while the second consideration is the open loop gain or stiffness of the system. These two points of view are not independent but are merely different ways of treating the same thing.

The desired (design goal) mirror motion of the interferometer is 2.0 complete back and forth cycles per second, with constant velocity within 1% during the scan. The minimum acceptable scan rate is 1

complete cycle per second. The frequency spectrum of this motion consists only of odd harmonics whose relative amplitudes decrease as the square of the harmonic number. For example, the amplitude of the fifth harmonic is only 4% of the fundamental amplitude. The eleventh harmonic is the lowest harmonic whose amplitude is less than 1% of the fundamental. To faithfully reproduce the input signal, the closed loop response should be good out to a frequency of 22 Hertz for the design goal of 2.0 mechanical cycles per second. A more conservative aim would be to have good closed loop response out to about the thirty-ninth harmonic since the sum of the amplitudes of all higher harmonics is less than 1% of the fundamental amplitude. On this basis the closed loop servo response should be good up to 78 Hertz. Good closed loop response means that the ratio of output to input as a function of frequency for sinusoidal input signals is constant to within +10% (+1db) and -30% (-3db). Limiting the frequency response to +10% ensures adequate damping and no ringing at the upper frequency limit of the servo system response.

Imagine that the interferometer slide is clamped so that it cannot move. In this condition there can be no displacement or velocity feedback. Now, compute the force produced for each volt of input from the displacement transducer. This open loop gain or stiffness is a measure of the ability of the servo to handle mechanical disturbances. Clearly the greater the force produced for a given displacement error indicated by the output of the displacement transducer, the more closely the servo can force the displacement to follow the input signal in spite of mechanical disturbances. Stiffness is a function of frequency. In the interferometer, velocity variations at frequencies much lower than the scan rate do not degrade the spectral resolution of the instrument. Therefore there is no need of stiffness at low frequencies except to overcome the force of gravity when the interferometer is operated vertically.

In a servo system, Figure 3.6.1, like that in the interferometer with strong tachometric feedback in a minor (inner) loop, the open loop response (stiffness) of the major (outer) loop tends to become inversely proportional to frequency. The closed loop response is flat out to the frequency at which the open loop gain is unity. Thus stiffness and frequency response are interdependent. Extending the frequency response to higher frequency automatically increases the stiffness of the system at lower frequencies.

The frequency response was measured on two interferometer servo systems. In the first test, both the open loop and closed loop responses were determined for the slide and servo system which were at ADL at that time for cold testing. Some overshoot and ringing were observed in the instrument at that time and the servo tests were made to try to identify the cause of these. The interferometer was operated at room temperature, and had no viscous damping.

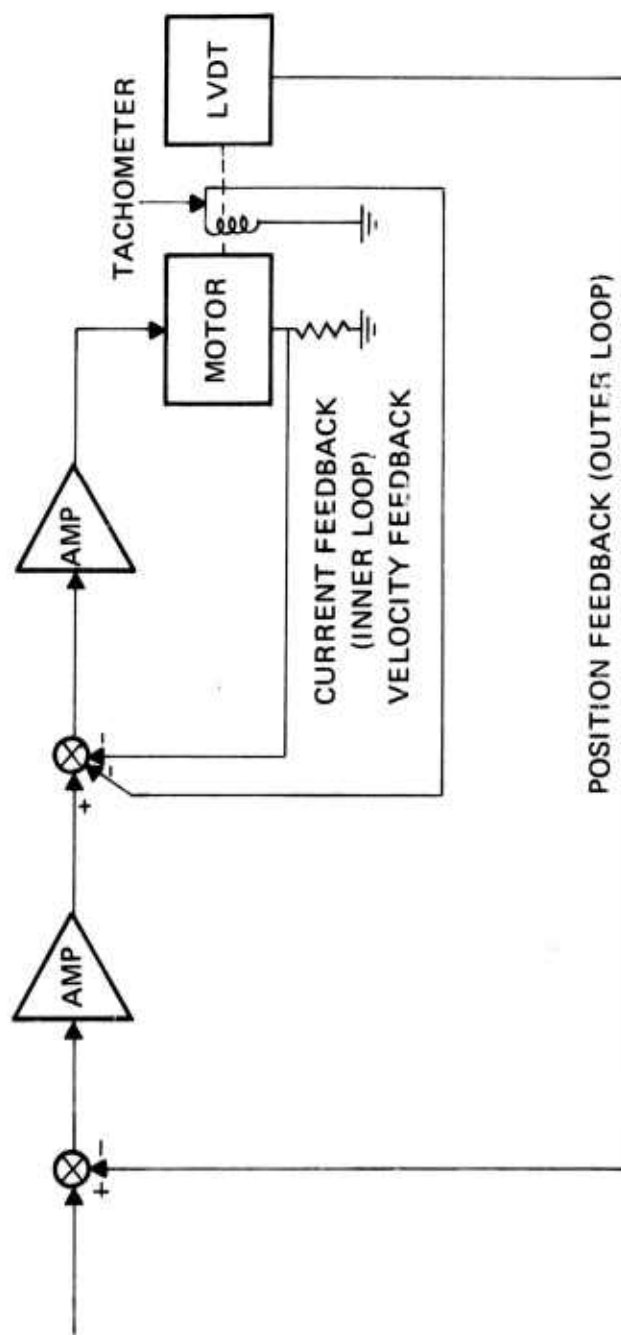


FIGURE 3.6.1 INTERFEROMETER SERVO SYSTEM – SIMPLIFIED SCHEMATIC

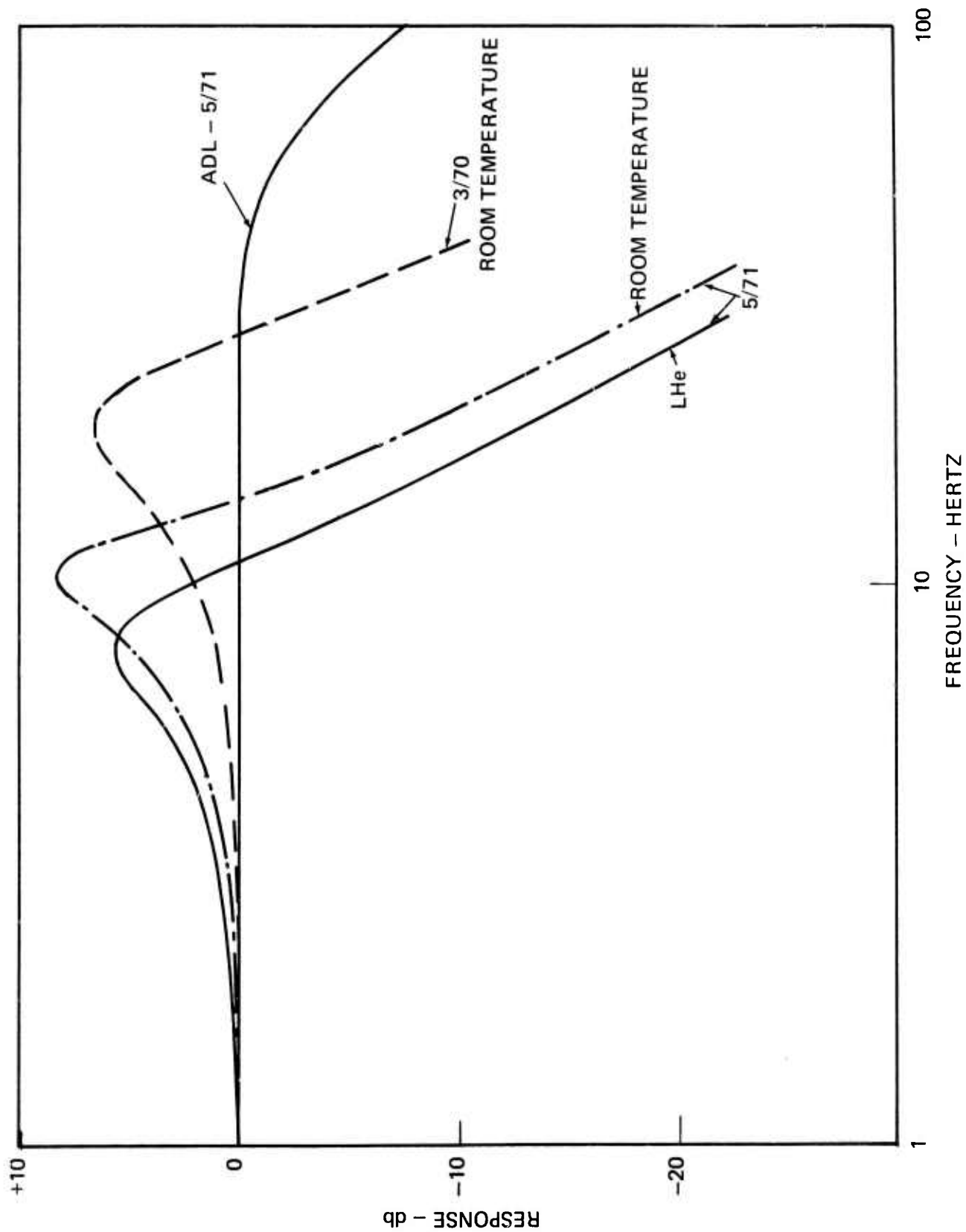


FIGURE 3.6.2 AMPLITUDE RESPONSE - INTERFEROMETER SERVO

In the second test, closed loop response tests were made on the instrument then undergoing cold tests at ADL, with measurements made at room temperature, liquid nitrogen temperature and liquid helium temperature since we had been informed that the servo had been optimized for low temperature operation. At a later date, some experiments were conducted with an Idealab Interferometer borrowed from AFCRL. The viscous damper was removed in order to make the mechanical system similar to that used in the cryointerferometer development program. Changes were made in the servo control circuits for both the inner and outer feedback loops in order to extend the frequency response and increase the loop stiffness. All servo measurements were made with an EMR Hatboro (Division of Weston) Model 1410 frequency response analyzer. The input test signal was inserted at the summing point of the first amplifier. The displacement transducer output was measured to obtain the closed loop response. The output of the first amplifier, the error signal, was also measured. The open loop response was obtained by treating this output as the input to most of the loop and adding the response of the first amplifier. The measured amplitude responses are compared in Figure 3.6.2. Note that between the first and second test periods servo response lost an octave in bandwidth and became more poorly damped. The following table summarizes the test results and compare them with the desired servo system response.

SERVO TEST SUMMARY

<u>Test</u>	<u>Peak Response (db)</u>	<u>Equivalent Damping (1%)</u>	<u>Frequency of Peak (Hertz)</u>	<u>Frequency of -3db Point (Hertz)</u>
<u>4/70</u>				
Room Temperature:	+6.6	24	19.5	32
<u>5/71</u>				
Room Temperature:	+8.3	19	10.5	16
Liquid Nitrogen Temp.	+6.3	25	8	13
Liquid Helium Temp.	+5.7	26	8	12.5
ADL Experiments 5/71	0	70	no peak	90
Desired response:	<+1.0	50 to 70	>50	>100

3.7 Slide Velocity Tests

A velocity constancy test set was designed and built as part of the interferometer development program. A block diagram of this instrument is shown in Figure 3.7.1. This tester has two input channels and can be used to measure the performance of the interferometer slide in a number of ways. The main input channel, the laser input, takes the a.c. coupled laser fringe signal from a photomultiplier, amplifies and

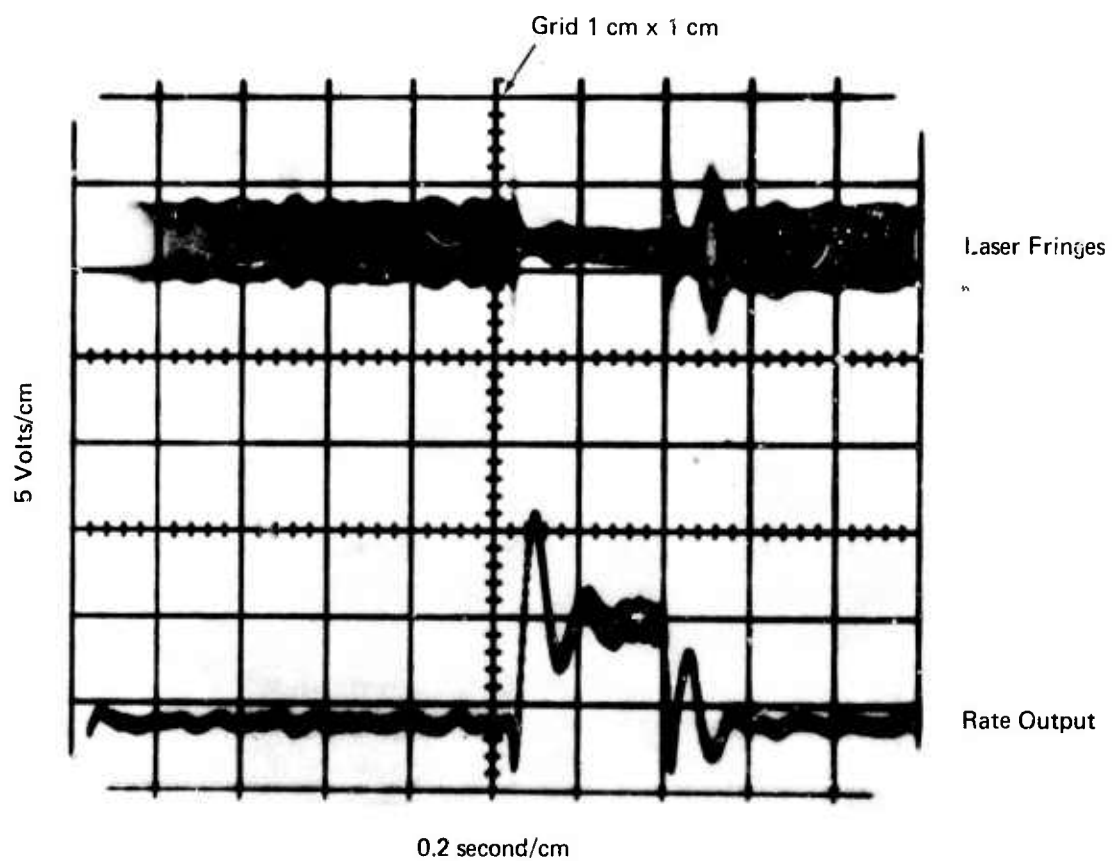


FIGURE 3.7.2 SLIDE VELOCITY TESTS AT LIQUID HELIUM TEMPERATURE

clips this signal. The signal is then differentiated and again amplified and clipped so as to produce pulses marking the positive going zero crossings of the laser fringe signal. These pulses trigger a monostable multivibrator producing standardized output pulses. Two outputs are now produced from the monostable output. The standardized pulses are integrated by a low pass filter to obtain the rate output, a signal proportional to the velocity of the interferometer slide as measured by laser interference fringes. The calibration of this output is 25 millivolts per kilohertz. Alternatively the monostable output is counted down by up to four flip-flop stages. The pulse output so obtained may be used to measure pulse to pulse jitter or high frequency velocity variations. The counter stages permit this type of measurement to be made for jitter averaged over two, four, eight or sixteen cycles of the interferogram.

The second channel in the velocity test set uses the tachometer signal from the interferometer servo. After amplification a delayed trigger is obtained from the tachometer waveform so that a selected portion of this waveform may be viewed in detail. An inhibit gate produced in the tachometer channel can be used to synchronize and control the laser fringe channel to examine the same selected portion of the scan.

The velocity constancy test set was used to test an interferometer slide delivered to us. Measurements were made at room temperature, liquid nitrogen temperature and liquid helium temperature. The rate output showed that overshoot and ringing at about 10 Hertz, which might be expected from the servo response. A 500 Hertz oscillation in the minor (velocity feed back) loop of the servo system was observed at liquid helium temperature. Figure 3.7.2 shows the laser fringes in the upper trace and the rate output in the lower trace for operation at liquid helium temperature. The vertical calibration is 0.5 volts/cm and the horizontal sweep speed is 0.2 second/cm. The ringing is obvious and the oscillation can be seen in the broadening of the velocity trace during the fly back portion of the scan. Pulse-to-pulse jitter measured in a .02 second portion of the comparatively flat part of the scan was approximately 10%, 20%, and 15% peak-to-peak variation for operation at room temperature, liquid nitrogen temperature and liquid helium temperature respectively.

The velocity constancy tests were concluded by recording the tachometer output and motor coil current with a strip chart recorder. Again the 10 Hertz overshoot and ringing due to the poor servo system characteristic were apparent. The velocity variations in the flat part of the scan are about 15% peak-to-peak for room temperature operation.

The same curves for liquid helium temperature operation show slight increases in both friction and roughness of the stroke by the changes in the current trace. These changes are insignificant and show that the slide performed well both cold and warm. The velocity trace shows

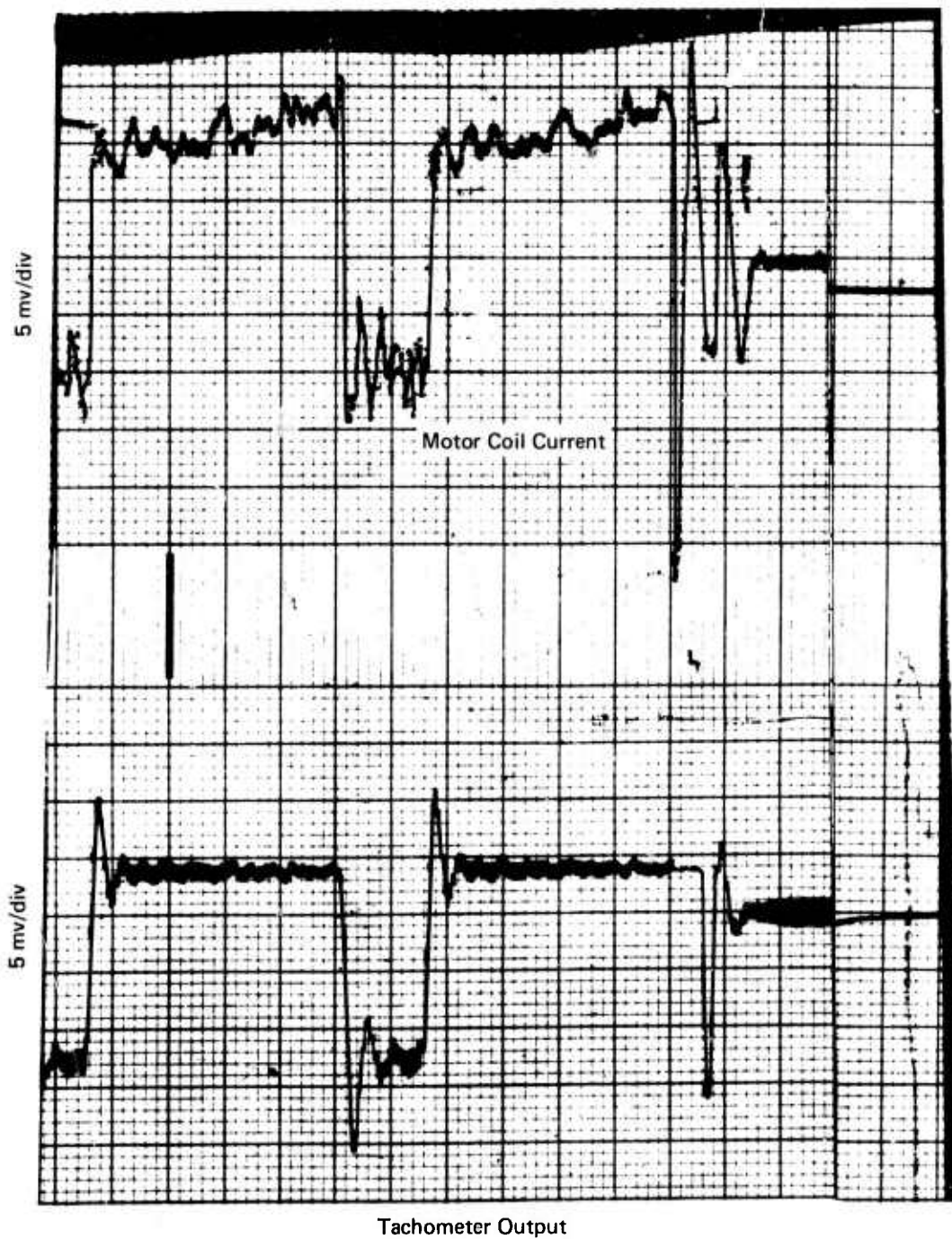


FIGURE 3.7.3 SLIDE VELOCITY TESTS, LIQUID HELIUM TEMPERATURE

slightly less ringing at low temperature as the result of decreased gain in the servo system. A typical curve for liquid helium operation is shown in Figure No. 3.7.3 in which the upper curve is the motor coil current recorded at 2 mv/div., the lower curve is the tachometer output at 5 mv/div. and the time base is 20 div/sec. The oscillation in the minor loop is shown by the wide trace of the tachometer output.

A full and proper evaluation of the slide could not be made because of the poor performance of the servo system.

3.8 Monochromatic Fringe Reference

An experimental program was undertaken to determine if cooled, gallium arsenide, solid state, laser diodes could be used as a fringe reference source for the cryointerferometer. The following experimental arrangement was employed. A glass helium dewar guarded with liquid nitrogen was used as a cold chamber. The laser diodes studies were attached to the end of a probe that could be immersed in the liquid helium. Radiation from the diodes was conducted out of the dewar through a flexioptics light pipe to the entrance slip of a Jarrell Ash .5m Ebert spectrometer with a 590 groove per mm grating. The resolution for this instrument is better than 14 Å in first order. The output of the spectrometer was monitored with an S1 photomultiplier and recorded by strip chart recorder.

Three different types of laser diodes were studied. These were an IBM diode, specifically designed for high-power cw operation procured previously under a NASA program, a Laser Diode Laboratory LD-22 diode, and an RCA 7606 diode. The IBM diode exhibited a rather broad emission band clearly unsuitable for the proposed application. Furthermore, the emitting wavelength was relatively insensitive to the current applied to the diode, Figure 3.8.1. The Laser Diode Laboratory LD-22 was somewhat better, exhibiting multimode emission. However, the modes were not clean, but relatively broad and overlapping. The emitted wavelength showed some dependence upon current through the diode, Figure 3.8.2.

The emission characteristics of the RCA diode were very much superior to those of the other diodes studied. Particularly near threshold very clean multimode operation was observed. The modes were spaced approximately 2.7μ apart, and the spectral width of individual modes was less than the resulting power of the instrument, that is less than .4 Å, Figures 3.8.3 and 3.8.4. Consequently the diode is suitable for use as a fringe reference source from the point of view of coherence length or monochromaticity. In addition to the clean emission characteristics, the diode could be temperature tuned, that is, the emission wavelength of any given mode varied depending on the current applied to the diode. For the strongest mode, this variation was from about 8,505 to about 8,590 μ as the current was increased from the threshold value of about 100 milliamperes to 500 milliamperes. Table 3.8.1 presents our results.

TABLE 3.8.1

SUMMARY OF LASER DIODE TEST RESULTS

IBM (special)				
$I, (mA)$	λ	$\Delta\lambda$	rel. energy	Notes
90	8420	100	-	Not lasing
--	8413	10	-	Lasing, wide slit
200	8410	5	-	30 μ slit. Noisy emission on wings of peak, $f \approx 160$ Hz first seen. Threshold ~ 130 mA
300	8425	6	2.7	--
200	8412	5	1.8	--
150	(8418)	-	.7	Very broad trashy spectrum
150	8411	-	-	Very broad trashy spectrum
1000	8412	15	-	" = multimode
Spectrum explored, using wide slits, from 1.6 μ to .3 μ and no emission found except the .84 line.				
200	-	400	-	Wings of line at high gain extend this far
Mode spacing apparently around 1.6 \AA				

RCA 7606				3 x .08 MILS
$I, (mA)$	λ	$\Delta\lambda$	rel. energy	Notes
200	8516 8517.5	$\sim .3\text{\AA}$	-	slitwidth .10 μ , inst. limit .4 \AA (but seem to get .3 \AA)
500	8588	$\sim .3$	-	Honks at ~ 160 Hz
1000	-	-	-	No output - overheated?
300	8532	$\sim .3$	-	[Hotter is redder]
150	8511	$\sim .3$	-	
110	8509	-	-	
98	8508	-	-	
92	8506	-	-	Threshold ~ 91 mA
Mode Spacing 2.75 \AA				

Laser Diode Laboratories LD - 22 Heterostructure 6 Mils Wide x junction thickness

150	8526	-	-	Threshold ~ 150 mA
200	8533	$\sim .3\text{\AA}$	-	Honk at ~ 160 Hz
300	8532	-	-	Multimodes cover 8507 to 8537 \AA
180	8526	-	-	
Mode Spacing 1.05 \AA				

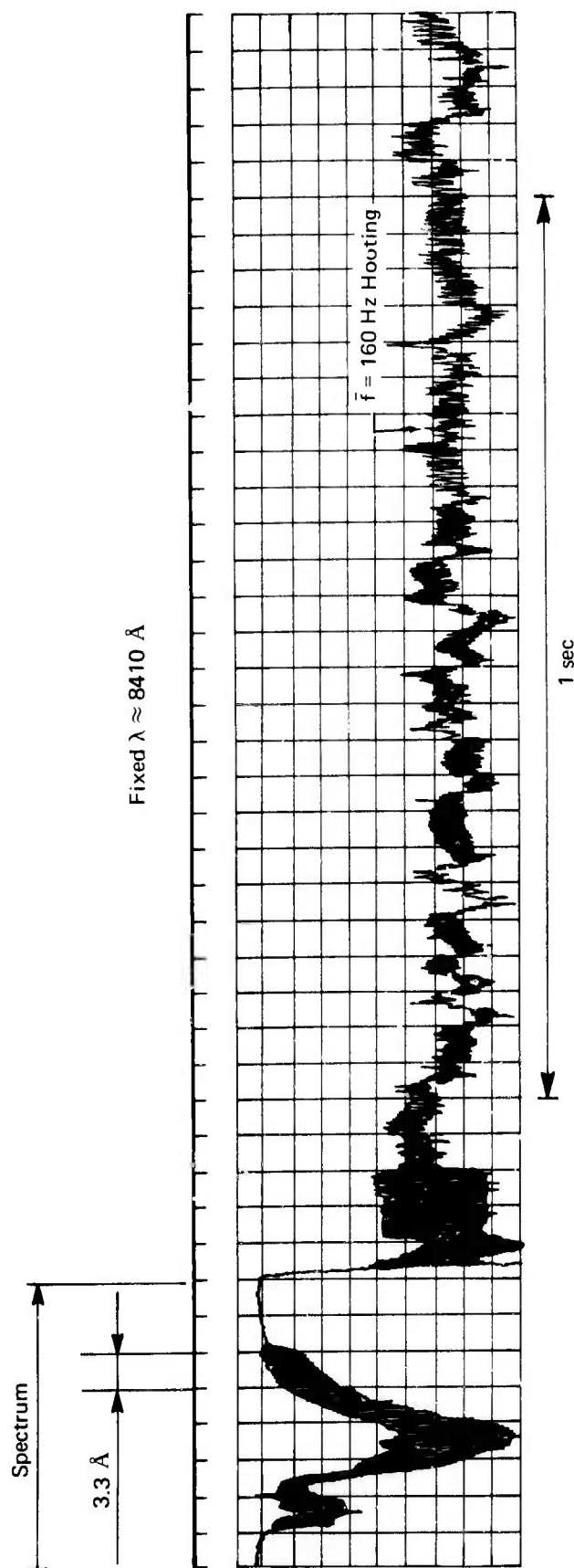


FIGURE 3.8.1 IBM DIODE SPECTRAL OUTPUT AT 200MA AND AT 4.2K

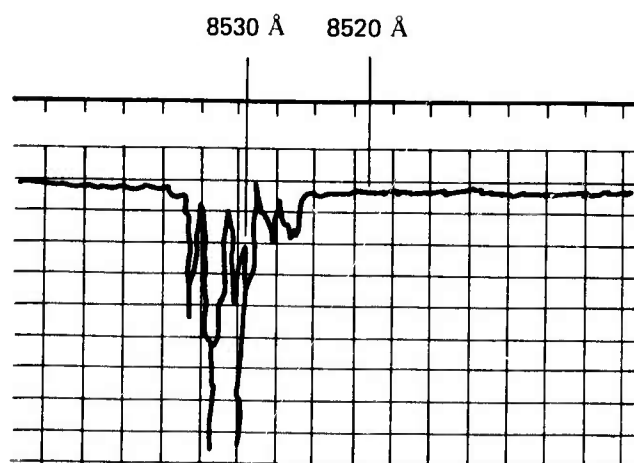


FIGURE 3.8.2 LASER DIODE LAB., INC., LD-22 AT 200MA AND 4.2K

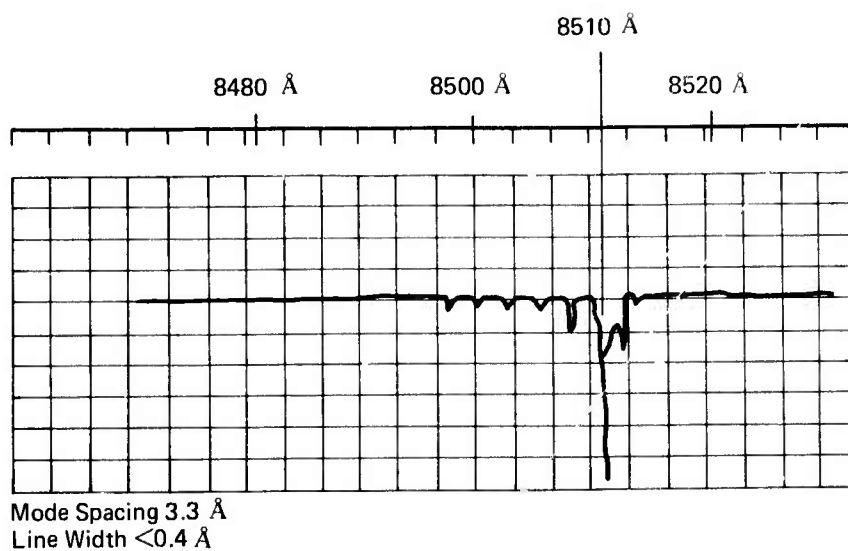


FIGURE 3.8.3 RCA 7606 DIODE SPECTRAL OUTPUT AT 150MA AND 4.2K

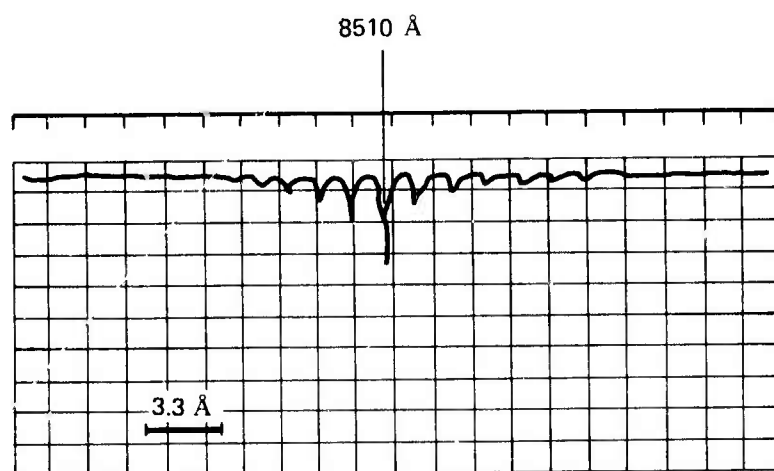


FIGURE 3.8.4 RCA 7606 DIODE SPECTRAL OUTPUT AT 95MA AND 4.2K

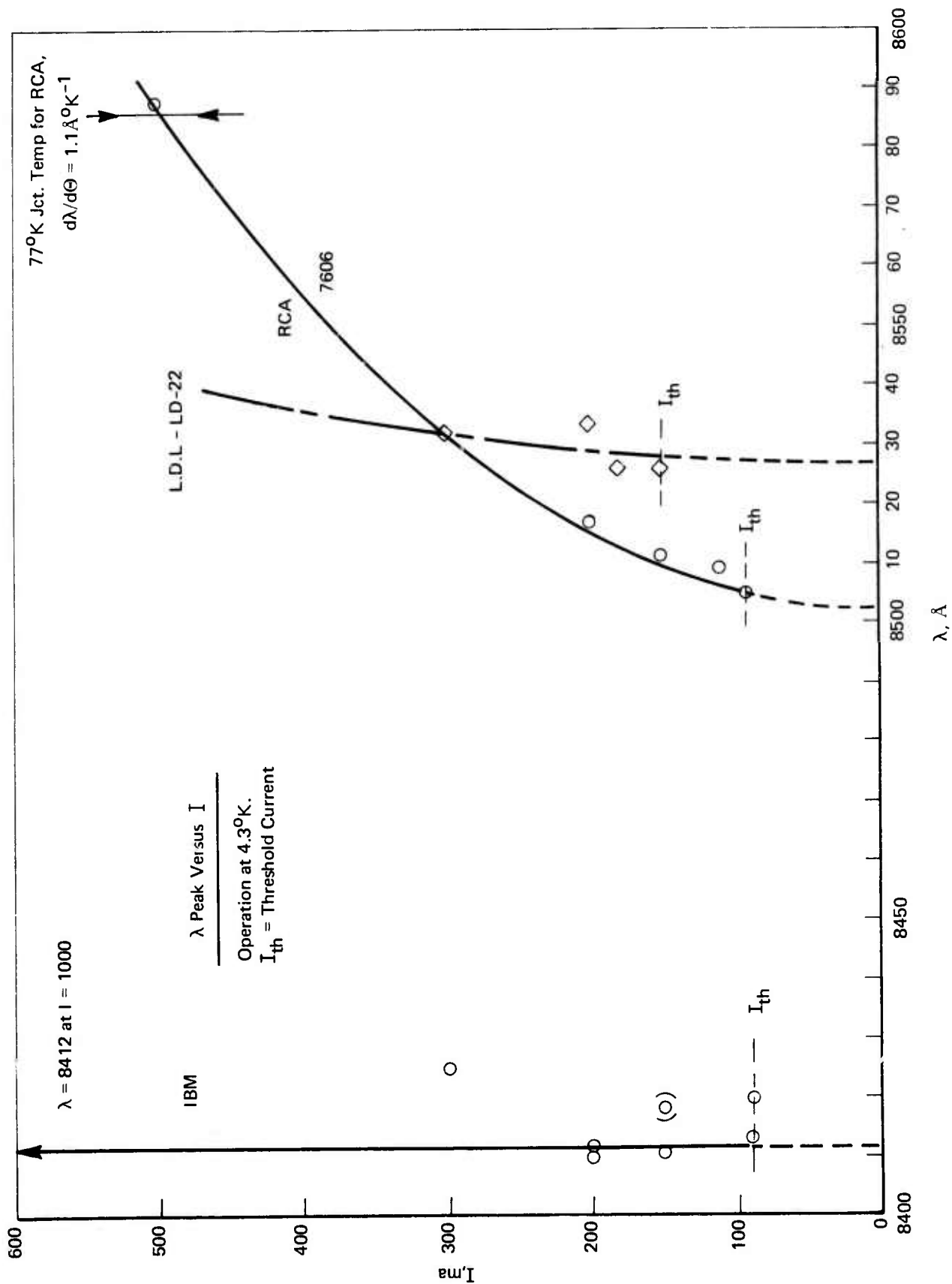


FIGURE 3.8.5 JUNCTION TEMPERATURE EFFECT, LASER DIODES

We have found that the RCA 7606 line center shifts with current which is a thermal effect. It is reasonable to operate the diode CW (continuous wave) when the junction (not the body) is at 77 K, and according to RCA, CW is possible with the 7606 for junction temperatures up to 200 K. Our measurements of this effect are shown in Figure 3.8.5.

We suggest use of the RCA 7606 diode as a fringe reference source. A narrow band filter can be used to select a single mode. Current tuning can be used to center the strongest mode in the filter pass band.

3.9 Monochromatic Fringe Reference Detector

Measurements were made of the response of several silicon photodiodes immersed in liquid helium. A PIN 040 diffused diode by United Detector Technology exhibited very good performance from room temperature to liquid helium temperature. At 4.2 K we observed a significant improvement in long wavelength response and a smaller improvement at shorter wavelengths. Our measurements show that the silicon photodiode will be a suitable detector for the gallium arsenide laser fringe laser source at or near liquid helium temperatures. Experimental results are presented in Table 3.9.1.

TABLE 3.9.1

Diode Type	Dark Current		% of Room Temp.		Response
	300 K	77 K	77 K	4 K	
UDT Pinspot 2 (3)	$6-2 \times 10^{-7} \text{ A}$	$1 \times 10^{-10} \text{ A}$	80%		
Fairchild FPM200	$7 \times 10^{-11} \text{ A}$	$< 1.5 \times 10^{-13} \text{ A}$	87%	unfiltered	IR ONLY
UDT PIN 040	$1-8 \times 10^{-10} \text{ A}$	$< 1-5 \times 10^{-13} \text{ A}$	63%	280%	440%

NOTE: All current measurements were made with Keithley feedback Electrometer, i.e., into a short circuit.

The PIN 040 photodiode is sensitive, much faster than required and will allow use of an $\text{H}^{\text{e}}-\text{N}^{\text{e}}$ laser for testing at room temperature and testing with a gallium arsenide diode at 4.2 K.

3.10 White Light Reference

3.10.1 Source

A low-power incandescent tungsten lamp is a suitable choice to provide broad band radiance. To reduce the heat load on the cube, the lamp will be heatsunk to the helium dewar, and the radiation conducted to the cube through a short length of light pipe. Good optical throughput will be obtained if the lamp is matched by a fast collimator to the pipe on the detector lens and if the detector lens images the exit face of the light pipe on the detector.

3.10.2 Detector

A lead selenide photo-conductive detector is probably the best compromise between the requirement for speed, sensitivity, cold operation and a wavelength range to match the optical bandwidth offered by the Tungsten lamp, glass optics and the beamsplitter. Santa Barbara Research, for example, makes PbSe detectors, specified to as low as 60 K and fast enough for reliable correlation of the white light signal with the laser reference signal.

An alternative might be the germanium photodiode - as for example made by Electro Nuclear Laboratories - which probably would provide sufficient optical bandwidth and high speed of response. We have not tested such a diode yet.

The exact choice of detector will depend on the selected beamsplitter material and the maximum permissible width of the central "white" fringe - given by requirements for co-addition and the nature of the recorded spectro.

3.11 Detector Optics

The optical system as studied consists of a Newtonian telescope followed by a collimator followed by a cassegrainian system. Figure 3.11.1 illustrates the system with lenses instead of mirrors. The field of view, the maximum diameter of the objective, and the clear aperture of the interferometer cube are specified as:

$$\begin{array}{ll} \text{F.O.V.} & 2\psi = 0.25^\circ = 4.36 \text{ mR} \\ \text{Cube} & D_s = 1 \text{ inch} \\ \text{Objective} & D_o = 11 \text{ inch} \end{array}$$

The objective and hence the entrance and exit pupil of the system are half moon shaped. The collimated beam at D_s will then have a half angle of divergence of:

$$\theta = \frac{D_o}{D_s} \psi = \frac{24 \text{ mR}}{1} \text{ i.e., the field of view}$$

This is substantially less than the maximum deviation allowable for the beam in the interferometer to maintain a resolution of $\Delta v < 2 \text{ cm}^{-1}$:

$$\frac{\Omega}{2\pi} = \frac{\Delta v}{v}$$

$$\theta \approx \sqrt{2 \frac{\Delta v}{v}} \approx \underline{40 \text{ mR}}$$

The detector's sensitivity is not uniform across its surface and the external field of view, i.e., the target, must therefore not be imaged on the detector surface. Normally, it would be possible to use a field lens and image the objective on the detector. For that case, we would require in front of the detector a two-lens system; one acting as the objective focussing the collimated exit beam from the cassegrainian system, and the second a field lens to image the objective on the detector.

The smallest detector size thus achievable will depend on the F/number of the field lens and if we assume F/1 as the practical limit, i.e., the cone at the detector to have a half angle of 30° , we find for the smallest possible detector size:

$$\begin{aligned} \frac{D_D}{D_o} &\approx \frac{\psi}{30^\circ} \\ D_D &\approx .046 \text{ inch} \\ D_D &\approx 1.2 \text{ mm.} \end{aligned}$$

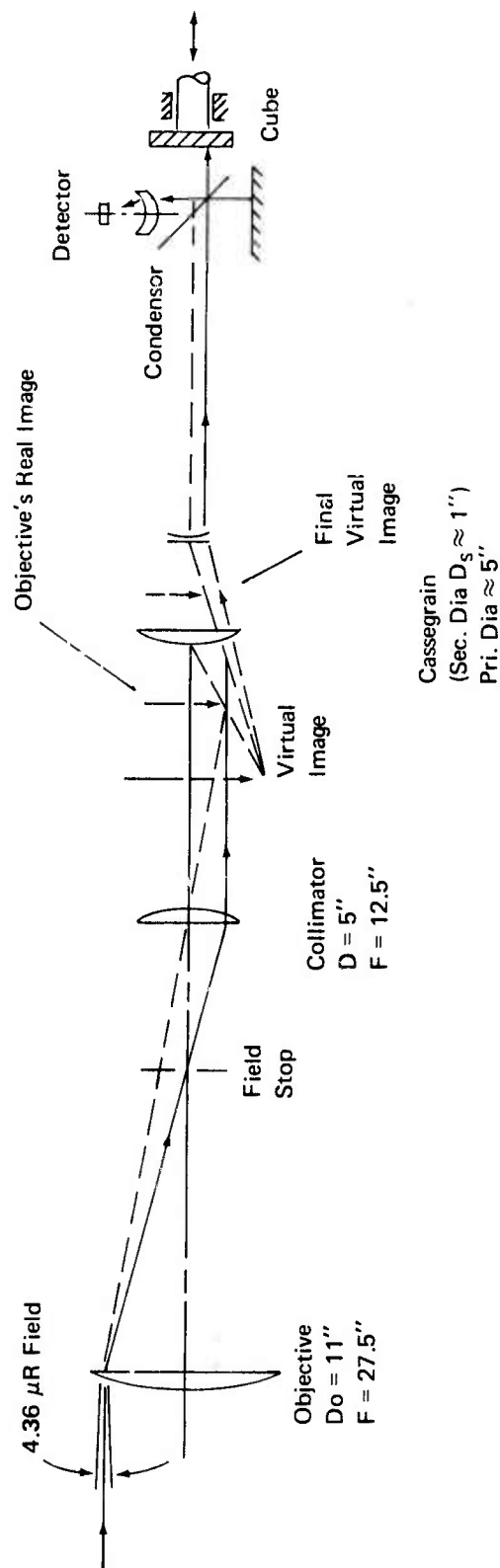


FIGURE 3.11.1 SUGGESTED DETECTOR OPTICS

However, a system of two lenses has substantial losses by reflection, and it will necessarily be rather longer than there is space between the side of the cube and the wall of the Dewar. Also, if the beam through the cube is focussed at infinity, appreciable vignetting will occur in the cube due to the divergence $\theta = 24 \text{ mR}$ (the field of view) of the beam.

To avoid most of these problems we can focus the exit beam of the cassegrainian at some spot behind the exit face of the cube with the convergence chosen so that no ray traverses the cube at more than 40 mR inclination and all rays fit through the cube's 1" clear aperture. A single condenser lens at the output of the cube of 1" focus and 1" diameter will then be used to image the objective on the detector.

A simple ray trace through the system shows that there is a real image of the objective about 5" in front of the cassegrainian primary and hence a virtual image a few inches in front of its secondary. When the system is adjusted as described above, this virtual image is slightly small than 1" and it is focussed on the detector by the condenser lens. (This is not a "field"-lens, since its position is not conjugate to the field of view!)

According to an approximate ray trace, the resulting image on the detector will be

$$D_D \approx \frac{0.9}{17.7} \approx 51 \text{ Mil} \quad \text{Dia}$$

$$D_D \approx 1.3 \text{ mm} \quad \phi$$

This is slightly larger than for the optimum system, because the lens will not be set for minimum blur circle but for focus on the objective in order to have precisely defined conditions and a uniform illumination.

A lens for the flight hardware can be made of IRTRAN 6 because that material promises good optical, mechanical and environmental performance.

Simple formulae (Jenkins & White, p. 137; Warren Smith, p. 401) can be used to estimate spherical and chromatic aberration to produce approximate blur circles of:

Spherical:	16 Mil	Dia.
Chromatic (4 - 10 μ)	3 Mil	Dia.

if the lens is bent for minimum spherical aberration.

Other aberrations will not be serious in this on-axis application. We therefore considered the following lens for the flight hardware:

material:	IRTRAN 6
diameter:	1 1/8 inch
effective focal length:	1 inch
shape:	meniscus for minimum spherical aberration at infinity focus

For a test program, one does not need the full wavelength range of IRTRAN 6 and can use quartz for all tests to 3.39μ or germanium or rock-salt for interferograms.

An estimate of the required detector size can be made from the theoretical diameter of the image, the spherical and chromatic aberrations and some allowances for angular misalignment of the detector assembly with respect to the telescope, for lateral misalignment of the detector and for inaccurate focus. Simple addition of these tolerances (a clearly pessimistic assumption) yields for 1" focus at F/1:

estimated image diameter	51
$1^\circ = 15$ mR angular tolerance	15
detector mounting tolerance	10
spherical aberration	16 (optimum lens made of IRTRAN 6)
chromatic aberration	3
10 Mil focussing error	5

$$D_D = \overline{100} \text{ Mil}$$

$$D_D = 2.5 \text{ mm}$$

We recommend this diameter for the first detector to be purchased by AFCRL.

An appreciable reduction in detector size can be achieved only by using a faster condenser. Such a condenser would require aspheric figuring to control aberrations, and the designer would also have to make sure that the wide cone of radiation does indeed enter the detector without too much reflection loss at the detector surface. The improvement in speed and noise that could be gained by such a size reduction would have to be weighed against the required effort.

3.12 Low Temperature Tests of KRS-5 for Beam Splitter

In the early months of this program Idealab developed a beam splitter concept utilizing an air gap. Their analysis based upon optical properties indicated that KRS-5 was the material most suited for this application. KRS-5 is a Thallium Bromiodide solid solution $[Ti(Br,I)]$ invented by Professor Alexander Smakula of MIT and available commercially from the Harshaw Chemical Company.

The very low temperature properties of this and other suitable materials are not yet well documented. When contacted, Professor Smakula indicated that the KRS-5 material which he had tested underwent physical deterioration in the temperature regime between 77 and 4.2 K. His tests were performed by rapidly immersing KRS-5 blanks into liquid helium, allowing them to remain submerged for 5 minutes and then bringing them rapidly into the room environment. After immersion the KRS-5 blanks were observed to have a yellow coating at the surfaces. This, he believed, was the result of a separation of the bromide from the iodide and a subsequent phase change in the iodide.

The deterioration observed by Smakula warranted experimental verification before any further efforts were expended in developing the KRS-5 air gap beam splitter. Further, in the actual application intended in this program, the cooling of the beam splitter to liquid helium temperatures would take place over a period of several hours. This lower rate of cooling might insure the survivability of the KRS-5 material.

We undertook this experimental effort with the objective to establish the survivability of KRS-5 at 4.2K with attendant mechanical stress. The experiment was designed to assure unidirectional heat flow into the blank while monitoring the surface temperatures to establish the temperature gradient and rate of temperature change in the material. The blank was to be cooled from room temperature to 4.2K over a period of approximately two hours.

The beam splitter and compensator of the interferometer were to be approximately 2 inch in diameter and 0.4 inches thick. However, because of the high cost of these blanks, tests were performed with 1 inch diameter and 0.25 inch thick blanks. Two of these blanks were placed together, face to face separated by .002 inch aluminum foil. The circumferential surfaces were insulated with urethane foam to reduce the heat flux from the edges. The outer surfaces of the blanks and foam insulation were covered with aluminum face plates .062 inches thick to assure a uniform distribution of temperature across the outer faces of the blanks. These plates were perforated in the area of the blanks to permit visual monitoring of the blank transparency during cooldown. The temperature of the aluminum face plates and center plane were monitored both during cooldown and warm-up of the blanks. The entire sample assembly was suspended from a string that was used to control the immersion rate. The assembly is illustrated in Figure 3.12.1.

Experimental Results with KRS-5

The first test was performed using liquid nitrogen as the heat sink. The sample assembly, consisting of KRS-5 blanks No. 1 and No. 2 was lowered very slowly into the dewar allowing it to cool by conduction with the gas before final immersion. The sample cooled from room temperature to 77 K in 151 minutes. The average differential temperature between the inside and the outside of the KRS-5 samples was 4.5°C during cooling, with a maximum of 15°C. The sample was removed from the liquid nitrogen dewar very slowly taking 51 minutes to raise the temperature from 77 K to room temperature. During warm-up the average temperature difference between the inside and the outside of the blank was 7.4°C with a maximum of 12°C being achieved. There was no observable effect on the KRS-5 during this test.

A second test was performed in the same manner using blanks No. 1 and No. 2 with the immersion time reduced to 53 minutes. The average temperature across the KRS-5 blank was 6.5°C with a maximum of 10°C. The warm-up was accomplished in the same manner as the first test in approximately 53 minutes with an average temperature of 8.75°C produced across the blank and a maximum of 14°C. During this test, the blanks showed no physical changes.

The KRS-5 blanks, No.1 and No. 2, were then immersed in liquid helium after a preliminary cooldown to 77 K using liquid nitrogen. The cooldown time from room temperature to 4.2 K was approximately 150 minutes. The average differential temperature measured across the faces of the crystal was 9°C. During immersion in the liquid helium, the sample was subjected to a series of mechanical shocks with a solid glass tube. The warm-up time was approximately 105 minutes and the average temperature difference across the faces of each blank was 8°C. On reaching room temperature, each of the crystals were carefully inspected.

Blank No. 1 was found to be intact while blank No. 2 had become opaque. This effect was produced by a series of parallel yellow streaks occurring at two principal angles within the bulk of the material. The surfaces of the blank were also upset in a regular pattern. One interpretation given to this phenomena is that slips in lattice arrangement of the molecules had occurred during cooldown.

Additional tests were performed with Blank No. 1 to determine if any physical deterioration could be induced by rapid cooling to 4.2 K. Smakula's test was performed in which the blank was immersed in liquid helium. The sample cooled to the sink temperature in approximately 10 seconds. There were no apparent physical changes after the blank was returned to room temperature.

Next, the transmittance of Blank No. 1 was measured in the range of 2-25 microns and found to be identical to Blank No. 3 of the same size, received from AFCRL, which had not undergone low temperature immersion. The average measured transmittance over this range was 71 percent.

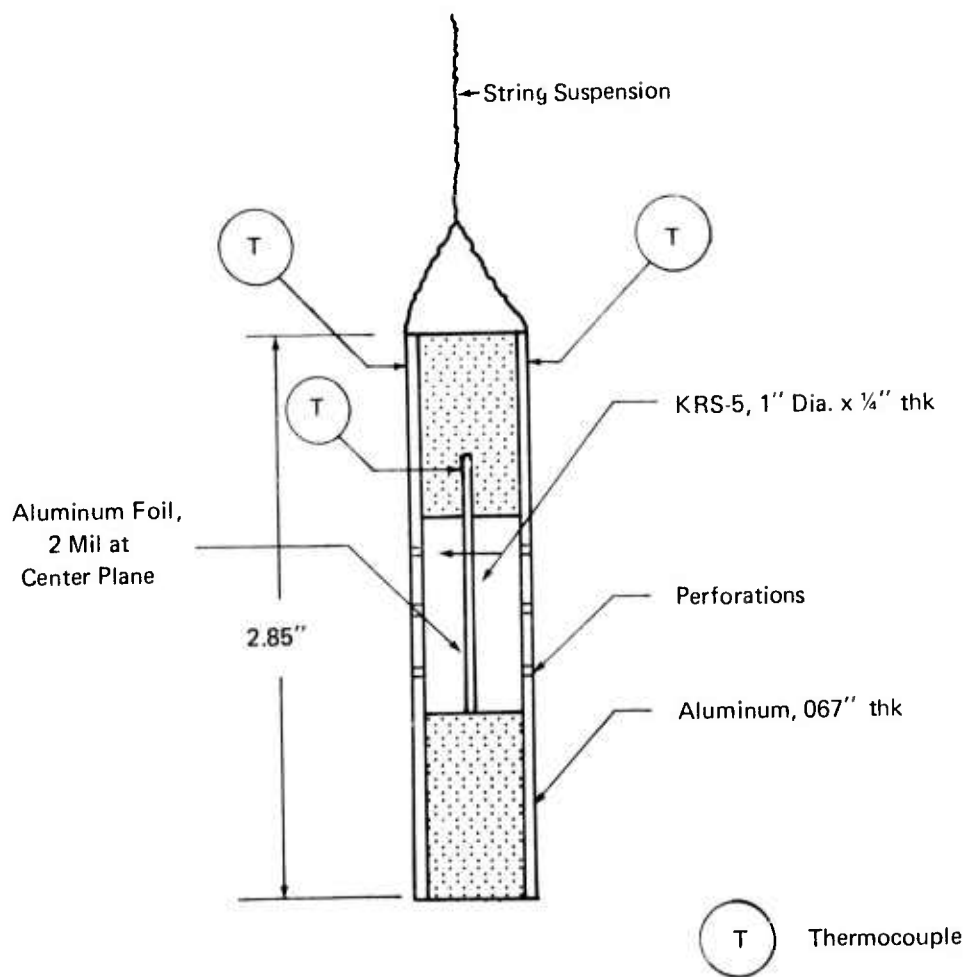


FIGURE 3.12.1 KRS-5 SAMPLE HOLDER FOR LIQUID HELIUM TESTS

It was concluded, therefore, that Sample No. 1 had not undergone any change in properties as a result of the multiple slow immersions and the single rapid immersion to liquid helium temperatures.

Samples one and two were returned to Idealab and these subsequently shipped to The Harshaw Chemical Company from the original supplier. After inspecting the crystals, Harshaw concluded that the KRS-5 Blank No. 1 which was still transparent appeared to be badly strained while the opaque Blank No. 2 was not. They suggested that the use of annealed samples could serve as the solution to the problem.

Idealab obtained four 1-inch diameter by 1/4 thick KRS-5 annealed samples from Harshaw Chemical Company, and we subjected these samples to a rapid immersion test. This was performed by placing each crystal in a string harness and rapid dunking in liquid helium. Observation of the helium pool indicated that cooldown of the sample occurred in about 10 seconds. Each sample was found to be opaque when removed from the liquid helium sink. These results and the previous immersion results substantiated the physical deterioration KRS-5 at liquid helium temperatures. Inasmuch as two blanks out of seven survived the immersion, there was a large uncertainty as to the cause of the phenomena. In any case, the results obtained seem to justify the evaluation of other materials to be used for the interferometer beam splitter.

We received two samples each of KBR, Cesium Iodide, and Irtran-6 from Idealab for further low temperature tests. The samples were approximately the same size as the previously tested KRS-5. Each of the samples was mounted into a harness and immersed in liquid helium by rapid dunking. The estimated cooldown time for the crystals from room temperature to 4.2 K was 10 seconds. We observed no physical degradation in any of the crystals after immersion. These results and those obtained with KRS-5 are summarized in Table 3.12.1.

TABLE 3.12.1BEAM SPLITTER MATERIALCOLD SHOCK TEST RESULTSImmersion

<u>Material</u>	<u>Sample</u>	<u>Temp(K)</u>	<u>Time</u>	<u>Result</u>	<u>Remarks</u>
KRS-5	1 & 2	77	151 min	No Change	-
KRS-5	1 & 2	77	53 min	No Change	-
KRS-5	1 & 2	4.2	150 min	#1 No Change	-
				#2 Opaque	-
KRS-5	1	4.2	10 sec.	No Change	Trans 71% 2-25 μ
KRS-5	3	--	--	--	71% 2-25 μ
KRS-5	1 & 3	4.2	10 sec.	No Change	-
KBR	1 & 2	4.2	10 sec.	No Change	-
CEI	1 & 2	4.2	10 sec.	No Change	-
IRTRAN-6	1 & 2	4.2	10 sec.	No Change	-
KRS-5	4,5,6,7	4.2	10 sec.	Opaque Annealed Material	

3.13 Beam Splitter Support System

The design of a support system for the beam splitter was undertaken at ADL and incorporated into the H-Cube test instrument by Idealab, mechanical evaluation tests were performed with this instrument by ADL.

The beam splitter is made up of two circular optical plates placed together with the flat surfaces facing each other but separated by a thin spacer. Because the material for the beam splitter had not been selected, the design was prepared for fused silica plates. These plates fit into the bore provided in the angled face of the cube and are held by the support system.

The support system is used to accurately maintain the angular position of the beam splitter, independent of the temperature environment, and to permit the beam splitter to survive the launch mechanical environment. In addition, the support cannot introduce excessive distortions in the plates.

In the present design the outer surface of the beam splitter is placed directly against an annular face plate that is mounted to the angled member of the cube. This establishes the angular position of the beam splitter and compensator. A spring force is applied to the outer face of the compensator to maintain contact with the beam splitter at 100 G's. The circular areas of both plates are supported by leaf springs inside of the bore in the cube.

The angled web of the cube structure establishes the angular position of the beam splitter and compensator. The clamping plate provides axial support to the beam splitter and compensator through the Wavy Washer. The point loads of the Wavy Washer are distributed over the compensator surface through the flat washer. Lateral support is provided through teflon rings and two 12-sided springs; the teflon rings serve to distribute the spring loads on the cylindrical surfaces of the beam splitter and compensator.

Both the Wavy Washer and the 12-sided springs also provide for differential expansion between the dissimilar materials.

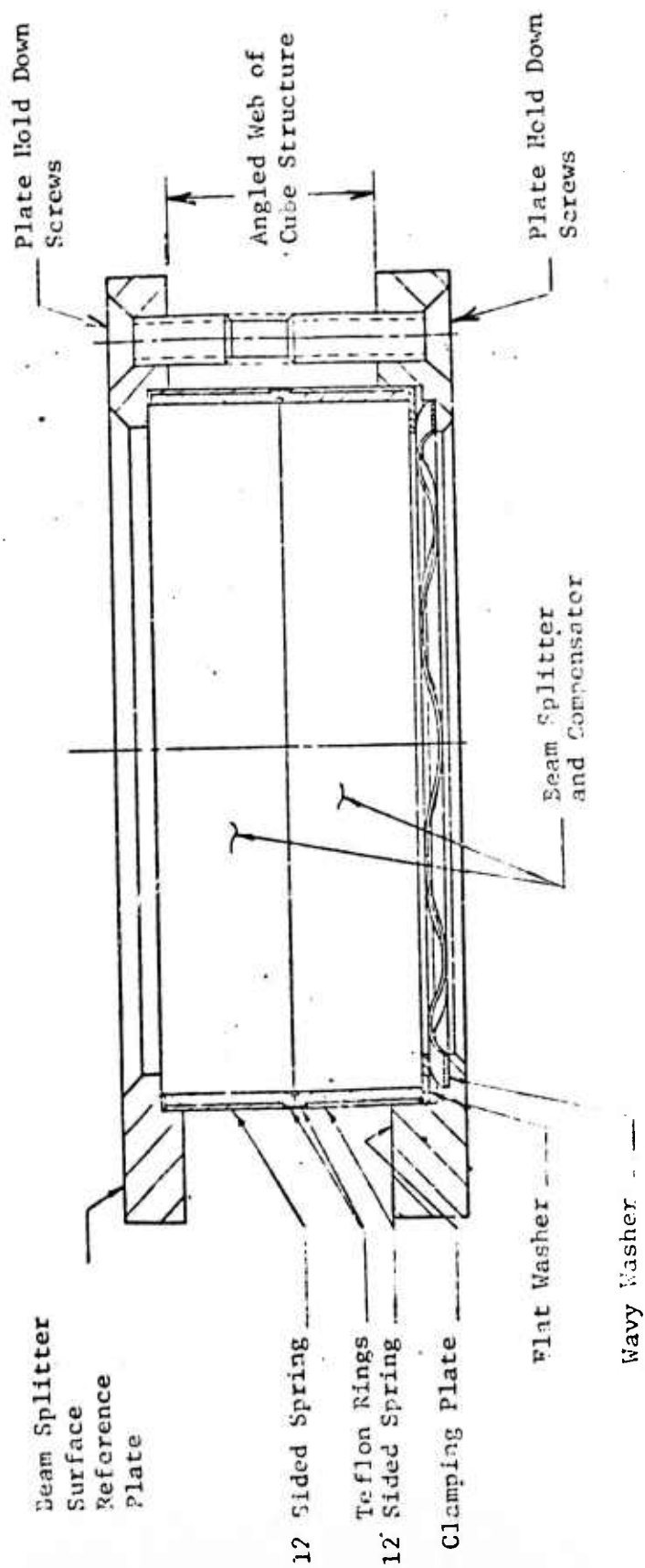


FIGURE 3.13.1 BEAM SPLITTER SUPPORT SYSTEM

3.14 Interferometer Slide Lock

The interferometer slide is vulnerable to damage during launch of the experiment because of the mechanical vibration environment produced by the Black Brant 5C sounding rocket. This mechanism, which is the only moving part in the interferometer system, must be restrained during launch and released after separation of the payload from the launch vehicle.

The launch phase has a duration of approximately 1/2 minute. In this period the interferometer will experience vibration inputs, at its supports, to levels indicated on page 11. Further, the launch acceleration along the flight axis will increase approximately 1 g to + 27 g.

Because the motor is in the aft location of the interferometer, it was decided to position the motor coil and slide mechanism against the motor magnet taking advantage of the 1 to 27 g axial acceleration present during launch. This positioning force is augmented by an additional force provided during launch only by a slide lock mechanism.

Two approaches were considered in the development of locking mechanism designs. The first is a mechanical lock involving a separate system from the interferometer and the second utilizes the interferometer motor to provide the locking force. Separate preliminary designs were developed for both these approaches. Further, an experimental program was undertaken at ADL to establish the feasibility of the second approach.

The experimental results indicate that the interferometer motor can produce a restraining force which is twice as large as the axial forces produced in the slide at 25 g. This restraining force, coupled with the force resulting from acceleration of the vehicle, will produce a restraining force up to three times the axial vibration forces.

This approach is feasible because the interferometer is in a helium gas environment. The helium gas at 4.2K provides sufficient cooling to prevent thermal runaway of the motor coil mounting at the large power levels (approximately 7 watts) in locking position.

The results of the slide lock tests performed with the interferometer motor in a helium gas atmosphere are summarized in the attached Table 3.14.1.

TABLE 3.14.1
INTERFEROMETER MOTOR
SLIDE LOCK TEST RESULTS

1. MOTOR CONSTANT - 4.3 POUNDS FORCE/AMPERE
2. MOTOR FLUX IN GAP - 175,000 MAXWELLS AT 300, 77 AND 4.2K
3. COIL RESISTANCE AT 4.2K - .086 OHMS, APPROXIMATELY 1 PERCENT OF 300K RESISTANCE
4. MOTOR COIL TEMPERATURE. 9 AMPS

<u>TIME (MIN)</u>	<u>TEMP (K)</u>
0	4.2
1	8
2	10
5	12
10	18
12.5	30

5. COIL ENERGY DISSIPATION FOR 1 MINUTE PERIOD IS 425 JOULES
6. MOTOR FORCE AT 4.2 AND 9 AMPERES - 39 POUNDS (CALCULATED)

The interferometer motor test at cryogenic temperatures were performed in a 10-inch diameter, 52 inch deep liquid helium dewar guarded on the outside with liquid nitrogen. A standard Idealab interferometer motor was suspended in the dewar with stainless steel wires. Initial cooldown was accomplished by placing the motor in the liquid helium dewar and cooling it with liquid nitrogen. When appropriate, the 77K tests were performed at this time. Cooldown to 4.2K was accomplished by the removal of liquid nitrogen from the dewar and replacing it gradually with liquid helium. The helium was filled into the dewar to a depth of several inches. The motor was suspended in the helium gas phase immediately above the liquid level to simulate the operational environment.

The motor flux measurement was performed using a 3 turn coil with taps at the ends and at coil No. 1. The test was performed with No. 24 Belden single strand wire wound on a NEMA-G-10 epoxy-fiberglass spool comparable in dimensions to the operational coil of the motor. At room temperature, 77K and 4.2K, a number of tests were performed with a flux meter connected to the flux measuring coil. The measured flux in the gap was 175,000 Maxwells. The spread of all the measurements taken at the three temperature levels was less than 0.5 per cent.

A group of tests were also performed to measure the maximum current carrying capacity of the motor coil before thermal run-away occurs. These tests were performed with the motor cooled to 4.2K suspended immediately above the liquid helium in the gas phase. The motor coil was positioned and held at center stroke in the motor with four NEMA-G-10 epoxy-fiberglass stand-offs. Two thermocouples were attached to aluminum spool to which the coil is mounted to monitor the coil temperature. The motor currents tested were 0.5, 1, 2, 3, 4, 5, 6, 7.5 and 9 amperes. The tests performed with motor currents of 7.5 amperes and under had a duration of approximately 30 minutes while the test performed with 9 amperes had a duration of 12.5 minutes.

At less than 7.5 amperes, the initial coil temperature rise rate remains less than 0.5K per minute. At 9 amperes this rate increases to approximately 4K per minute. This latter rate of rise is at an acceptable level provided that the motor is not energized for a period greater than 1 to 2 minutes. At 9 amperes the motor force is calculated to be 39 pounds, based upon the room temperature motor constant and on a constant motor flux.

We conclude that the use of the interferometer motor for locking the slide is feasible. The detail design of the electrical system utilizing this approach should, therefore, be undertaken.

4. APPENDICES

4.1 Mechanical Environment Specification for Interferometer Tests

In April 1969, personnel at AFCRL were asked about the vibration environment for the Black Brant VB with the following result.

There is very little specific vibration information available for the payloads for this sounding rocket. The environment is strongly dependent upon the flexibility of the payload instruments and its mounts, so no formal environmental specification has ever been issued by AFCRL. The following information, however, is known.

The vibration acceleration loads to the payload nose are about 5 g from 10 to about 2500 HZ. There is a motor case resonance at 110 to 120 HZ. Transmissibilities are from 5 to 20 depending upon the payload carried. AFCRL suggests that the payload be designed to take 25 g, 10 to 2000 HZ with a sine sweep rate of 2 to 4 octaves per minute along the flight axis. This results in about 8 octaves for a duration (at 4 octave/min) of about 120 seconds. Lateral accelerations are very low, but a 5 g sweep is recommended for design and development tests. The powered flight time is about 26 seconds so the specification on duration is conservative. This type of test would constitute a qualification test and does not include the mounts or attaching means to the rocket.

The acceptance test by AFCRL consists of vibration tests on the real payload mounting ring. The first test is a 2 g sine sweep as a search for any obvious resonances. The second is a 5 g, 10 to 2000 HZ axial sweep, and the third is a 5 g RMS random for 26 seconds.

In January 1971, the above environment was reviewed along with the document "General Environmental Test Specifications for Design Qualification and Flight Acceptance of Sounding Rocket Payloads and Components", S-320-SR-2 dated 20 June 1968 by NASA GSFC. This document describes in great detail the environments of all the U.S. sounding rockets. Another source consulted is the Journal of Spacecraft paper "Development of the Aerobee 350 Sounding Rocket", Vol. 4, No. 10, October 1967 by Lane and Chalfant which describes the extensive instrumentation used during the development of this vehicle. This paper confirms the quality of the data appearing in the NASA document.

To clarify the purposes of the test levels, the following definitions are quoted from the NASA document, pages 1 and 2:

DESIGN QUALIFICATION. This test program consists of tests which subject the prototype payload or component to environmental levels more stringent than those expected from transportation, handling, acceptance test, prelaunch, launch, and flight. The purpose is to demonstrate the ability of the design to meet all performance requirements and suffer no harmful degradation when exposed to environments more stringent than predicted.

PRECEDING PAGE BLANK - NOT FILMED

FLIGHT ACCEPTANCE. This test program subjects flight payloads or components to environmental levels equal to those expected in ground handling, launch, and flight. The purpose is to locate latent material and workmanship defects in a proven design.

From this review it was concluded that the previous vibration levels were reasonable and the following specification was established as the design qualification levels for the input to the interferometer base.

DESIGN QUALIFICATION LEVELS
FOR BLACK BRANT V

1. Sinusoidal, 2 octaves/minute

Thrust, Z axis

20-40 HZ	0.31 inches D.A.
40-2000 HZ	25 g, 0-peak

Lateral, X and Y axes

14 HZ	0.5 inches D.A.
14-2000 HZ	5 g, 0-peak

Note: There is a motor case resonance at 100 to 120 HZ.

2. Random, 30 seconds duration

All axes

20-2000 HZ	$0.0126 \text{ g}^2/\text{HZ}$, 5 g, RMS
------------	---

3. Acceleration, 30 seconds duration

Thrust, Z axis only

+Z	27 g
-Z	3.8 g

To date, no information is available on the automatic guidance control system. Hence, the design of the experiment includes the dynamics only of the powered portion of the flight. The effect of system natural frequencies on the control system is unknown.

It has recently come to our attention that vibration levels in the form of an environmental specification for the Black Brant have been published. These levels are roughly comparable to the levels used in the program and do not invalidate the approach taken here.

4.2 Interferometer Mounting Plate

The interferometer mounting plate provides a base both for the linear drive motor and for the base supporting the slide mechanism and the cube. The two principal requirements for the interferometer mounting plate are (1) that it have a magnetic permeability near the permeability of air and (2) that the coefficient of thermal expansion (contraction) match this coefficient for A2 steel as closely as possible. The recommended material is Type 310 Stainless Steel.

The reasons for selection of Type 310 Stainless Steel for this base were (1) it is the only austenitic stainless steel which is fully stable at cryogenic temperatures and (2) it has the lowest coefficient of expansion of all the 300 series stainless steel. Steel in the austenitic or face-centered condition is non-ferromagnetic (see Ref. 1,2).

Many materials change from magnetic to non-magnetic as the temperature of the material increases, or conversely, change from non-magnetic to magnetic as the temperature decreases. The temperature at which the change occurs is known as the Curie temperature (Ref. 2,3). At room temperature, all the 300 series stainless steels have a magnetic permeability at 200 H annealed of 1.02 and below (Ref.4). Air has a magnetic permeability of 1.00. As the temperature is decreased, all these austenitic stainless steels undergo some degree of transformation to martensite except Type 310 (Refs. 5, 6, 7). Even when subjected to cold work, the value of magnetic permeability for Type 310 remains at about 1.004 (Ref. 7). Therefore, Type 310 appears to be the logical choice for the IRIS base.

In addition to its low permeability, Type 310 also has the coefficient of thermal expansion of all the 300 series stainless steels of which data was available on the magnetic permeability. (Ref. 7,8). The contraction in cooling from 70°F to -300°F is .0026 in/in. By comparison, the contraction for a low alloy carbon steel for the same temperature range is .0018 in/in, and for A2 tool steel it is .0017 in/in (Ref.9).

REFERENCES

(Note: Pertinent pages from these references are attached to this Memorandum.)

1. Magnetic Materials, by F. Brailsford. John Wiley & Sons, Inc. 1951. Pages 138, 139.
2. Engineering Materials Science, by Cedric W. Richards, Wadsworth Publishing Co., Inc., 1961. Pages 429, 430.
3. Physical Constants -- Monel, Inconel, Nickel and Nickel Alloys, Section E, by The International Nickel Co., Inc., 1947. Pages 4, 5, 8.
4. Stainless Steel Handbook. Allegheny Ludlum Steel Corp. 1956. Pages 2, 3, 27, 28.
5. "A Study of Austenite Decomposition at Cryogenic Temperatures," by J. F. Watson and J. L. Christian. 9 June 1961. General Dynamics/Astronautics Materials Research Report No. ERR-AN-057. Pages 22, 23, 51, 66, 72.
6. "The Effect of Experimental Variables Including the Martensitic Transformation on the Low-Temperature Mechanical Properties of Austenitic Stainless Steels," by C. J. Guntner and R. P. Reed. Transactions of the ASM, Vol. 55, 1962. Pages 400, 402.
7. Heat Treatment and Physical Properties of the Chromium-Nickel Stainless Steels -- Nickel Alloy Steels, Section 7, Data Sheet A. The International Nickel Co., Inc., 1947. Pages 18, 19.
8. "Thermal Expansion Characteristics of Stainless Steels Between -300° and 1000°F," by D. E. Furman. Journal of Metals, April 1950, Transactions AIME, Vol. 188. Page 690.
9. Distortions in Tool Steels, Lement, B. S., American Society of Metals, Novelty, Ohio, 1959.

4.3.1 Idealab Test Dewar

In November of 1970, a requirement was established for a dewar to be used by Idealab to test the beamsplitter and mirror components of the IRIS under vacuum and at 77K, both separately and assembled in the H-Cube and in the Interferometer Spectrometer. A system meeting the requirements noted below was fabricated, assembled and delivered to Idealab by ADL on January 8, 1971.

The dewar had a working volume of 1 foot in diameter and 2 feet in length. This volume was required to achieve a temperature of 77-80K and a vacuum of 25 microns. The dewar could be mounted in both the vertical and horizontal position. Windows were provided for beam entry and exit.

The system provided Idealab is shown in Figure 4.3.1.1 exclusive of the liquid nitrogen supply. It consisted of the test dewar, vacuum pumping and measuring systems. A temperature read-out for both the dewar and experiment and a dewar warm-up control system.

The test volume of the dewar consisted of a stainless steel cylinder 1 foot in diameter by 2 feet long. Copper tubing was wrapped around the cylinder and soldered to the wall. The cylinder and tubing were sealed in a rigid urethane low density thermally insulating foam. The interior of the test volume contained a removable base for mounting experiments in the horizontal dewar position. Internal longitudinal flanges were also provided in the test volume for support and positioning of mirrors and components used during the tests.

The cold section of the dewar extended approximately 1 foot outside of the foam insulation. This formed the transition from the cold working space to the room temperature flange to which was attached the cover of the chamber opening. The cover contained three window apertures and two 18 pin Amphenol feedthrough connectors were made in the chamber transition area.

The chamber is cooled by admitting liquid nitrogen under pressure to the copper tracing line from the supply dewar. See Figure 4.3.1.2. The liquid flow rate was manually regulated by a cryogenic valve, and adjusted to maintain the appropriate temperatures with minimum liquid utilization. The vacuum system was utilized to evacuate the chamber space, when the test instruments were sufficiently cooled.

A complete set of operating procedures were prepared and delivered with the system to Idealab. In addition, instructions in the use of the system were given to Idealab personnel.

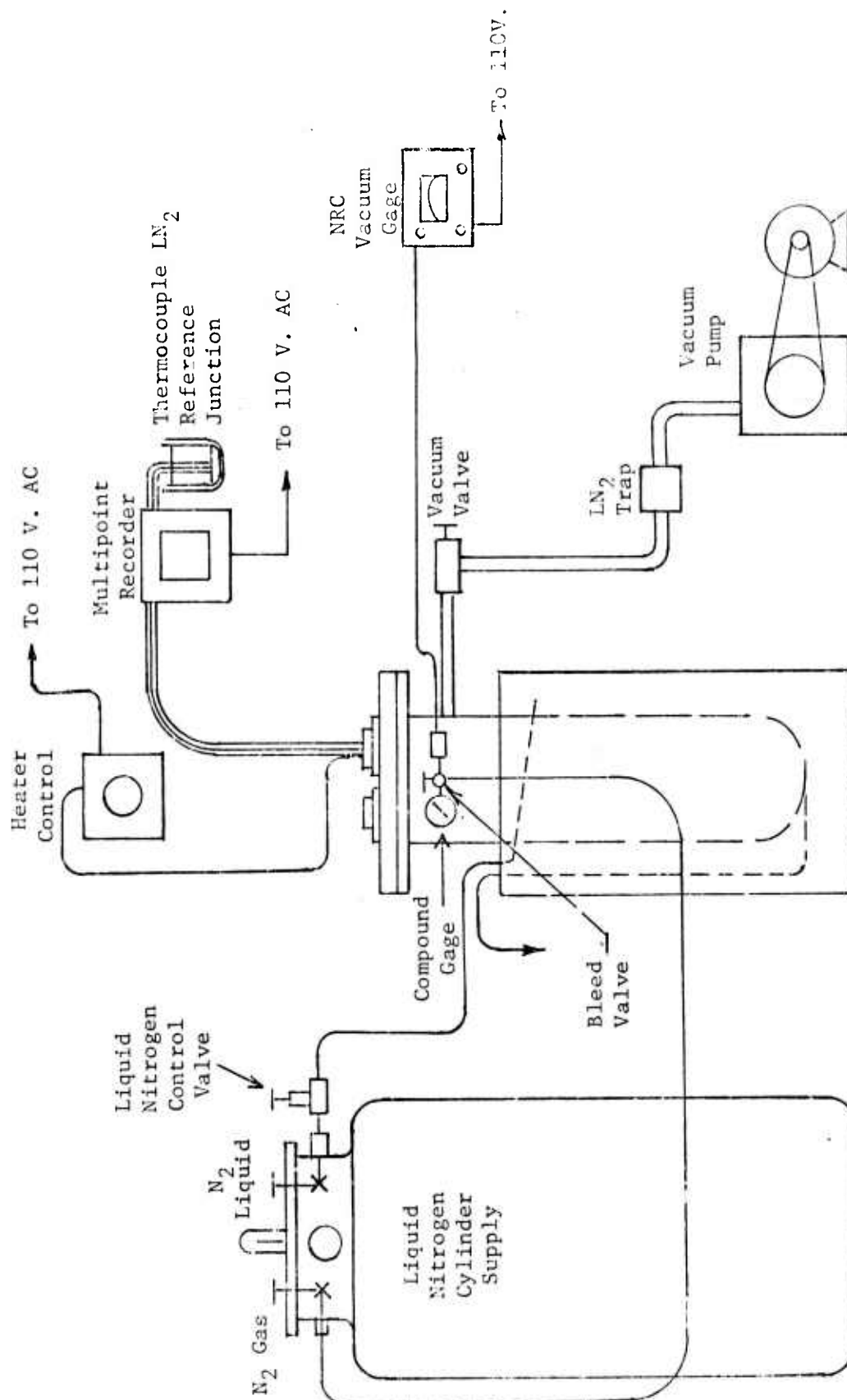


FIGURE 4.3.1.1 IDEALAB DEWAR

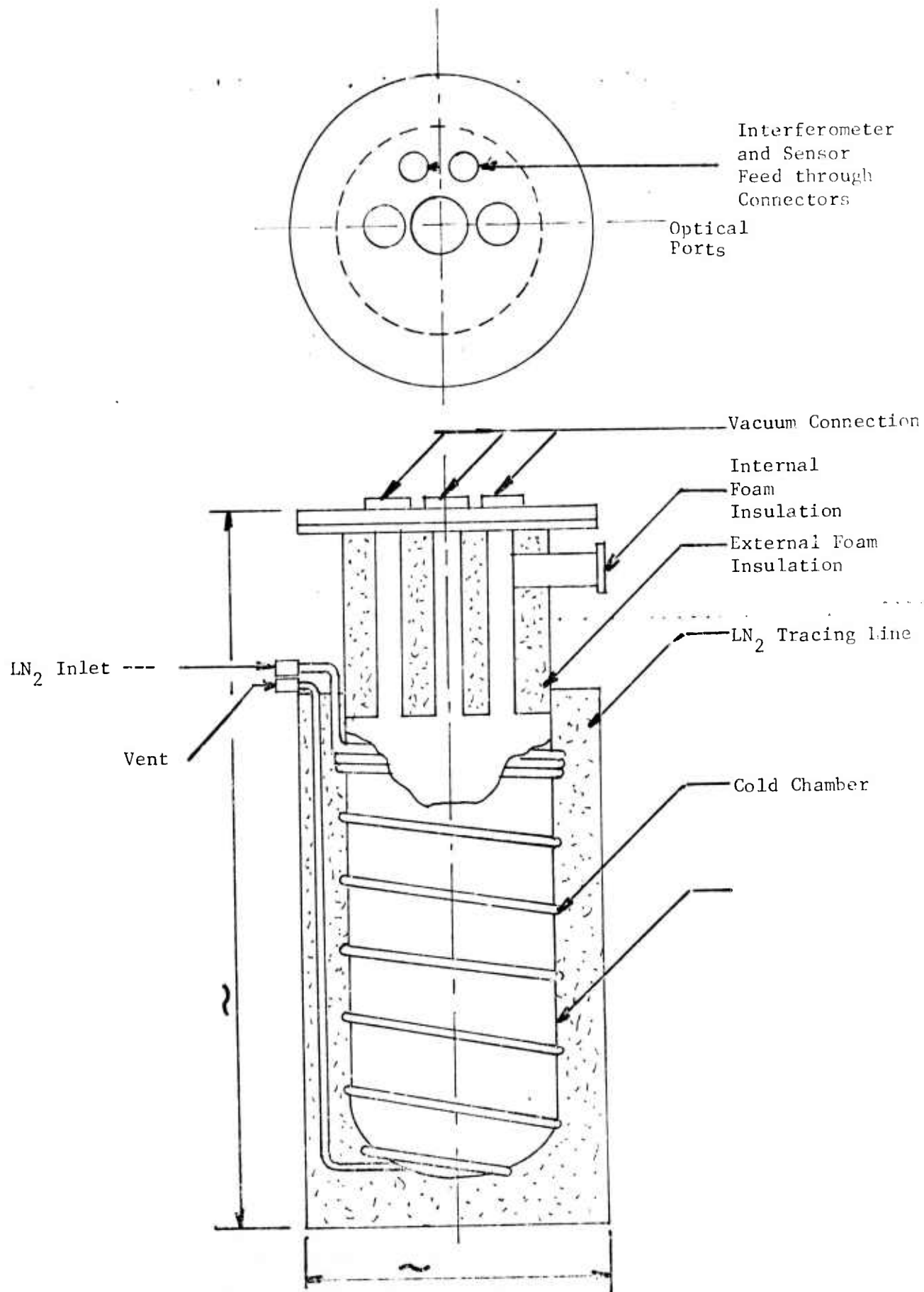


FIGURE 4.3.1.2 LIQUID NITROGEN TEST CHAMBER

4.3.2 ADL Liquid Helium Test Chamber

The existing ADL test facility was used to perform the H-Cube and IR interferometer Spectrometer optical tests at liquid helium temperatures. This facility consists of a thermal-vacuum chamber and associated optical table, a high-speed data acquisition system, liquid helium and liquid nitrogen supply systems, optical instrumentation including beam sources, beam detectors, and electronic analyses used with the interferometer electronics. The configuration of the facility is shown in Figures 4.3.2.1, 4.3.2.2, and 4.3.2.3.

The ADL test chamber has an evacuated space of 2 feet in diameter and 4 feet long, and a vacuum system capable of achieving pressures less than 10^{-6} torr. The chamber is supported upon pneumatic mounts to minimize vibrations to the test and measuring instruments and source beams. An optical viewing port is provided in the chamber cover between the optical bench and chamber interior.

Suspended in the evacuated space of the chamber is a liquid nitrogen-cooled shroud. (See Figures 4.3.2.1 and 4.3.2.4.) The shroud is traced with copper lines through which the liquid nitrogen coolant flows. The walls of the shroud are of heavy copper construction to assure a uniform temperature near 77 K. The front of this shroud facing the optical table contains an optical aperture; the opposite end contains a flanged cover for inserting the experiment.

This chamber is adapted to achieve a liquid helium temperature environment for the H-Cube and interferometer tests. A second shroud was fabricated, as shown in Figure 4.3.2.1, containing a liquid helium supply tank. This shroud was placed inside of the liquid nitrogen shroud where it was thermally protected from the room temperature walls of the chamber. The test instruments were placed inside of the liquid helium cooled shroud from a back opening which was covered with a copper plate during the tests. The front of the shroud contained an aperture for optical access to the instrument.

The liquid helium reservoir and the fill and vent lines were of stainless steel. The shroud was constructed of OFC copper brazed to the reservoir. The shroud was also traced with 3/16 inch copper line to make maximum use of the refrigeration present in the boil-off helium gas during initial cooldown.

All interferometer power and control leads and temperature measuring leads attached to the interferometer instrument were heat stationed to both the liquid nitrogen and liquid helium shrouds. Chromel-Constantan thermocouples using the liquid helium for a reference junction heat station were used for temperature measurement. The thermocouple signals were readout with a Vidar Data Acquisition System and the data recorded on a teletype printer.

The interferometer instruments were heat stationed to the liquid helium shroud using copper straps and lead or indium support washers. Initial cooldown of the instrument was accomplished with 1,000 micron nitrogen gas pressure in the chamber at 77 K. The chamber was evacuated to the low 10^{-6} torr range. The innermost shroud was then cooled with a flow of liquid helium which was maintained throughout the test after cooldown of the shroud and instrument was achieved.

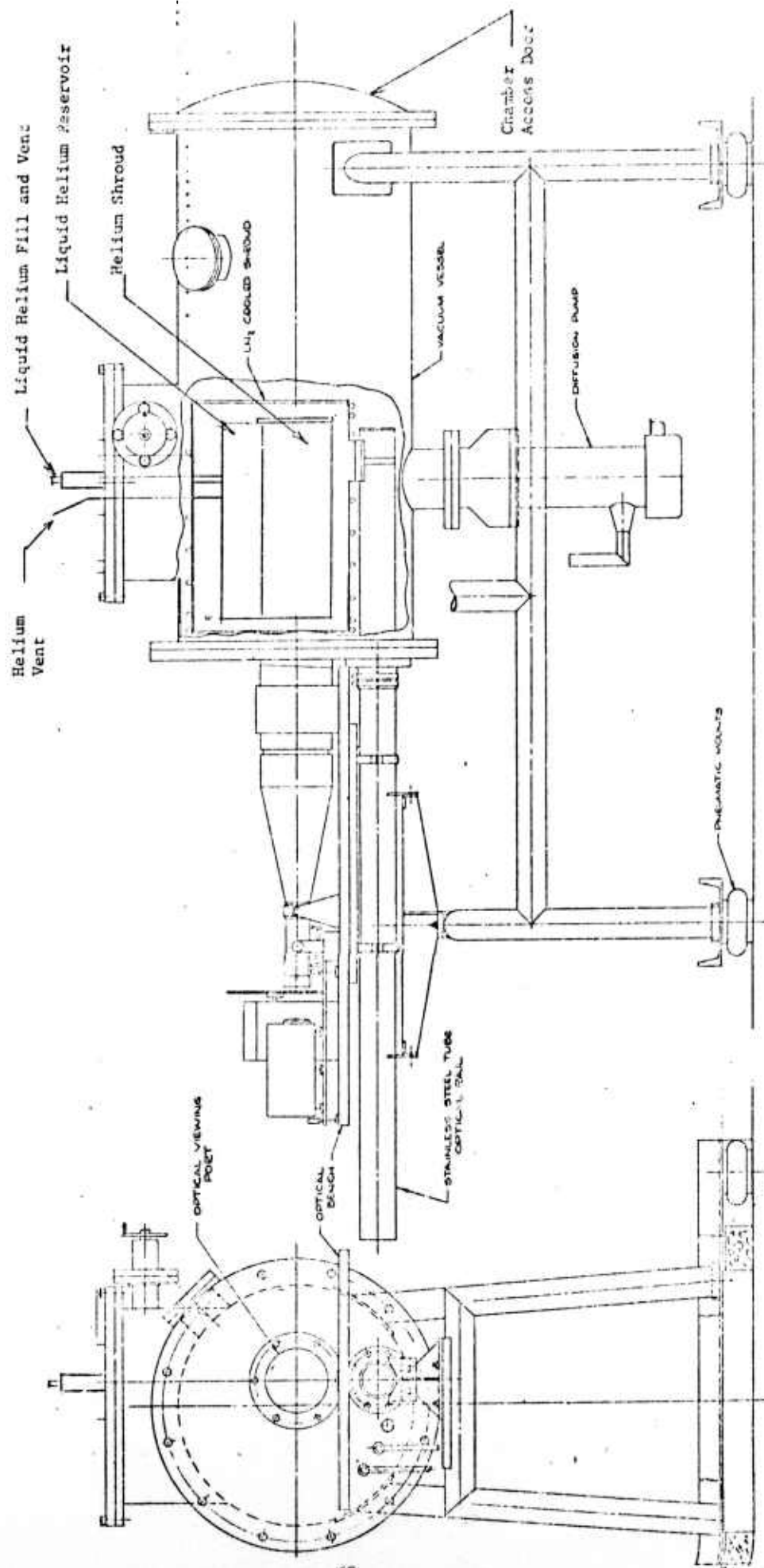


FIGURE 4.3.2.1 OPTICAL, THERMAL, VACUUM TEST CHAMBER FOR HELIUM TEMPERATURE TESTS

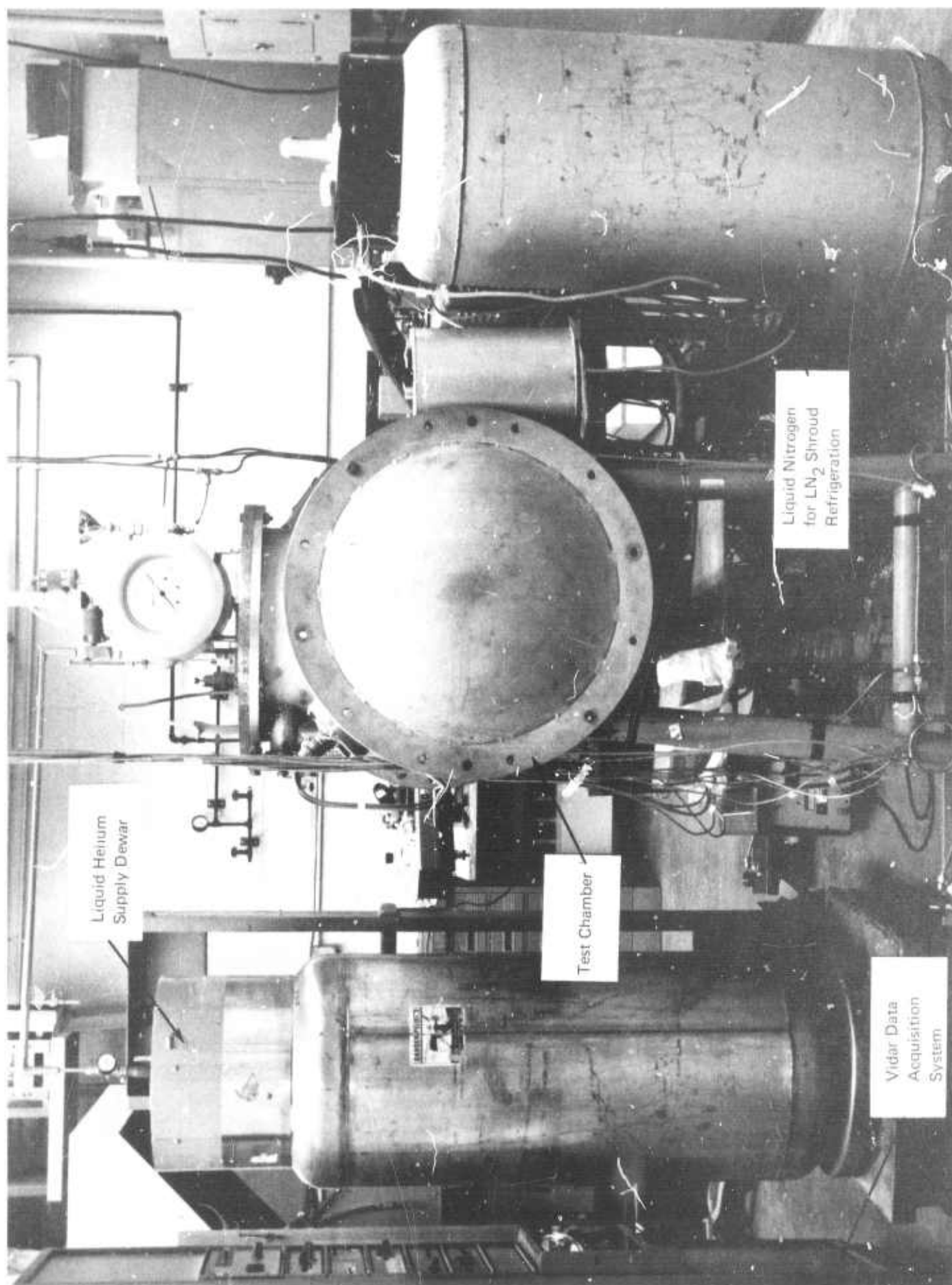


FIGURE 4.3.2.2 HELIUM THERMAL, OPTICAL, VACUUM TEST FACILITY

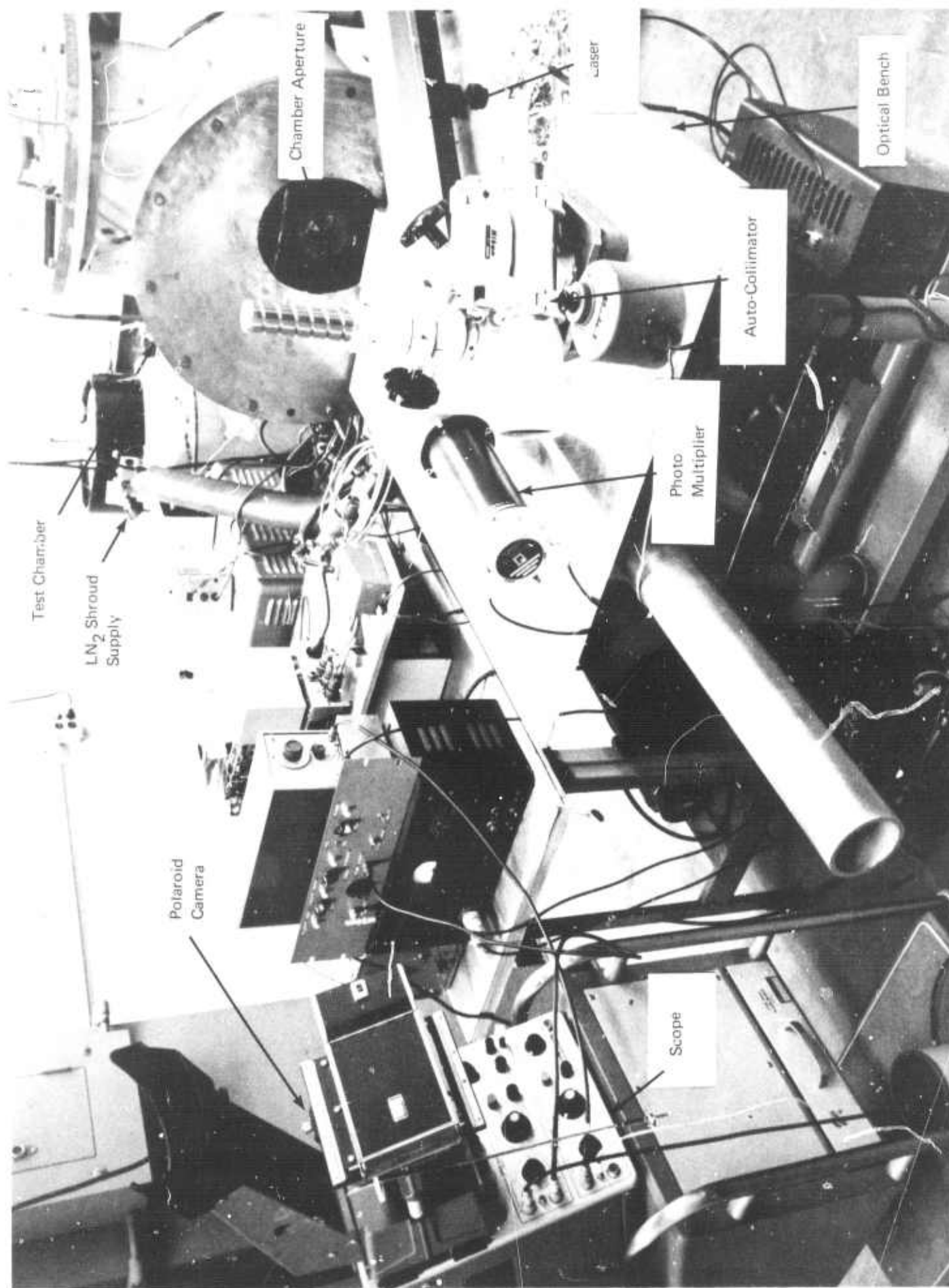


FIGURE 4.3.2.3 HELIUM TEST FACILITY, OPTICAL SET UP

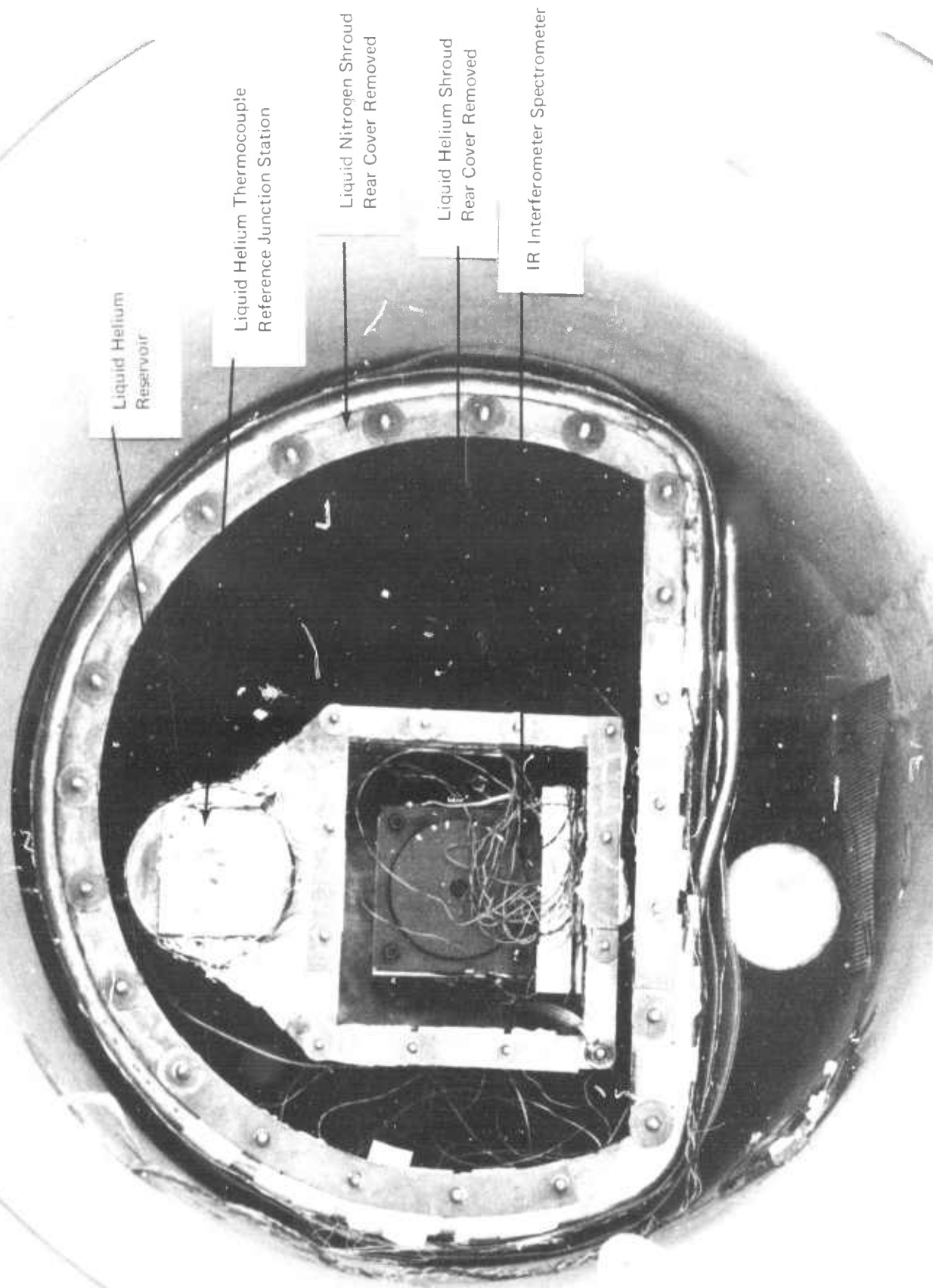


FIGURE 4.3.2.4 LIQUID HELIUM TEST CHAMBER, NITROGEN AND HELIUM SHROUD CONFIGURATION

4.3.3 Helium Test Dewar - Flight Simulation

Under this program a design was prepared for a test dewar that can be used to simulate the launch vehicle vibration environment, the IRIS thermal and optical environments, and the appropriate gas environment. The test simulation conducted with the dewar would include the following principal steps.

- (a) Optical checkout of the IRIS at room temperature.
- (b) Cooldown of the instrument to liquid helium temperatures.
- (c) Qualification level vibration (three axis) of the IRIS and test dewar with IRIS at liquid helium temperature.
- (d) Measurement of the IRIS performance at liquid helium temperatures without warm up after the vibration tests and in both the vertical (pointing upward) and horizontal IRIS positions.
- (e) Warm up of the instrument to room temperature.
- (f) Optical checkout of the IRIS at room temperature.

The facility to conduct this series of tests were to consist of a test dewar into which the IRIS is mounted, the liquid helium and liquid nitrogen coolant supplies, the dewar associated vacuum system including pumps and measuring instruments, the optical instruments and beam sources, and the data acquisition system. All the sub-systems were available as existing equipment at the Arthur D. Little, Inc. test facilities. The test dewar necessary for the tests was not, however, available as a standard item because of the special requirement for the simulation of the launch mechanical environment.

A dewar design was prepared and fabrication was initiated prior to termination of the program. The basic configuration of the dewar is shown in Figure 4.3.3.1. It consists of an outer vacuum shell, a liquid nitrogen dewar-shield, and a liquid helium dewar-shield. The helium-cooled shield encloses the IRIS test volume.

The liquid nitrogen and liquid helium dewar-shields are supported to the vacuum shell primarily through a low conductive conical washer support system. This support was successfully tested in the liquid nitrogen dewars designed and built by Arthur D. Little, Inc. for the fuel inerting system of the XB-70 aircraft. This system provides lateral as well as axial support of the inner shells. The thermal path between the vacuum shell and the 77K shield is through two washer stacks. Likewise, the path between the 77K shield and the 4.2K shield is through two washer stacks. Each stack consists of approximately 200 washers each, .002 inches in thickness and each separated by a microscopic coating of magnesium dioxide. Under vacuum conditions, the large number of series surface contact resistances produce a low thermal conductance.

In addition to the low conductance and high load capabilities of this support, it is an excellent vibration damper and it can be tuned off of the critical vibration modes of the shells. This type of support is utilized in the test dewar because it is a candidate for the flight system. The additional operating experience obtained with the support could be utilized in the design of the flight dewar support.

The aperture ends of the 77K and 4.2K shields as provided only with lateral support and are permitted to move axially relative to one another and to the 300K vacuum shell in accordance with the temperature induced length variations. The supports are formed from annular rings of NEMA G-10, Epoxy-Fiberglass material. The cross-section of the thermal path is greatly reduced to minimize the support heat leak between the two sets of temperature levels, i.e., 300K to 77K to 4.2K.

The liquid nitrogen shell is maintained at 77K by an annular liquid nitrogen dewar that utilizes the 77K shell for one of the two cylindrical dewar walls. The dewar section and head at the support end are of 300 series stainless steel. The 77K shell at the aperture end is of aluminum and it is conductively tied to the liquid nitrogen dewar. The 77K shield is thermally isolated from the 300K shell by a high performance multilayer insulation having an effective emittance of approximately .0024 in the unperturbed areas.

The liquid helium section of the test dewar is approximately 9 inches in diameter and 2 feet in length. The support for the IRIS instrument. Because the instrument has a helium gas environment of one atmosphere, the aperture end of the enclosure is sealed with a cover plate; the aperture itself is sealed with a window. It is to be noted that the spaces outside of the helium section and inside of the 300K shell are evacuated to less than 10^{-6} torr during operation.

Boil-off helium gas is used to cooldown the IRIS instrument and to maintain it at 4.2K during operation as in the flight operating mode. This is accomplished by venting the liquid reservoir into the IRIS instrument space before venting it to the atmosphere. The helium section is isolated from 77K shield through the conical washer support previously described and through an annular support at the aperture end similar in design to the 300K to 77K support. Addition isolation of the 4.2K section is obtained with a multilayer insulation.

The IRIS instrument is supported within the test chamber at two locations; one through the mass center of the motor and the other under the base supporting the slide mechanism and cube. The former support is an annular stainless steel ring which forms a part of the dewar and shield. The main base of the IRIS instrument

is attached to this ring through a hinged connection; the hinge point provides a moment-free axial and lateral support. The forward support is attached to the main IRIS base and provides a moment-free lateral support because it is free to move axially relative to the 4.2K shield.

The electrical leads between the IRIS instrument and the controls and electronics exterior to the 300K shell require both heat stationing and vacuum wall feedthroughs. This is not shown in the figure. However, the electrical leads are heat stationed on the outside of the 77K shield and on the outside of the 4.2K shield. The heat stationing consists of thermally bonding the individual lead wires to the heat station while at the same time maintaining electrical isolation of the leads from the shields and from each other. The vacuum feedthroughs are required at the 300K and 4.2K shells. Feedthroughs are required at the 4.2K shield because the interior is pressurized with one atmosphere of helium gas and the outside is evacuated.

In addition to the specific items mentioned above, fill and vents are provided to each liquid reservoir. A vacuum connection is provided in the 300K shell. The 300K shell contains provisions for supports appropriate for mounting to the shake machine along the three principal axis and for mounting to the optical bench in both the horizontal and vertical orientation.

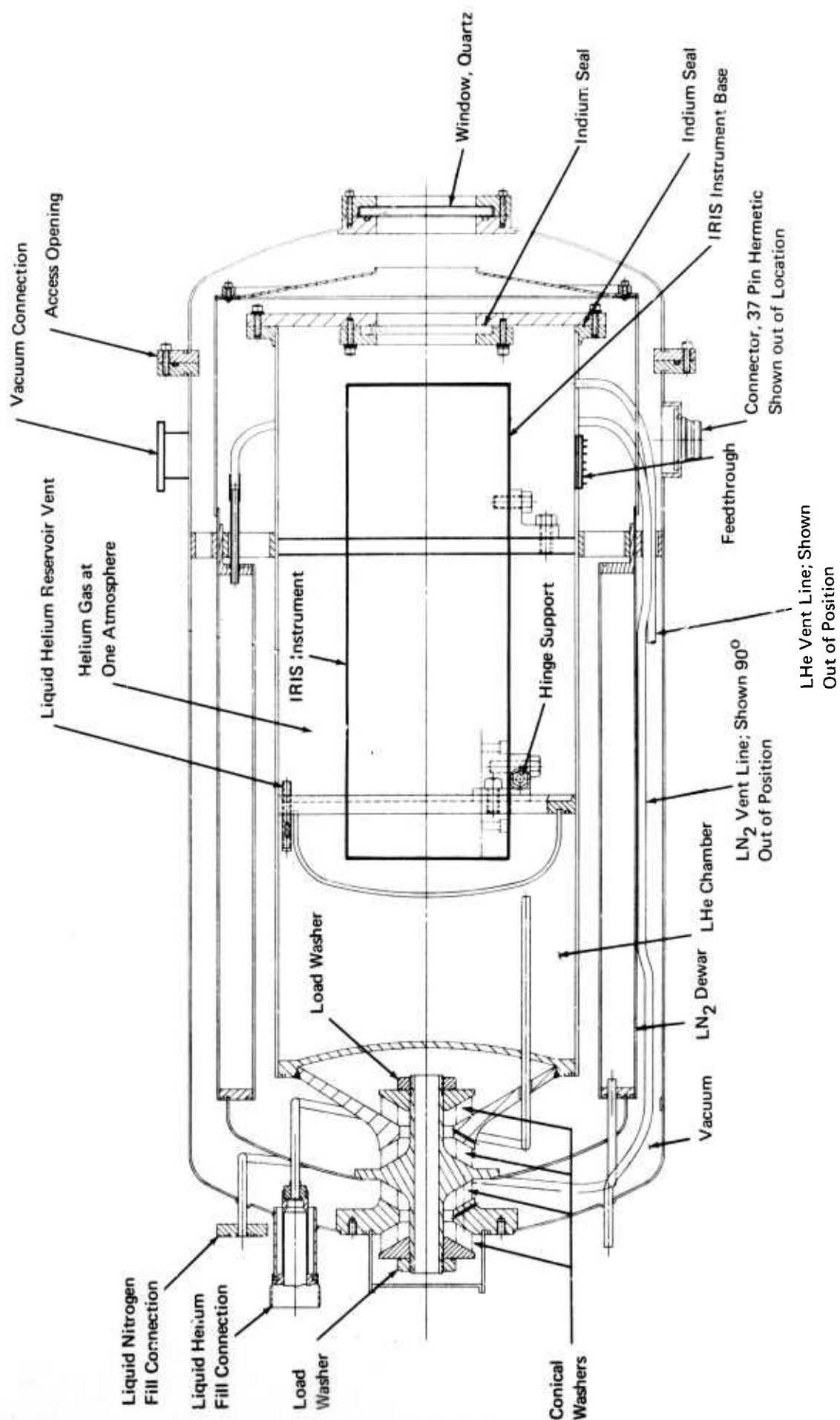


FIGURE 4.3.3.1 HELIUM TEST DEWAR

4.4 System Operating Temperature Requirement

To optimize system performance, it is necessary that the effective spectro radiance due to emission from the optical elements be less than the system noise equivalent spectro radiance has determined from the detector noise equivalent power. The radiance of the optical elements depends on the emissivity of the elements and their temperature. In the sensor system described in our design evaluation report for a cryogenically cooled rocket borne interferometer under Contract F19628-70-C0068 only the primary mirror will be at a temperature significantly above 4.3 K. We will now determine the maximum permissible operating temperature for the primary mirror.

System NESR is given by

$$\text{NESR} = \frac{\text{NEP}}{A_c \Omega T (\Delta\lambda)}$$

where

NEP is noise equivalent power
 A_c is collector area
 Ω is field-of-view in steradians
 T is system transmission
 $\Delta\lambda$ is spectral resolution

A_c and Ω are related by resolution requirements. For 2 cm^{-1} resolution at 5 microns, the maximum permissible cone of rays through the interferometer is $\delta = 2\pi \frac{\Delta\nu}{\nu} = 6.3 \times 10^{-3}$ steradians, corresponding approximately to an F/11 system.

If we take the noise equivalent power of a good cooled detector as $10^{-15} \text{ watts/Hz}^{1/2}$ and require detector limited performance at 1 scan per second for a spectro resolution of 2 wave numbers then the values noise equivalent spectro radiance as given in Table 4.4.1 are obtained as a function of wavelength from 5 to 25 microns,

where we have used

$A_c = 250 \text{ mc}^2$
 $\Omega = 1.3 \times 10^{-5} \text{ Btu } (1/4^\circ \text{ FOV})$
 $T = 0.1$
Scan rate 1/sec

NOTE: The values are taken from our design evaluation report.

TABLE 4.4.1
NOISE EQUIVALENT SPECTRO RADIANCE

λ (μ)	NESR (watts/cm ² ster. μ)
5	6×10^{-10}
10	1.5×10^{-10}
15	6.8×10^{-11}
20	3.7×10^{-11}
25	2.4×10^{-11}

The radiance of the primary mirror must be less than these values to give detector limited performance.

Table 4.4.2 summarizes computed mirror radiance for the same wavelengths at emissiveness of .05, .01, and .001 for mirror temperatures of 80K, 60K, 50K and 40K. If we take an emissivity of .05 as a likely value for the primary mirror, then the mirror temperatures must be maintained at 40K or less. For a well designed dewar, this can be readily achieved.

II MIRROR RADIANCE

40 K or less with $\epsilon = 0.05$

(Sensitivity 10^3 worse at 80°K)

III PHOTON FLUCTUATIONS AND SENSITIVITY

$$NEP = \left[\frac{\pi h \nu}{4 \eta \tau F^2} \int_{\lambda_1}^{\lambda_2} R_{\lambda} d_{\lambda} \right]^{1/2}$$

$$\int_{\lambda_1}^{\lambda_2} R_{\lambda} d_{\lambda} \approx R_{\lambda_2}$$

TABLE 4.4.2

MIRROR RADIANCE

		NESR		
		(1) $\epsilon = .05$	$\epsilon = .01$	$\epsilon = .001$
T	λ (μ)			
80 K	5	4.5×10^{-17}	9×10^{-18}	9×10^{-19}
	10	9.0×10^{-11}	1.8×10^{-11}	1.8×10^{-12}
	15	5.0×10^{-9}	9.7×10^{-10}	9.7×10^{-11}
	20	2.3×10^{-8}	4.6×10^{-9}	4.6×10^{-10}
	25	4.6×10^{-8}	9.2×10^{-9}	9.2×10^{-10}
60 K	5	2.5×10^{-22}	5×10^{-23}	5×10^{-24}
	10	2.3×10^{-13}	4.6×10^{-14}	4.6×10^{-15}
	15	9×10^{-10}	1.8×10^{-11}	1.8×10^{-12}
	20	1.1×10^{-9}	2.3×10^{-10}	2.3×10^{-11}
	25	4.1×10^{-9}	8.3×10^{-10}	8.3×10^{-11}
50 K	5	2×10^{-26}	3.9×10^{-27}	3.9×10^{-28}
	10	1.9×10^{-15}	3.8×10^{-16}	3.8×10^{-17}
	15	3.6×10^{-12}	7.3×10^{-13}	7.3×10^{-14}
	20	1.1×10^{-10}	2.1×10^{-11}	2.1×10^{-12}
	25	6×10^{-10}	1.2×10^{-10}	1.2×10^{-11}
40 K	5	1.1×10^{-31}	2.2×10^{-33}	2.2×10^{-34}
	10	1.4×10^{-18}	2.9×10^{-19}	2.9×10^{-20}
	15	3.0×10^{-14}	6.1×10^{-15}	6.1×10^{-16}
	20	2.9×10^{-12}	5.8×10^{-13}	5.8×10^{-14}
	25	3.4×10^{-11}	6.9×10^{-12}	6.9×10^{-13}

(1) Emissivity of surface.

$$\text{LET} \quad \nu = 10^{14} \text{ cps } (\sim 25 \mu)$$

$$F = 1$$

$$\text{NEP} = 10^{-15} \text{ Watts}$$

Then

$$R_{25\mu} = 10^{-11} \text{ Watts/cm}^2 \text{ ster. } \mu$$

or if

$$\epsilon = .05$$

$$T_{\text{Mirror}} \approx 37 \text{ K}$$

APPENDIX 4.5
SERVO CONTROLLED
MICHELSON INTERFEROMETER SPECTROMETER

FINAL REPORT

Contract F19628-71-C-0090

IDEALAB, INC.
UNION STREET
FRANKLIN, MASSACHUSETTS 02038

PREPARED FOR
ARTHUR D. LITTLE, INC.

The final report on this contract will cover two principal aspects of the work done under the contract. The first matter that received our consideration was an attempt to determine materials suitable for operation in the prescribed wavelength region and materials which would hopefully be able to survive the particular environment of temperature and vibration which were called out in the specifications.

Our approach to this matter was to first search the literature and attempt to find all possible materials which could be used for this purpose. After looking through a number of different publications we were able to narrow the choice of material down to the following:

Potassium Bromide (KBr)

Thallium Bromide (TlBr)

Potassium Iodide (KI)

Cesium Bromide (CsBr)

Cesium Iodide (CsI)

Rock Salt (NaCl)

Thallium Bromide-Iodide (KRS-5)

Thallium Bromide-Chloride (KRS-6)

Thallium Chloride (TlCl)

The material which at first seemed to be the most promising of the above list of materials we studied was KRS-5. This material had the advantage of an extremely wide transmission range as the enclosed graphs will demonstrate. We had had, prior to this contract, a considerable amount of experience in the design of a special beamsplitter using this material. This beamsplitter is the so-called "Air Gap Beamsplitter". The "Air Gap Beamsplitter" has many aspects to it which make it very interesting for this particular problem. The design was such as to produce a beamsplitter which if there was any motion of one of the substrates vis-a-vis the other substrate there would be no deterioration to the coating which would essentially be an air or gaseous coating or a vacuum coating which could not be destroyed. This consideration in terms of the fact that we were obliged to come up with a design which would withstand considerable vibration was a very important factor. Consequently we were immediately led to make certain tests. The first test that we attempted on this material was to submerge it to the liquid nitrogen and see if the crystal would survive this temperature. We did this and we were gratified to find that the material would indeed survive the temperature.

At this point it was decided that we would make the next logical step and that we would turn over samples of the material to Arthur D. Little and have them make tests on the material at liquid helium. It turned out that of a number of crystals tested only one crystal survived the liquid helium tests. This was most disappointing because this material had so much promise in terms of its use in the manner in which we have already described. Consequently, we felt it was worthwhile to try to investigate just what the physical property was which made it possible for the crystal to survive liquid nitrogen but not to survive the liquid helium.

In this connection we contacted Professor Smakula at M.I.T., the originator of this material, and we discussed the problem with him. Our discussions with Professor Smakula were somewhat inconclusive and we decided that we would take the matter up with the principal manufacturer of this material, Harshaw Chemical. We spoke to a Mr. Kasulones there and he in turn put us in touch with their chief scientist, Dr. Swinehart. We posed the problem to Dr. Swinehart and it was decided that the material had not been properly annealed so we agreed to

have them anneal some of this material for us; which they did. We received the material back and we went through the tests which we have already described. The results were again inconclusive. It was also suggested that the difficulty was because of the fact that the material had not been cut out of the bauble in the proper orientation. This matter was unsuccessfully pursued and finally the whole matter came to a more or less inconclusive result when Harshaw admitted to us that they really didn't understand just what was going on and in the time frame in which we were working in made it impossible for us to consider this material seriously any further.

Of the other materials that remain the material which appeared to be most interesting was Potassium Bromide. This material we had already had tested for survival to liquid nitrogen and to liquid helium temperature. It has the necessary transmission properties to be an acceptable material. It is, however, not as good in this respect as KRS-5. Beamsplitters made of this material using a germanium coating have produced very satisfactory results in normal ambient temperatures so

that all things considered it was decided to experiment with this type material. We had several of these pieces polished and we have started to make plans to test this type of material to determine the transmission reflective properties and optical flatness at the operating temperature . This was as far as we were able to go on the materials aspect of the beamsplitter compensator problem.

While the matter of selection of material for the beamsplitter and compensator was taking place a parallel effort was also being undertaken to design and fabricate a suitable beamsplitter and compensator holder. The problem here essentially was to determine a method whereby the beamsplitter and compensator substrates could be held in a position vis-a-vis the fixed and movable mirrors with great precision. Also it was required that the fidelity of the geometry of the beamsplitter and compensator as held by the holder would be maintained in the face of severe vibration and extreme cold. This meant that the beamsplitter compensator holder had to be designed in such a fashion as to insure essentially no distortion whatsoever of the geometry after having arrived at the liquid helium temperature. Such a beamsplitter and compensator holder was designed and

after a substantial amount of experimentation a method of holding the beamsplitter and compensator in this holder was evolved and we were able to maintain the optical fidelity of two crystals which we were using as test crystals. These two crystals were quartz crystals coated with a zinc sulfate coating such as to make them operate reasonably efficiently in the visible.

In terms of the total interferometer, a design philosophy was agreed upon at the beginning. The philosophy was essentially one that said that every effort should be made to design the equipment in such a fashion that its total geometry would remain invariant with temperature under a steady state condition. That is to say that we were willing to anticipate distortions in going from one temperature to another. However, after the total unit had arrived at a given temperature and all of the component parts and pieces had stabilized at a particular temperature then the geometry of the unit should be the same as it was at the ambient temperature. It was felt that this was a design goal which, even if it were not achieved, would lead to either one or two circumstances. We would be able to more readily correct for any distortions because of necessity such a design

goal would attempt to minimize all geometric distortions. Secondly, it was postulated that if we were able to observe the interferometer in a convenient dewar and notice the way in which the fringe patterns changed we would know to within an ambiguity as to how to maladjust the interferometer at the ambient temperature in such a fashion as to have the interferometer come into precise alignment at the desired temperature.

In order to accomplish this end, it was decided that the best approach was to try to use the same material in the construction of all of the parts and pieces insofar as this was possible. This meant that whereas in our standard instrument we used dissimilar metals, that is to say we used hardened A2 steel for slide and rails and in general for the moving mirror configuration and bolted this member to a tenzalloy base. In our present configuration, we had to abandon this type of construction and go to a construction which would be essentially all hardened A2 steel. It was decided also in this connection that the beamsplitter and compensator holder should be made of A2 steel. The bottom base plate of the unit was made of a 303 stainless steel. The reason that we used this material was

simply because it was the only material that was available which had a coefficient of expansion which was roughly similar to that of A2 steel and also because it was non-magnetic. The non-magnetic properties of the material was necessitated by the fact that one of its primary functions is to support a large Alnico magnet and this Alnico magnet would be short circuited by a material such as A2 steel. In order to minimize any communication of stresses of the A2 steel moving mirror assembly, it was decided that a key type arrangement or a one point line suspension system would be used. This keyed assembly was placed in a position where if there were any stresses whatsoever they would have minimal effect on the geometry of the A2 movable mirror platform.

It should be mentioned at this time that all of the A2 steel members that go into making the interferometer have to be machined to great precision because of the fact that we were attempting to have a unit which when assembled would automatically be in alignment. This factor not only makes it necessary to give careful attention to all of the usual design parameters that go into such a design but also

it was necessary to contemplate the various types of jigs and fixtures which are available for such precision grinding.

In our first test with this configuration we used conventional quartz mirrors. These mirrors were held in place by various types of spring mechanisms and one of the great difficulties that we had here was the fact that although the front surfaces of the mirrors were extremely precise, that is to say they were 10th wave, the parallelism of the mirrors was not all that was desirable. Consequently, it was necessary for us to work these mirrors in order to be able to mount them in a fashion that we desired and end up with a configuration which was in alignment. We tested these types of configurations and although the results were not entirely disastrous they certainly were not as encouraging as we had hoped for.

While doing this we were driven by the consideration of trying to use some form of metal to make the fixed and movable mirrors. We hoped by this procedure to be able to completely eliminate the fixtures holding the mirrors in their relative positions and use the metal mirrors alone as their

own support fixtures. We had rather early in the part of this contract talked to a number of fabricators and we had suggested the possibility of making the mirrors out of hardened A2 steel. In this connection a number of test blanks were machined up and ground flat and parallel. These blanks were polished and processed by Hudson Optical Company of New Hampshire and after having been polished and processed they were tested for their reflectance properties by Arthur D. Little. The results were very encouraging. Because of the urgency in regard to time on this program, we decided that we would investigate the possibility of making and polishing our own metal mirrors. A2 steel blanks were fabricated in various design configurations. These mirror blanks were hardened in precisely the same fashion as the other A2 steel members of the moving mirror assembly. They were then polished and figured and we were able on the first go-around to achieve something in the order of half wavelength of flatness. However, these mirrors were not altogether satisfactory and it was decided that we would attempt to make the mirrors using a slightly different geometry. So new blanks were fabricated,

hardened, ground, and polished. The second set of mirrors were polished to a flatness of something approaching quarter wavelength. They were tested and the results proved to be very gratifying.

At this time the total unit was assembled with the beamsplitter compensator and A2 metal mirrors. We placed the instrument in the test chamber and lowered the temperature down to the liquid nitrogen. The instrument had been previously aligned and as it went down in temperature there was a pronounced change in its alignment. This change in alignment was more than what the specifications would allow. A number of these tests were repeated in a effort to determine just where the fault lie. By the simple process of elimination and trying one thing after another, we finally found that by taking a top plate off the beamsplitter configuration we were able to get much more satisfactory results then we had been able to get before. However, the instrument when arriving at the liquid nitrogen temperature was still not in sufficiently good alignment for excellent data taking. At this point it was decided that we would attempt to determine a method whereby we could

misalign the instrument and have the instrument come back into alignment at the temperature. That is to say we would purposely misalign it at the room ambient temperature and we would expect that the distortions that would take place in going down to the liquid nitrogen temperature would be of such a fashion as to bring the instrument into as nearly exact alignment as possible. By very carefully noting the fashion in which the interference fringe pattern took place as we went from room temperature to liquid nitrogen temperature and by experimentally misaligning the instrument at room temperature in such a fashion as to reproduce the same transition in the fringe pattern, we were able to determine in what fashion we should introduce a misalignment at the room temperature and have it come into alignment at the liquid nitrogen temperature. This we were able to do successfully.

The next question that occupied our attention was the question as to whether or not such an instrument would produce results which were repeatable. It should be pointed out that our criteria was a five point check over equally spaced distances of the travel of the movable mirror. These checks were made over a total excursion which would be double the excursion that

the instrument would have to travel in order to meet the resolution requirements of the particular job that it was designed to do. This test, that is taking the instrument from room temperature down to liquid nitrogen temperature, was done seven times. The results achievable every time was such as to have the instrument arrive at the liquid nitrogen temperature in an alignment which would be completely acceptable for the wavelength region that the instrument is ultimately to be designed for. Furthermore, these tests also indicated that the movable slide mechanism was indeed maintaining its fidelity as the check of alignment was made for five different positions along the slide travel. The results of these tests have been reasonably gratifying and have led us to believe the fundamental philosophy which we expected at the beginning was a tenable one. That is to say, that an instrument made in the manner in which we have described can be built such that it will arrive at the operating temperature of liquid nitrogen and be in acceptable alignment. It should, however, be pointed out that this procedure does not preclude the use piezo electric crystals or such other devices to bring the instrument into even

better alignment should that prove to be necessary. However, since such devices as piezo electric crystals have not been thoroughly tested at liquid nitrogen or helium temperatures and certainly not at these temperatures plus ambient vibrations such as are expected, it is far from certain as to how they would perform. Furthermore, these devices are of such a nature as to increase the possibility of malfunctioning. In other words, by using such devices one has of necessity to trade down in the overall reliability of the system. We believe that our fundamental philosophy in regard to the design of the interferometer has been justified.

The servo system used in making the various optical checks on this instrument was a design which had been built around an interferometer having a very substantial amount of viscous damping. No attempt was made to optimize this design because at the very beginning it had been decided that we were going to attempt to design a servo which would suit the particular needs of the environment which this instrument was to exist in.

Preliminary study of this design problem showed that there would be certain major changes that would be necessary in order to produce a servo which would give optimal performances. Consequently, no attempt was made to optimize the performance of the servo that we planned to use for making the optical checks. The main thing that we desired of this system was a means whereby we could measure the system friction profile which in practice meant measuring the current through the drive motor coil in order to determine if there was any binding at the liquid nitrogen temperatures. This we were able to do quite satisfactorily. In the meantime we have breadboarded a new servo system specifically designed for the environment in which this instrument is to operate and we have begun to make preliminary checks on its performance. A complete frequency response and phase shift characteristics is in the process of being determined. It is assumed that at an appropriate stage in this design, we will incorporate into the system certain equalizing networks to bring about an optimal performance of the system at the environmental conditions under which it will operate.

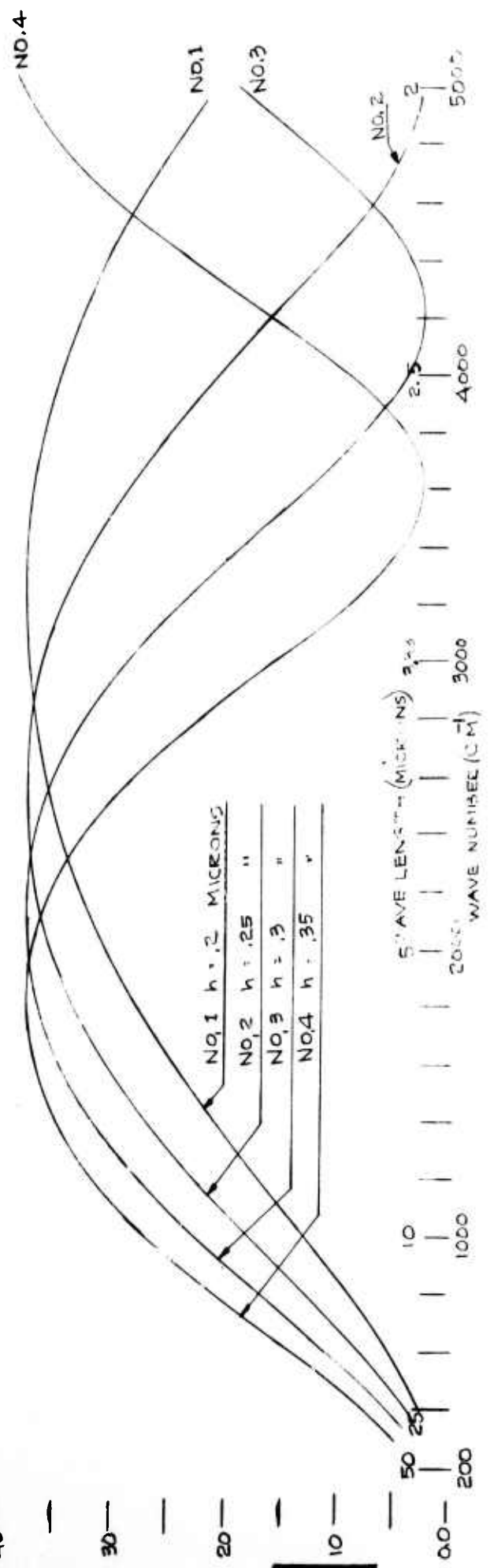
100 —
—
90 —
—
80 —
—
70 —
—
60 —
—
50 —
—
40 —
—
30 —
—
20 —
—
10 —
—
00 —

SUBSTRATE KRS-F

COATING 5.2

θ 1 45°

% EFFICIENCY

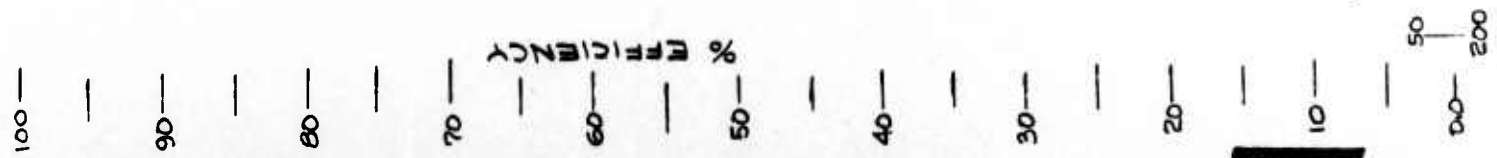


SUBSTRATE KRS 2

COATING Ge

Θ 45°

EFFICIENCY %



NO. 1 $h = .2$ MICRONS
NO. 2 $h = .25$ "
NO. 3 $h = .3$ "
NO. 4 $h = .35$ "

5 WAVELENGTH (MICRONS) 3.32
2000 WAVELENGTH (CM⁻¹) 3000

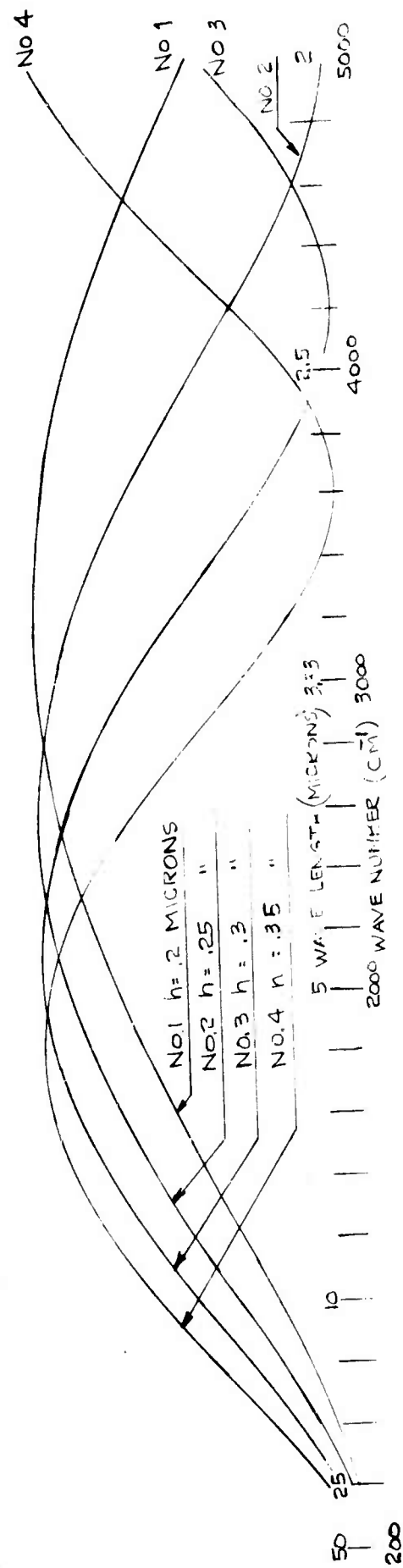
100 —
90 —
80 —
70 —
60 —
50 —
40 —
30 —
20 —
10 —
0.0 —

SUBSTRATE IRTRAN 4

COATING SE

Θ_1 45°

% EFFICIENCY



SUBSTRATE K B L

COATING Ge

Θ 1 45°

% EFFICIENCY

No. 2
No. 1
No. 3

IDEALAB, INC.

No. 1 $h = .1$ MICRONS

No. 2 $h = .15$ "

No. 3 $h = .2$ "

No. 4 $h = .25$ "

No. 4

5 WAVELENGTH (MICRONS) 3.33

2000 WAVE NUMBER (CM⁻¹) 3000

2.5

4000

2

5000

3.33

3000

1000

10

25

50

200

500

1000

2000

3000

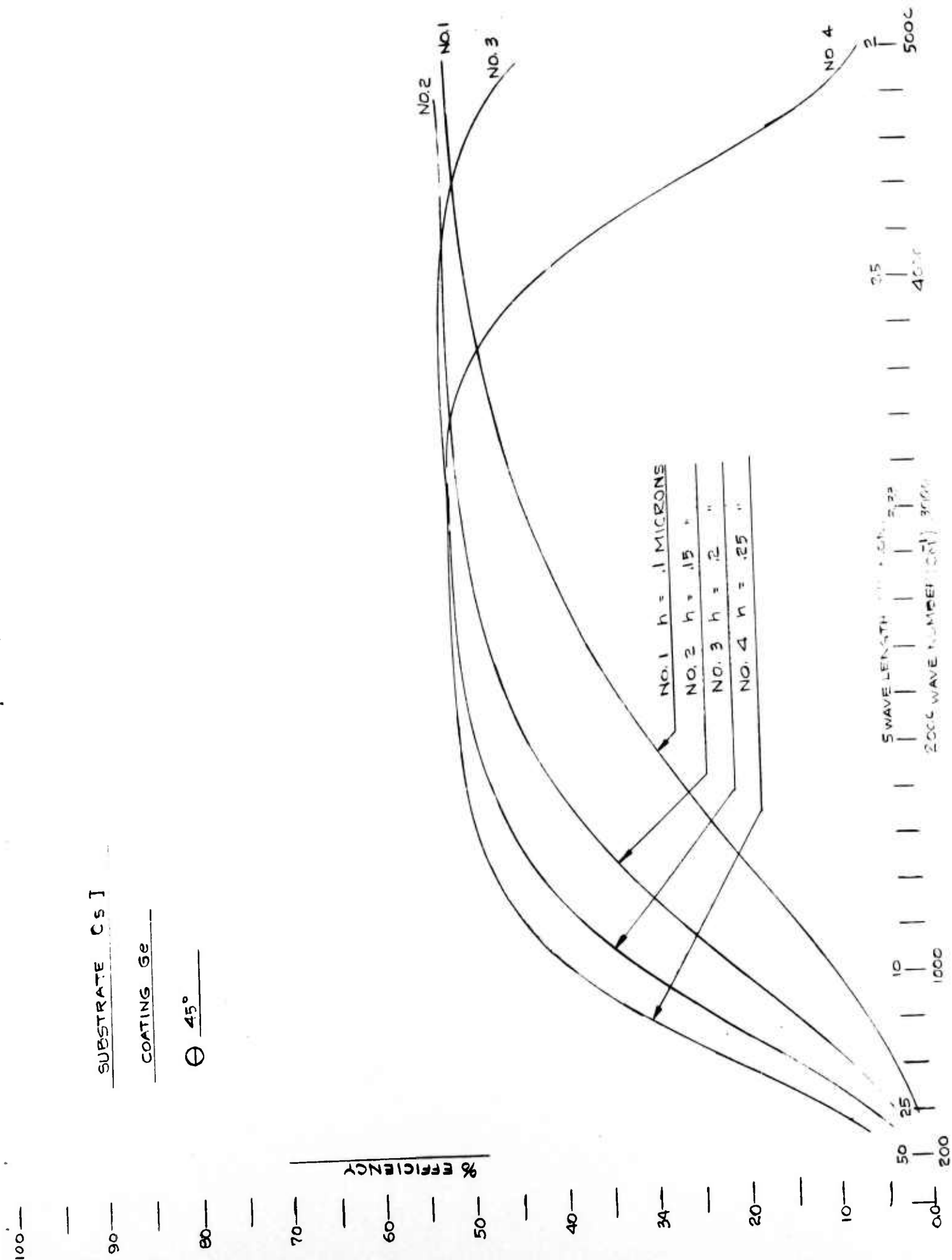
4000

5000

SUBSTRATE [Cs]

COATING Ge

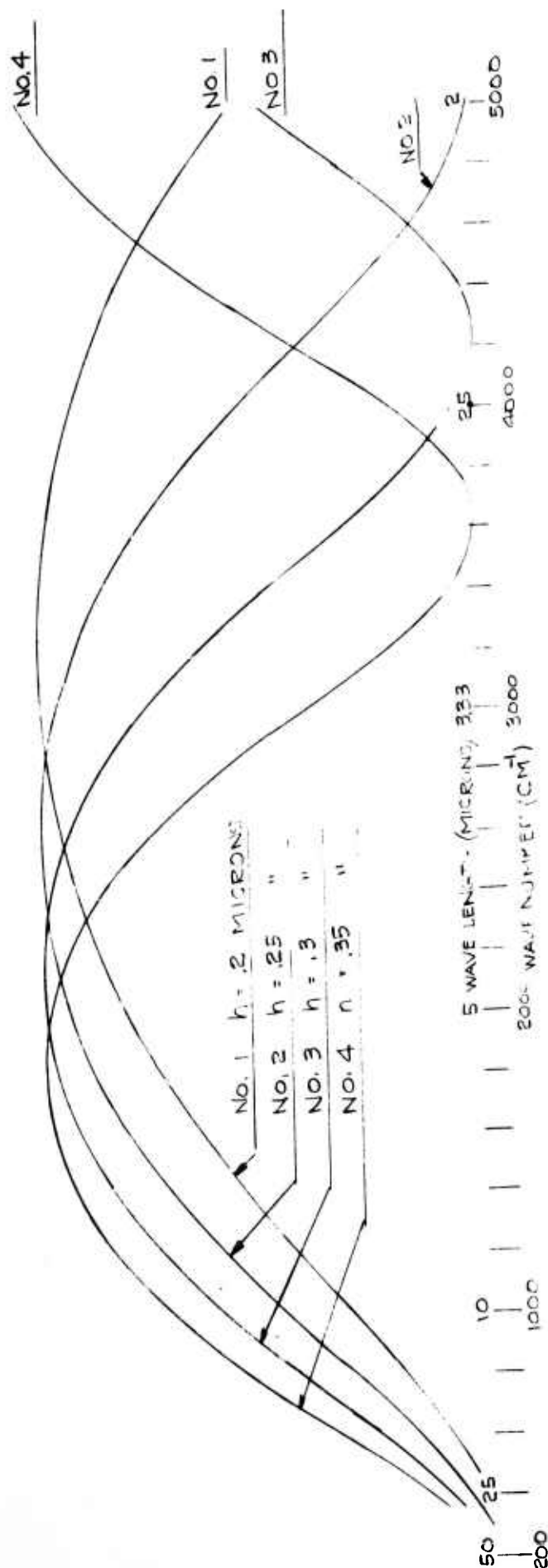
θ 45°



COATING Ge

$$\Theta \quad \frac{I}{45^\circ}$$

% EFFICIENCY



IDEALAB, INC.

100—

90—

80—

70—

60—

50—

40—

30—

20—

10—

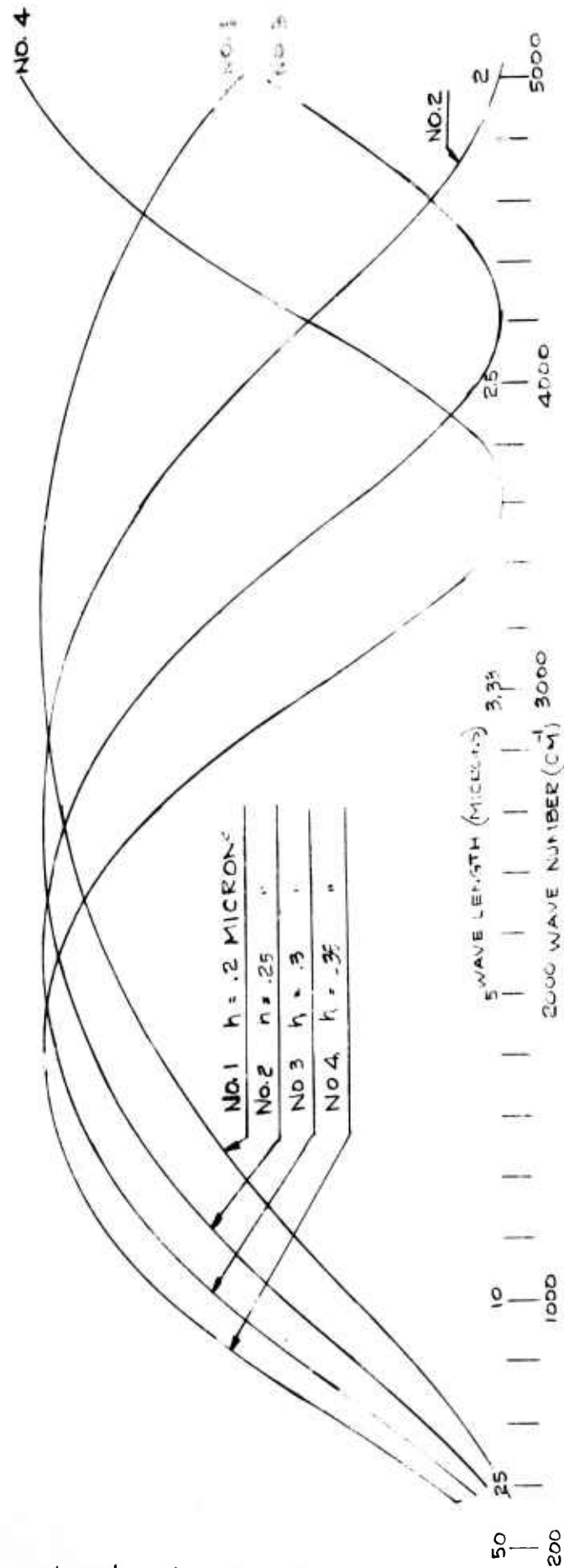
0.0—

SUBSTRATE TQCL

COATING Ge

 Θ_1 45°

% EFFICIENCY



100—

—

90—

—

80—

—

70—

—

60—

—

50—

—

40—

—

30—

—

20—

—

10—

—

0.0—

200

1000

25

10

2.5

3.33

4000

2

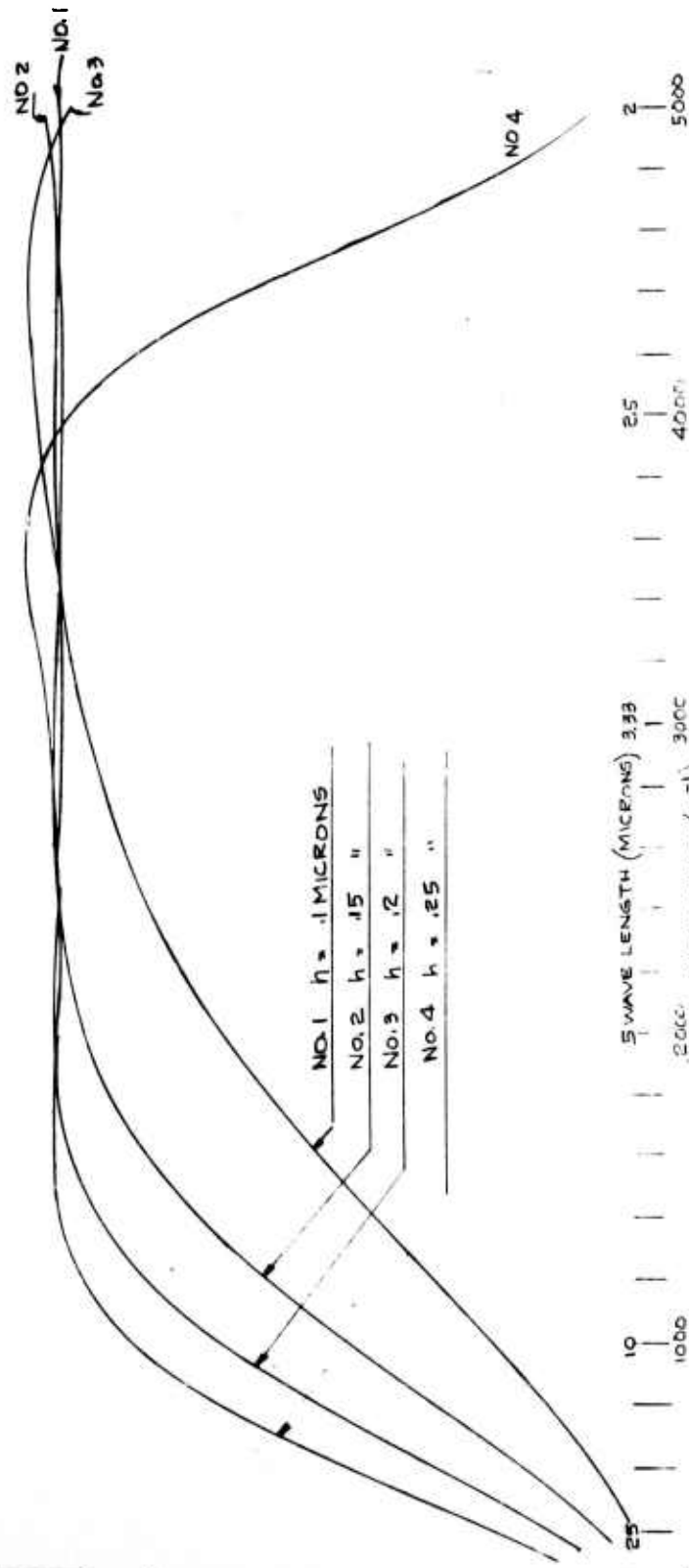
5000

WAVE NUMBER (CM⁻¹)

WAVELENGTH (MICRONS)

NO. 1 $h = .1$ MICRONSNO. 2 $h = .15$ "NO. 3 $h = .2$ "NO. 4 $h = .25$ "

% EFFICIENCY

SUBSTRATE CsBrCOATING Ge Θ_1 45°

DOCUMENT CONTROL DATA - R&D		
(Security classification of title, body of abstract and indexing annotation must be entered when the overall report is classified)		
1. ORIGINATING ACTIVITY (Corporate author) Arthur D. Little Incorporated Acorn Park Cambridge, Massachusetts 02140		2a. REPORT SECURITY CLASSIFICATION Unclassified
		2b. GROUP
3. REPORT TITLE DESIGN AND DEVELOPMENT OF A CRYOGENICALLY COOLED HIGH RESOLUTION INTERFEROMETER		
4. DESCRIPTIVE NOTES (Type of report and inclusive dates) Scientific. Final. 12 November 1970 3 November 1971 Approved 21 Jul 72		
5. AUTHOR(S) (First name, middle initial, last name) Henry H. Blau, Jr. Richard B. Hinckley Frank E. Ruccia		
6. REPORT DATE November 1971	7a. TOTAL NO. OF PAGES 103	7b. NO. OF REFS 9
8a. CONTRACT OR GRANT NO. F19628-71-C-0090	9a. ORIGINATOR'S REPORT NUMBER NOT APPLICABLE	
b. PROJECT, TASK, WORK UNIT NOS. 8692 n/a n/a		
c. DOD ELEMENT 62301D	9b. OTHER REPORT NO(S) (Any other numbers that may be assigned this report.) AFCRL-72-0329	
d. DOD SUBELEMENT n/a		
10. DISTRIBUTION STATEMENT B - Distribution limited to U.S. Government agencies only: Test and Evaluation, 21 July 1972. Other requests for this document must be referred to AFCRL (OPR), L.G. Hanscom Field, Bedford, Massachusetts 01730.		
11. SUPPLEMENTARY NOTES This research was supported by the Advanced Research Projects Agency.	12. SPONSORING MILITARY ACTIVITY Air Force Cambridge Research Laboratories (OP) L.G. Hanscom Field Bedford, Massachusetts 01730	
13. ABSTRACT The intent of the development called for under this contract is to produce a prototype liquid-helium cooled instrument, consisting of a cooled interferometer spectrometer, telescope, optical system and sensor, having a resolution of about two wavenumbers and suitable for flight on vertical sounding rockets such as the Black Brant V for the purpose of making measurements of the spectral radiance of the airglow and aurora. This development was initiated under Contract No. F19628-70-C-0068. Development, fabrication and testing of a prototype optical cube suitable for use at liquid helium temperatures and capable of surviving the environment of a rocket launch is described. A prototype interferometer was exposed to mechanical vibration at room temperature; the results of these tests are reported. The results of an experimental program to determine the feasibility of using a laser diode as a fringe reference source at liquid helium temperatures are cited. The preliminary design of a test dewar designed to permit both vibration and optical tests of the interferometer at cryogenic temperatures is presented.		

Unclassified

Security Classification

14.	KEY WORDS	LINK A		LINK B		LINK C	
		ROLE	WT	ROLE	WT	ROLE	WT
	Infrared Spectrometer Cryogenic Interferometer Auroral Spectrometer Cryogenic Sensor Infrared Sensor						

Unclassified

Security Classification